INTERNATIONAL ATOMIC ENERGY AGENCY
UNITED NATIONS EDUCATIONAL, SCIENTIFIC AND CULTURAL ORGANIZATION

INTERNATIONAL CENTRE FOR THEORETICAL PHYSICS
34100 TRIESTE (ITALY) - P.O.B. 586 - MIRAMARE - STRADA COSTIERA 11 - TELEPHONE: 2240-1
CABLE: CENTRATOM - TELEX 460392 - 1

SMR/390 - 8

WORKING PARTY ON "FRACTURE PHYSICS"
(29 May - 16 June 1989)

FROM DISLOCATION DYNAMICS TO SELF ORGANIZATION OF DISLOCATIONS (Part II)

G. ANANTHAKRISHNA
Indira Gandhi Centre for Atomic Research
Materials Science Laboratory
603 102 Kalpakkam
India

J. Phys. D: Appl. Phys., 14 (1981) 699–713. Printed in Great Britain

A statistical theory of dislocation dynamics with application to creep in LiF†

G Ananthakrishna and Debendranath Sahoo
Materials Science Laboratory, Reactor Research Centre, Kalpakkam 603 102, Tamil Nadu, India

Received 17 June 1980

Abstract. A statistical theory of dislocations has been proposed with specific application to creep in LiF and materials like it. The velocity of a dislocation is chosen to be a random variable. Based on various established mechanisms contributing to glide-controlled plastic flow, a semi-empirical continuity equation is set up for the velocity distribution function. The solution is obtained in terms of a power-series expansion of two small parameters, and the first four cumulants have been calculated within a certain approximation in which the third and fourth turn out negative, resulting in a distribution function having sharp edges on both sides. The average velocity of dislocations is shown to reduce linearly with the average density of dislocations, leading to an internal stress which is linear in the average density. The equation of motion of the dislocations exhibiting the drag, an equation for population dynamics of dislocations during creep, and a creep law proposed by Webster (1966) follow from our work. The theory is applied to creep in LiF with excellent agreement. It also explains the shift in the stress–velocity relation in prestrained samples.

1. Introduction

Gilman (1968a) has emphasised that a statistical description is inevitable for motion of dislocations in a material undergoing plastic deformation. In simple theories, only average values of parameters are considered as in the Orowan equation

$$\dot{\varepsilon} = bVN \tag{1}$$

where $\dot{\varepsilon}$ is the strain rate, V the *average* velocity of dislocations, N the *average* density and b the magnitude of the Burger vector. Clearly, if one writes the above equation in terms of a (nonstationary) velocity distribution function $\rho(v, t)$, it would lead to a statistical description. If one sets up an equation of motion for $\rho(v, t)$, and solves it with suitable boundary conditions pertaining to all aspects of plastic flow, then one would have a description of plasticity which would be an improvement over the usual phenomenological treatment. This is a difficult task, as the laws governing plastic flow are 'nonlinear'. For example, in a tensile test for polycrystals (in general), the stress $\sigma \sim \varepsilon^{1/2}$, and as $\varepsilon \sim N$ (for not too high levels of strain), $\sigma \sim N^{1/2}$. There are less common materials where $\sigma \sim N \sim \varepsilon$. This is also true in stage II of work hardening of simple crystals. A typical example is LiF where $\sigma \sim \varepsilon$ in a tensile test (Gilman and Johnston 1960) and the internal

† A preliminary version of this work was presented at the DAE Symposium on Nuclear Physics and Solid State Physics, Bombay, 1978.

0022-3727/81/040699+15 $01.50

stress is $\sigma_i \sim N$ (Gupta and Li 1970). In this paper we propose a statistical theory of dislocation dynamics applicable to materials with $\sigma \propto \varepsilon$ and apply it to LiF. We expect that the basic feature of plasticity, namely nonlinearity (at the microscopic level) would be common to these and the other type of materials mentioned above. There are two reasons for choosing LiF as a reference material for our theory. First, it is extensively studied (Gilman and Johnston 1962, Gilman 1969, Gupta and Li 1970). Secondly, the mechanisms of plastic flow are well known: dislocations multiply rapidly by the cross-glide mechanism (Gilman and Johnston 1962) with a rate proportional to the flux NV of dislocations.

For simplicity we consider plastic flow to be homogeneous in the sample and consider the flow to be one-dimensional, i.e. we assume v to be a scalar variable v. To see the range of v, consider a stress acting on positive and negative dislocations with $b_+ (= |b|)$ and $b_- (= -|b|)$ as their respective Burgers vectors. We regard the velocity of a dislocation as positive if it moves in the direction of the applied stress and negative if it moves opposite to the applied stress. Hence the velocity v_+ of positive dislocations can take on values from 0 to $+\infty$, and the velocity v_- of negative dislocations can range from 0 to $-\infty$. (Note $v_+ = -v_- = |v|$.) Then the range of v is from $-\infty$ to $+\infty$. However, both positive and negative dislocations contribute positively to creep. Using the appropriate ranges of $v_\pm$, we get

$$\begin{aligned}\dot{\varepsilon} &= b_+ \int_0^{+\infty} v\,\rho(v,t)\,\mathrm{d}v + b_- \int_{-\infty}^{0} v\,\rho(v,t)\,\mathrm{d}v \\ &= |b| \int_{-\infty}^{+\infty} |v|\ \rho(v,t)\,\mathrm{d}v \\ &= b\langle |v| \rangle N \end{aligned} \tag{2}$$

where

$$N(t) = \int_{-\infty}^{+\infty} \mathrm{d}v\ \rho(v,t). \tag{3}$$

In §2 we propose an integro-partial-differential equation for ρ, which turns out to be a Fokker–Planck equation with some source and sink terms. We confine ourselves to the phenomenon of creep (i.e. stress is held constant). The main result we are able to derive (§3) is that during creep V decreases linearly with N, thus resulting in an internal stress $\sigma_i \sim N$. The relation was *assumed* in the creep model of Webster (1966). The population dynamics equation for the evolution of N during creep, and the Newtonian dynamics equation for V (Webster 1966, Gilman 1968a, 1969, Li 1963) are derived (§2) from our theory. In addition to a creep law (§4) (derived with the approximation that $\langle v \rangle = \langle |v| \rangle$ justified in §6 by the form of ρ, and then applied to LiF), which is similar to Webster's (1966), our theory can also account for the shift in the stress–velocity curve (§5) for a prestrained sample (Gilman and Johnston 1962, 1960). Also derivable from it is the linear ε versus N law (§4). We have derived four cumulants of the distribution $\rho(v,t)$ (§3); the third and the fourth ones, corresponding to the coefficients of asymmetry and excess (Stratonovich 1963), turn out to be negative. This implies that the distribution $\rho(v,t)$ has sharp edges on both sides.

There are other statistical theories dealing with one aspect or the other of the phenomenon of plastic flow. We mention the following, with no elaboration of the contents, as there is little in these in common with our work—Gilman (1968b), Ostrom and Lagneborg (1976), Lagneborg and Forsen (1973), Feltham (1968, 1973), Mott and Nabarro (1948) and Welch and Smoluchowski (1972).

2. The proposed model

As the distribution function is nonstationary, a central role is played by the conditional velocity distribution function $\rho(vt|v_0t_0)$ (synonymous with conditional probability density if probability were conserved) which is the probability of dislocations having the velocity v at time t given that these had the velocity v_0 at an earlier time t_0. The velocity distribution function, which should also depend on t_0, is derivable from $\rho(vt|v_0t_0)$:

$$N_0\rho(v,t,t_0)=\int \mathrm{d}v_0\,\rho(vt|v_0t_0)\,\rho(v_0t_0) \tag{4}$$

where $N_0\equiv N(t_0)$. However, in the present problem, $\rho(vt|v_0t_0)$ loses memory of v_0 in an extremely short time (short compared to the time over which the material deforms, as will be shown later), but retains memory of the initial state $\rho(v_0t_0)$ through the initial dislocation density N_0 and t_0. Because of this, $\rho(vt|v_0t_0)$ is for all practical purposes equal to $\rho(v,t,t_0)$. The dependence on time is only through $t-t_0$. However, as the single particle distribution has an explicit time dependence (although in the form $t-t_0$), the process is nonstationary (Stratonovich 1963). We do not distinguish between $\rho(vt|v_0t_0)$ and $\rho(v,t,t_0)$ unless otherwise required. Further, we suppress t_0, and write $\rho(v,t,t_0)$ as $\rho(v,t)$.

The problem of dislocation motion under stress has some similarities with the problem of Brownian motion with the most obvious difference that the total number of dislocations is not conserved. We momentarily disregard the production and annihilation of dislocations. (This would be true if the time over which the stress is applied is short compared to the time constant associated with production and loss of dislocations.) The lattice friction of dislocations and the force acting on these due to the applied stress, respectively, assume the roles of the viscous drag and the gravity force of the Brownian motion. (The lattice friction constant in our problem is regarded as a parameter to be supplied empirically.) Now we can include the production and the loss of dislocations by a term representing sources and sinks. Then the equation of continuity for $\rho(v,t)$ can be written as

$$\frac{\partial\rho}{\partial t}+\frac{\partial J}{\partial v}=S \tag{5a}$$

and

$$J=-\left(\frac{B_0}{M}v-\frac{b\sigma_a}{M}\right)\rho(v,t)-\frac{Q}{M}\frac{\partial\rho(v,t)}{\partial v}$$

$$=-(\beta v-f)\rho(v,t)-q\frac{\partial\rho(v,t)}{\partial v}. \tag{5b}$$

Here, J is the current associated with $\rho(v,t)$. In the above equation, B_0 is the drag coefficient, $b\sigma_a$ is the force acting on a unit length of a dislocation and Q, the velocity diffusion coefficient. (M is the effective mass of a dislocation of unit length, appearing due to the fact that we have considered the velocity rather than the momentum as the random variable.)

The sources and the sinks can include many different types of contributions. We shall include only those which are well established and are simple in form. Some of these are linear in $\rho(v,t)$ and others, bilinear. The first linear contribution comes from the stopping of dislocations at precipitates, grain boundaries, etc. Let the rate of loss due to this be $-\alpha\rho(v,t)$ where α is a constant. The second contribution is the breeding of dislocations due to the well established (Gilman and Johnston 1962) cross-glide mechanism. The rate

of generation due to this process is denoted by $\theta v\rho(v,t)$, where θ is a constant called the breeding coefficient (Gilman 1968a). Adopting the chemical kinetic approach, the mutual interaction of dislocations should be bilinear in $\rho(v,t)$ in the simplest case (analogous to the collision integral in the Boltzmann transport equation). If we consider two dislocations with arbitrary velocities v' and v'' with their respective velocity distributions $\rho(v,'t)$ and $\rho(v'',t)$, then the contribution to $\partial\rho/\partial t$ should be of the form $\rho(v')\rho(v'')$. It should represent such well known mechanisms as mutual annihilation of a pair of dislocations of opposite sign, formation of dislocation dipoles, formation of stair-rod dislocations of the Lomer–Cottrell type, etc. The resulting species can in principle have a velocity $v=v'+v''$. (This resultant velocity could be zero also.) Thus the interaction term will be of the form $\rho(v-v')\rho(v')$. It is clear that if $|v|<|v'|$, $v-v'$ has a sign opposite to that of v' for $-\infty\leqslant v'\leqslant\infty$. Thus we expect this term to represent all pairwise interactions which arise when the participating dislocations have some velocity component having opposite signs. Here again, $|v|$ being small would possibly represent the formation of dipoles and other types of locks, which physically should have small velocities. Other values of v represent dislocations interacting weakly (with their slip planes far apart). Some pairwise interactions corresponding to the case $|v|>|v'|$ have been discussed by Gilman (1969). We represent all such interactions by integrating over the variable v' and obtain the overall contribution as

$$-\mu\int_{-\infty}^{\infty}\mathrm{d}v'\,\rho(v-v',t)\,\rho(v',t)$$

where μ is the effective rate constant for all these processes. In addition, when two dislocations of velocities v' and v'' interact with each other, their resultant velocities are also reduced. Associated with these velocities, their respective distributions should change differentially, their total contribution to $\dot{\rho}$ being proportional to

$$\tfrac{1}{2}\int\mathrm{d}v''\,\rho(v')\partial\rho(v'')/\partial v''+\tfrac{1}{2}\int\mathrm{d}v'\,\rho(v'')\,\partial\rho(v')/\partial v'.$$

But v' and v'' are not independent since $v=v'+v''$. This leads to an interaction having the form

$$h\int_{-\infty}^{\infty}\mathrm{d}v'\,\rho(v-v',t)\partial\rho(v',t)/\partial v'$$

where h is a rate constant. Now, summing up all contributions, we may write the source and sink function as

$$S=(-\alpha+\theta v)\rho(v,t)-\mu\int_{-\infty}^{\infty}\mathrm{d}v'\,\rho(v-v',t)\,\rho(v',t)$$
$$+h\int_{-\infty}^{\infty}\mathrm{d}v'\,\rho(v-v',t)\partial\rho(v',t)/\partial v'. \tag{5c}$$

It is clear that we have taken simplified forms for f and θ terms in equation (5) to facilitate a closed form solution. Although terms representing interaction of positive and negative dislocations have correct forms as explained above, the f and θ terms should have appropriate step functions multiplying them. The above simplified version, we believe, still represents the physical situation adequately enough, with the basic difference that the actual distribution should be bimodal when appropriate forms for θ and f terms are considered. (See discussion, §6, where this point is discussed in detail.)

To solve equations (5 *a–c*), we impose natural boundary conditions

$$\rho(v,t),\ v\rho(v,t),\ \partial\rho(v,t)/\partial v\to 0 \qquad \text{as} \qquad v\to\pm\infty. \tag{6}$$

As there are several parameters entering into equation (5), we list their magnitudes in table 1. All measurable quantities occur as ratios with respect to β ($\gg 1$), the largest being f/β; this is much larger than h/β, q/β, α/β and μ/β. The quantity $(h/\beta)N$ could be comparable to f/β, which will be shown to be approximately equal to the average velocity. Even before we solve the central equations (5 *a–c*), we derive the essential results by a short cut but in an approximate way; the deficiencies are then removed in the next

Table 1. Values of the parameters used in equation (5).

Parameter	Value	Remarks
$B \approx B_1 = \frac{f}{\beta}$	3.033×10^{-3} cm s^{-1}	Value for $\sigma_a = 380$ g mm^{-2} using power law†.
θ	30 cm^{-1}‡	
β	10^9 s$^{-1} \sim 10^{13}$ s^{-1}	Estimated in §2
α	1.82×10^{-3} s^{-1}	From case (2) of creep
μ	2.271×10^{-10} cm^2 s^{-1}	From case (1) of creep
h/β	3.535×10^{-10} cm^3 s^{-1}	From case (1) of creep
N_s	8.4×10^6 cm^{-2}	From case (1) of creep
N_0	7.5×10^4 cm^{-2}	From case (1) of creep
q/β	B^2	From the condition $k_2 > 0$

† Johnston (1962).
‡ Gilman (1968a).

section. The purpose of doing so is to establish connections with some well known phenomenological relations.

First we derive the equation governing population dynamics of dislocations. Integrating equation (5 *a*) over v and using equations (5 *b*, *c*) and (6), we obtain

$$dN/dt = (-\alpha + \theta V)N - \mu N^2 \tag{7}$$

where V refers to the average velocity, an expression for which will be obtained from our theory. This equation, apart from a constant term, has been used earlier, with V assumed to decrease linearly with N (Webster 1966, Li 1963, Gilman 1968a, 1969)—a result which we will derive.

The equation governing Newtonian dynamics of dislocations is similarly obtained by multiplying equation (5*a*) by v and then integrating over v

$$(dV/dt) + (\beta + \mu N)V = f - hN + \theta(\langle v^2 \rangle - V^2) \tag{8}$$

where

$$N\langle v^2 \rangle = \int_{-\infty}^{\infty} dv\, \rho(v,t) v^2. \tag{9}$$

Under the approximations (to be justified later in §4)

$$\mu N \ll \beta \qquad \text{and} \qquad \theta(\langle v^2 \rangle - V^2) \ll hN$$

and ignoring the quantity hN, we get the familiar equation

$$M(dV/dt) + B_0 V = b\sigma_a. \tag{10}$$

(See Gilman 1968a, 1969 for more explanations.)

As it turns out the quantity hN is not necessarily small compared to f when N is large

(see table 1). Then a better approximation to equation (8) would be the equation

$$M(\mathrm{d}V/\mathrm{d}t)+B_0V=b\sigma_a-hNM\equiv b(\sigma_a-\sigma_i)\equiv b\sigma_d. \tag{11}$$

The quantity

$$\sigma_i\equiv hNM/b\equiv f_iM/b \tag{12}$$

is to be identified with the internal stress in the sample and σ_d with the effective driving stress. The steady state solution of equation (11) is

$$V=\frac{b\sigma_d}{B_0}=\frac{b(\sigma_a-\sigma_i)}{B_0}=\frac{f-hN}{\beta}. \tag{13}$$

In the following we argue that the time constant $\tau_1=\beta^{-1}$ is small. Roughly, the minimum value of β, $\beta_{\min}$, can be estimated by considering the lower limit of σ_d, namely the threshold stress σ_T of the material (Gilman and Johnston 1962) and the upper limit of V, i.e. the velocity of sound, V_{sound}. This leads to

$$\beta_{\min}=b\sigma_T/MV_{\text{sound}}\sim 10^9\ \mathrm{s}^{-1}.$$

(We have used a typical value $\sigma_T\sim 10^7$ dyn cm^{-1}.) The upper limit of β is set by the Debye frequency. This means that τ_1, the time constant for dislocations to attain a steady velocity is small (Gilman 1968a, 1969). Thus we have a natural expansion parameter β^{-1}.

In contrast to the above short time scale in the problem, there is another time scale which is large and is associated with the growth of N. This should be physically easy to see, since the growth of N corresponds to the duration of deformation. If we assume that a larger time scale associated with N exists, then we can use equation (13) in equation (7) to obtain

$$\mathrm{d}N/\mathrm{d}t=(-\alpha+B_1\theta)N-\mu N^2-(h\theta/\beta)N^2 \tag{14}$$

where $B_1=f/\beta$. The solution is

$$N=N_{s1}\{1+(N_{s1}/N_0-1)\exp[-(B_1\theta-\alpha)t]\}^{-1} \tag{15}$$

where

$$N_{s1}=(B_1\theta-\alpha)\beta/(\mu\beta+h\theta) \tag{16}$$

and $N_0\equiv N(t=0)$. Using the values of $V\simeq B_1$, and θ from table 1, we see that

$$\tau_2=(-\alpha+B_1\theta)^{-1}\sim 10\ \mathrm{s}\gg\tau_1.$$

Also note that if we take $\alpha=0$, and since $f\lesssim\beta$

$$\tau_2=f\theta\tau_1\gg\tau_1.$$

Thus the quantity occurring on the right-hand side of equation (13) in fact represents its instantaneous value, and every time N changes, V reaches its steady value in a time τ_1 so small that V and N are always in phase.

3. The distribution function

Equation (5*a–c*) cannot be solved exactly. In this section we calculate the moments/cumulants of $\rho(r,t)$ in an approximate manner. In addition to the boundary conditions

(6), we need to prescribe the initial condition for $\rho(v,t)$ at the time $t=t_0$, when a constant stress σ_a is applied. We note that for time $t\sim t_0+\tau_1$, the sources and sinks do not operate as τ_1 is so small and N remains practically at its initial value $N_0(=N(t_0))$. For such short times we shall therefore set $S=0$; then the asymptotic solution of equation (5*a*,*b*) is well known (Wang and Uhlenbeck 1945)

$$\rho(v_0)=\frac{N_0}{(2\pi q/\beta)^{1/2}}\exp\left(-\frac{\beta}{2q}(v_0-B_1)^2\right)\qquad(t\ll\tau_2). \tag{17}$$

Note that just before the start of the creep test, i.e. for $t\leqslant t_0$, $B_1=0$ (as $f=0$), and the distribution $\rho(v_0)$ is centred around $v_0=0$. More generally however, one has $v_0\neq 0$, and

$$\lim_{t\to t_0}\rho(vt\,|\,v_0t_0)\to N_0\delta(v-v_0). \tag{18}$$

We use the method of Fourier transform to obtain a solution of characteristic function $\chi(\omega,t)$ of $\rho(v,t)$ given by equation (A1) in powers of ω for small ω, which is sufficient, as we wish to calculate only the cumulants by using equation (A13). The details are given in the appendix. Using equation (A15) in (A10) we get

$$\chi(\omega,t)=N_s/Z(\omega,t) \tag{19}$$

with

$$\begin{aligned}Z(\omega,t)=\psi^\eta[(N_s/N_0)\exp(-\theta v_0/\beta)-1]\exp(\mathrm{i}B\omega+C\omega^2)\\ +1+\gamma\omega+\delta\omega^2+\nu\omega^3+\xi\omega^4+\mathrm{O}(\omega^5,\beta^{-1})\\ \psi=\exp[-\beta(t-t_0)]\end{aligned} \tag{20}$$

and

$$N_s=N(t\to\infty)=\eta\beta^2/(h\theta+\mu\beta).$$

All the other constants are given in the appendix. We obtain by setting $\omega=0$ in $\chi(\omega,t)$,

$$N=N(t-t_0)=N_s\{1+\psi^\eta[(N_s/N_0)\exp(-\theta v_0/\beta)-1]\}^{-1}. \tag{21}$$

The moments are calculated by using equation (A13). We quote the first four cumulants:

$$k_1=\langle v\rangle=V=B-(h/\beta)N. \tag{22}$$

$$k_2=2C-(h/\beta)NV. \tag{23}$$

$$k_3=-(h/\beta)N\langle v^2\rangle. \tag{24}$$

$$k_4=-(h/\beta)N\langle v^3\rangle. \tag{25}$$

Equation (22) is our main result—i.e. the average velocity of dislocations decreases linearly with N during creep. This result is applied to the velocity-shift experiment in §5. The dispersion k_2 given by equation (23) also decreases with the passage of time. As k_3 is negative, ρ is of negative skew type and hence it has a sharp leading edge. In addition, k_4 is also negative, thus contributing an additional platykurtic character (i.e. concentration of area around the mean value with a flat top). The combined effect is a distribution having sharp edges on both sides, but the leading edge is sharper than the trailing edge (Kendall and Stuart 1969).

Our earlier remark that $\rho(vt\,|\,v_0t_0)$ is equivalent to $\rho(v,t,t_0)$ is transparent from the expression for N (equation (21)). N contains information about the initial velocity v_0 only through the factor $\exp(-\theta v_0/\beta)$ which is essentially unity, as $\beta\gg 1$. It depends on

the initial state only through N_0, i.e. the value of N at t_0. All cumulants depend on the initial state only through N which in turn depends on N_0.

We now remove the deficiencies in our earlier derivations of equations (7) and (13). The first cumulant $k_1 = V$ (equation (22) with B defined by equation (A7)) shows that the quantitity B_1 occurring in equations (14) and (15) and in equation (17) is to be replaced by $B = B_1 + (q\theta/\beta^2)$. In fact the correct equation corresponding to equation (14) is obtained by differentiating N as given by equation (21). Note that the difference between B and B_1 is $q\theta/\beta^2 = 2C\theta/\beta$ which is negligible due to the factor β^{-1}. This is because $2C$ is the dispersion and is of the order of B^2.

4. The creep law and its application to LiF

In order to obtain the creep law, we need $\langle|v|\rangle$ and not $\langle v\rangle$. This cannot be obtained easily from $\chi(\omega,t)$. From the discussion about the general form of $\rho(v,t)$, it is clear that the spill-over to the negative region of velocity should be expected to be small (see also §6). Thus, we approximate $\langle|v|\rangle$ to $\langle v\rangle$ and use it in equation (2) along with equations (21) and (22). Integrating the strain rate with respect to t, with the initial conditions $\varepsilon(t_0)=0$, we obtain the following creep law:

$$\varepsilon(t-t_0) = bN_s\left(B-\frac{h}{\beta}N_s\right)(t-t_0) + \frac{bN_s}{\eta\beta}\left(B-\frac{h}{\beta}N_s\right)\ln\left(\frac{N_0}{N}\right) + \frac{hb}{\theta h+\mu\beta}(N-N_0). \qquad (26)$$

This creep law is very similar to Webster's (1966) second creep law (his equation (14)). It differs from his equation in the following way: the saturation value of dislocation density in equation (26) is given by

$$N_s = (B\theta-\alpha)\beta/(h\theta+\mu\beta)$$

where α corresponds to the stopping of dislocations at precipitates, grain boundaries etc. In Webster's law, this rate of loss is assumed proportional to the dislocation velocity—in other words this process has been included along with the breeding term. However, if we set $\alpha=0$ in the expression for N_s in equation (26) and also set the corresponding (velocity-dependent) loss term in his equation, then our creep law is identical to his.

We now apply equation (26) to creep in LiF (Johnston 1962). Among the parameters occurring in the creep law, only h is adjustable. Consider creep at $\sigma_a = 380$ g mm^{-2} for which $B = 3.033\times10^{-3}$ cm s^{-1} (see table 1). We have calculated creep in two ways. In the first case (case 1) we have assumed $\alpha=0$ and $\mu\neq0$, and in the second (case 2) $\alpha\neq0$ and $\mu=0$. The values of N_0 chosen in both cases fall within the range quoted by Gilman and Johnston (1962). N_s, as determined by the near saturation value of ε (see equation 26), is $\sim10^7$ cm^{-2}. As V is always positive, we must have $(h/\beta)N_s \leqslant B$. Our calculation of creep curves for cases 1 and 2, presented in figures 1 and 2 respectively, shows excellent agreement with Johnston's (1962) experimental data. For case 2, the value of α is obtained from the relations

$$\gamma = \alpha/B\theta \qquad N_s = (1-\gamma)B\beta/h.$$

One observes transient creep (TC) when there appears a point of inflection on the ε–t curve. Let t_1 be the time of inflection and let ε_1, N_1 and V_1 denote the corresponding values of ε, N and V. From the condition $\ddot{\varepsilon}(t_1)=0$, one obtains $N_1 = B\beta/2h$. Four different classes of creep curves result: (1) if $N_0 < N_1 < N_s$, TC is observed (figure 1, curves B and C); (2) if $N_1 < N_0 < N_s$, N_0 is so large that there is no incubation time for creep

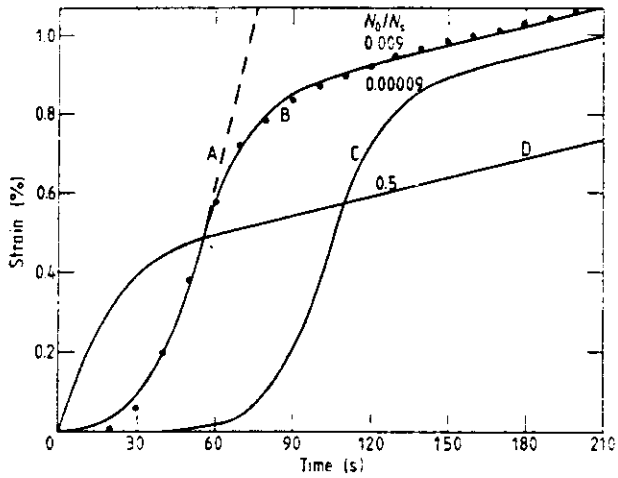

Figure 1. Calculated and experimental creep curves for case 1. Variation with respect to N_0 is also shown. $N_s = 8.4 \times 10^6$ cm^{-2}, $\mu \neq 0$, $\alpha = 0$, $h/\beta = 3.535 \times 10^{-10}$ cm^3 s^{-1}; ——— theory; ● experiment.

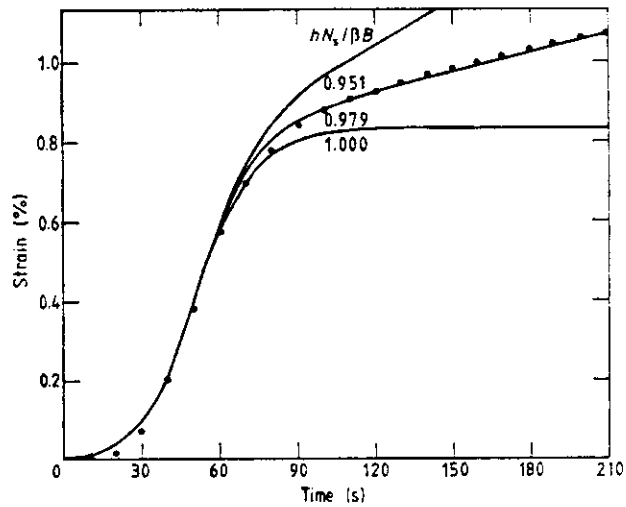

Figure 2. Calculated and experimental creep curves for case 2. Variation with respect to h/β is also shown. $N_0 = 7.5 \times 10^4$ cm^{-2}, $N_s = 8.4 \times 10^6$ cm^{-2}, $\mu = 0$, $\alpha \neq 0$, $\alpha/\beta\theta = 0.02$, $h/\beta = 3.45 \times 10^{-10}$ cm^3 s^{-1}; ——— theory; ● experiment.

and hence no TC is observed (figure 1, curve D); (3) if $N_0 < N_s < N_1$, TC appears as $N_0 < N_1$, but the point of inflection receeds to 'infinity' (figure 1, curve A); (4) if $N_1 < N_0 = N_s$, only secondary creep is exhibited, and $N(t) = N_s$ for all t. The case $N_0 = N_s < N_1$ is similar to this. (This is not shown in figure 1.)

Creep is not as sensitive to changes in α and μ as it is to h/β. The variation of creep with the dimensionless parameter $hN_s/\beta B$ is indicated in figure 2.

We now show that the linear N–ε relation follows from equation (26). At any time t, consider this equation for various stresses. Then we obtain a linear relation between

$N(\sigma_a)$ and $\varepsilon(\sigma_a)$. We may rewrite equation (26) as

$$\varepsilon = -\frac{bN_s}{\eta\beta}\left(B-\frac{h}{\beta}N_s\right)\ln\left(\frac{N_s-N}{N_s-N_0}\right)+\left(\frac{bh}{h\theta+\mu\beta}\right)(N-N_0). \tag{27}$$

For N not too close to N_s, the dominant term in the right-hand side of this equation is linear in N.

Previously (§2) we had assumed that $\mu N \ll \beta$ and $\theta[\langle v^2\rangle - V^2] \ll hN$. Below we show that these relations are valid. The first one follows from $N < N_s$. This implies that

$$\mu N/\beta < (B\theta-\alpha)/\beta - h\theta N/\beta^2 \ll 1.$$

To see the second, it is reasonable to assume that the dispersion

$$\langle v^2\rangle - V^2 \sim 2C \sim B^2.$$

Although V reduces monotonically, as for the order of terms

$$B \sim (h/\beta)N \sim [\langle v^2\rangle - V^2]^{1/2}.$$

As $\beta \gg 1$, we have

$$hN \gg [v^2 - V^2]^{1/2}.$$

Noting that in our theory $B \sim f/\beta \leqslant 1$, we have

$$[\langle v^2\rangle - V^2]^{1/2} \lesssim 1.$$

Therefore

$$hN \gg \theta[\langle v^2\rangle - V^2]^{1/2}.$$

Further justification can be found in table 1, where we have listed the values of the various parameters for the creep case considered.

5. Velocity reduction in strained crystals

According to the experiment of Gilman and Johnston (1962) involving the stress-pulse technique of measuring V, the graph for the unstrained and strain-hardened ($\sim 0.1\,\%$) samples of LiF are shifted with respect to each other. The values in these samples were respectively $N(\text{unstrained}) \sim 10^4$ and $N(\text{strained}) \sim 5 \times 10^6\ \text{cm}^{-2}$. From equation (22) one obtains the following relations between the velocities $V(\text{strained})$ and $V(\text{unstrained})$ in the two crystals:

$$V(\text{strained}) = V(\text{unstrained}) - (h/\beta)\,[N(\text{strained}) - N(\text{unstrained})]$$

$$R \equiv \frac{V(\text{strained})}{V(\text{unstrained})} \approx 1 - \frac{h}{\beta}\frac{N(\text{strained})}{V(\text{unstrained})}.$$

(Here $N(\text{unstrained})$ has been neglected compared to $N(\text{strained})$.) Since the values of V, N, σ_a and ε pertaining to creep at $t \sim 210$ s (see §4) are in the range covered by the present case, we use $N(\text{strained}) \approx N_s$ and $V(\text{unstrained}) \approx B$ and obtain (using table 1) $R \approx 0.02$. From the results of Gilman and Johnston (1962), $R \approx 0.001$. Thus there is order-of-magnitude agreement.

A few more comments will be made. As σ_i is proportional to $N(t)$, it has the same time dependence as $N(t)$. It starts almost from zero value, saturates during secondary

creep. The driving stress

$$\sigma_d = \sigma_a - [N(t) - N_0]hM/b \tag{28}$$

has the same functional form as that of the velocity V. It is at its maximum initially, and attains a constant value as $N \to N_s$, during secondary creep. After N saturates, the strain rate becomes constant. Equation (28) also provides insight into the situation prevailing in a tensile test. Kocks *et al* (1975) made the observation that the inference drawn from the secondary creep region is equally applicable to conditions during a tensile test which corresponds to the same strain rate. Let σ_a' and σ_i' respectively be the stress sensed by the load cell and the internal stress developed in the specimen during a tensile test. The quantity corresponding to σ_d in this experiment is $\sigma_d' \equiv \sigma_a' - \sigma_i'$. As σ_d is constant during secondary creep, one would expect σ_d' to remain so during a tensile test. This is in fact confirmed by the stress relaxation data for LiF obtained by Gupta and Li (1970)—see their figure 8.

6. Discussion

The main result of our theory is the derivation of the evolution of the internal stress σ_i (equation (12)) during creep of materials like LiF. Our theory unifies several well known phenomenological relations; these are expressed by equations (10) and (12–14). It leads to a creep law (equation (26)) in excellent agreement with the experimental data on LiF, and it explains successfully the reduction of the velocity of dislocations in strained crystals of LiF. There are no data available to check the expressions for the cumulants (equations (22–25)) of the velocity distribution.

The distribution, strictly speaking, should be bimodal. The absence of this correct feature in our present calculation is due to the unsatisfactory way in which we have modelled the f and the θ terms to help us obtain the solution. However, we argue below that the actual distribution should be very nearly the one obtained by appending to the present $\rho(v,t)$ (for $v \geqslant 0$) its mirror reflected part $\rho(-v,t)$. To see this, consider the contribution to $\partial\rho/\partial t$ arising due to the f term alone. This should have the form

$$-f\frac{b_+}{|b|}\frac{\partial}{\partial v}[\rho(v)\Theta(v)] - f\frac{b_-}{|b|}\frac{\partial}{\partial v}[\rho(v)\Theta(-v)]$$
$$= -f\frac{\partial}{\partial v}[\rho(v)\Theta(v) - \rho(v)\Theta(-v)] \tag{29}$$

where $\Theta(v) = +1$ for $v \geqslant 0$ and zero otherwise. In a similar way the breeding term should contribute equally to positive and negative dislocations. We retain all other terms which include interaction between dislocations as they have been correctly modelled. Then we have the equation

$$\frac{\partial\rho(v,t)}{\partial t} = -\alpha\rho(v) + \beta\frac{\partial}{\partial v}(v\rho(v)) + q\frac{\partial^2\rho(v)}{\partial v^2} + [\Theta(v) - \Theta(-v)]\,\theta v\rho(v)$$
$$-f\frac{\partial}{\partial v}[(\Theta(v) - \Theta(-v))\rho(v,t)] - \mu\int_{-\infty}^{\infty}\rho(v-v',t)\rho(v',t)\,dv'$$
$$+h\int_{-\infty}^{\infty}\rho(v-v',t)\frac{\partial\rho(v',t)}{\partial v'}\,dv'. \tag{30}$$

We now show that the solution of the above equation is essentially the same as the earlier

one except that it is bimodal. To see this, consider only the β, f and q terms. Without the f term the solution is a Gaussian centred around the origin. Including the f term changes the nature of the solution to a bimodal form.† With these terms $\rho(-v,t)$ satisfies the same equation as $\rho(v,t)$ (with the same initial conditions). Thus

$$\rho(v,t)=\rho(-v,t).$$

Using this and defining

$$\chi_c=\int_0^\infty \rho(v,t)\cos(\omega v)\,dv$$

after some algebra, we get

$$\frac{\partial \chi_c}{\partial t}=\beta\omega\frac{\partial \chi_c}{\partial \omega}+if|\omega|\chi_c-q\omega^2\chi_c. \tag{31}$$

Clearly, this leads to a bimodal distribution with the peaks appearing asymptotically at

$$\langle|v|\rangle=\pm f/\beta.$$

Now consider the effect of including other terms except the μ and the h terms. All these terms are symmetric in v. *Thus the addition of these terms does not destroy the bimodal nature.* The μ term also gives a symmetrical contribution. To see this, consider this term in the Fourier transformed space, i.e. consider the term $-\mu\chi^2(\omega)$. If

$$\rho(v,t)=\rho(-v,t)$$

then

$$\chi(\omega,t)=\chi(-\omega,t)$$

and vice-versa, thus proving our assertion. The contribution from the h term is

$$ih\omega\chi^2(\omega).$$

Changing $v\to -v$ corresponds to changing

$$ih\omega\chi^2(\omega)\to -ih\omega\chi^2(-\omega).$$

Thus the h term makes opposing contributions for $v\to -v$, which still retains the symmetry of $\rho(v,t)$ about the origin. On the basis of present calculation, we recognise that the time variations of all cumulants arise from the h term, in particular, k_3 and k_4 becoming progressively negative. Since the h term in equation (30) also contributes in the same way as it did to equation (5), the bimodal distribution should have sharp edges on both sides.

To see the relationship of this distribution to the one governed by equation (5), it is fair to assume the same *initial* density of positive and negative dislocations. Let

$$\int_{-\infty}^0 \rho(v,t)\,dv=N_-(t)$$

and

$$\int_0^\infty \rho(v,t)\,dv=N_+(t).$$

Then the above statement means $N_-(0)=N_+(0)$. With the evolution of time, the equality of the densities N_+ and N_- is maintained except for the fact that the contributions due to μ and h terms to N_+ and N_- are negative. In addition, the h term has the effect of moving

† Note that the bimodal form arises only due to the f term.

both the edges towards the origin. For this reason, it is clear that the bimodal distribution should have the form $\rho(v,t)$ that we obtained as a solution to equation (5) for $v \geqslant 0$ and should have in addition, a mirror-reflected part for $v \leqslant 0$. (Note that $N=2N_+=2N_-$, i.e. the areas under the distribution to the left and to the right of the origin are equal.) We therefore feel that the present calculation does indeed represent the physical situation quite well.

Finally we wish to mention one curious fact regarding the last term in S (equation (5*c*)) relating to the internal stress field. As is clear by now, the relation $\sigma_i \sim N$ is a consequence of the term

$$h \int_{-\infty}^{\infty} dv' \rho(v-v',t) \partial\rho(v',t)/\partial v'.$$

One might suspect that other complex terms in ρ may lead to different relations for the internal stress. We were however unable to find any other suitable forms in ρ. For example the form

$$\mu \int_{-\infty}^{\infty} dv' \rho(v-v') \exp[-(h/\mu)\partial/\partial v']\rho(v')$$

leads to a constant internal stress which is unphysical. *It appears that it is difficult to postulate terms which lead to the more common form* $\sigma_i \sim N^{1/2}$. It may be necessary to modify the continuity equation from, say, a two-particle distribution function to a multiparticle one. The reason lies in the fact that the present approach leads only to σ_i proportional to a power of N (by including more convolutions). However, it is unreasonable to expect a nonanalytic function $N^{1/2}$ to be derivable from any finite sequence involving powers of N.

Acknowledgments

We thank Dr JJ Gilman for his reply to our queries, Dr PRodriguez for many useful discussions, Dr GVenkataraman for arousing our interest in this field, and Dr V Balakrishnan for reading the manuscript. We are thankful to the referee for his valuable comments on equation (5).

Appendix

Introducing the characteristic function of $\rho(v,t)$

$$\chi(\omega,t)=\int_{-\infty}^{\infty} dv\, \rho(v,t) \exp(-iv\omega) \tag{A1}$$

and using it in equation (5), we get

$$\frac{\partial\chi}{\partial t} = -(\alpha+i\omega f+q\omega^2)\chi-(\beta\omega-i\theta)\frac{\partial\chi}{\partial\omega}-(\mu-ih\omega)\chi^2. \tag{A2}$$

The first independent solution is

$$(\omega-i\theta/\beta)\exp(-\beta t)\equiv(\omega-i\theta/\beta)\varphi(t)=C_1' \tag{A3}$$

where C_1' is a constant. The second independent solution can be written in the form

$$\chi^{-1}(\omega)=(I(\omega)+C_2')\exp\left(\int^{\omega}d\omega'\frac{(\alpha+if\omega'+q\omega'^2)}{\beta\omega'-i\theta}\right) \tag{A4}$$

where C_2' is a constant, and

$$I(\omega)=\left(\frac{\mu}{\beta}+\frac{h\theta}{\beta^2}\right)I_{\eta-1}(\omega)-\frac{ih}{\beta}I_{\eta}(\omega) \tag{A5}$$

with

$$I_{\eta-m}(\omega)\equiv\int^{\omega}d\omega'(\omega'-i\theta/\beta)^{\eta-m}\exp(-iB\omega'-C\omega'^2) \qquad m=0,1. \tag{A6}$$

In the above equations

$$B=(f/\beta)+(q\theta/\beta^2) \tag{A7}$$

$$C=q/2\beta \tag{A8}$$

and

$$\eta=(-\alpha+B\theta)/\beta. \tag{A9}$$

Eliminating C_1' and C_2' from equations (A3, A4) and using the initial condition (18) we get

$$\chi^{-1}(\omega,t)=N_0^{-1}\psi^{\eta}\exp[i\omega_{\psi}t_0-iB(\omega_{\psi}-\omega)-C(\omega_{\psi}^2-\omega^2)]+J_{\psi}(\omega)\exp(iB\omega+C\omega^2) \tag{A10}$$

where

$$J_{\psi}(\omega)=(\omega-i\theta/\beta)^{-\eta}[I(\omega)-I_{\psi}(\omega)] \tag{A11}$$

with $I_{\psi}(\omega)$ standing for $I(\omega)$ (equation A5) with ω replaced by

$$\omega_{\psi}=\omega\psi+i(\theta/\beta)(1-\psi) \qquad \psi=\varphi(t)/\varphi(t_0)$$

in the limit of the integral. J_{ψ} contains the integral

$$I_{\eta-m}(\omega)-I^{\psi}_{\eta-m}(\omega)=\int_{\omega_{\psi}}^{\omega}d\omega'(\omega'-i\theta/\beta)^{\eta-m}\exp[-iB\omega'-C\omega'^2]. \tag{A12}$$

As $\eta>0$ and is not an integer, the above integral cannot be carried out exactly. As we are interested in obtaining only the first few moments, given by

$$N\langle t^n\rangle=i^n(\partial^n\chi/\partial\omega^n)_{\omega=0} \tag{A13}$$

it is sufficient to attempt a power series solution in ω. It is clear that around $\omega=0$, the exponential varies slowly with ω, and a dominant contribution of ψ^{η} arises from $(\omega-i\theta/\beta)^{\eta-m}$ near the lower limit (for $m=1$). Thus the larger time scale emerges naturally as the η power of ψ. Performing a series of partial integrations, we get

$$\begin{aligned}I_{\eta-m}(\omega)-I^{\psi}_{\eta-m}(\omega)&=\sum_{k=0}^{l}(-)^k\frac{(\omega'-i\theta/\beta)^{\eta-m+k+1}}{(\eta-m+1)(\eta-m+2)\ldots(\eta-m+k+1)}\\&\times\frac{d^k}{d\omega'^k}\exp(-iB\omega'-C\omega'^2)\Big|_{\omega_{\psi}}^{\omega}-\frac{(-)^l}{(\eta-m+1)(\eta-m+2)\ldots(\eta-m+l+1)}\\&\times\int_{\omega_{\psi}}^{\omega}d\omega'(\omega'-i\theta/\beta)^{\eta+l-m+1}\frac{d^{l+1}}{d\omega'^{l+1}}\exp(-iB\omega'-C\omega'^2).\end{aligned} \tag{A14}$$

We have two small parameters β^{-1} and ψ. Using equation (A14) in (A11), and dropping all power of ψ larger than one and of β^{-1} larger than two, the expression for J_ψ up to ω^4 is

$$J_\psi(\omega) = -N_s^{-1} K_0 \psi^\eta + N_s^{-1} \exp(-iB\omega - C\omega^2) \times (1 + \gamma\omega + \delta\omega^2 + \nu\omega^3 + \xi\omega^4) + O(\beta^{-2}, \psi, \omega^5) \tag{A15}$$

where

$$K_0 = \exp[(B\theta/\beta) + (C\theta^2/\beta^2)] \simeq 1 \tag{A16}$$

$$N_s = \eta\beta^2/(\mu\beta + h\theta) \tag{A17}$$

$$\gamma = \frac{iB}{\eta+1} - i\frac{h}{\beta}\frac{N_s}{\eta+1} \tag{A18}$$

$$\delta = \frac{2C}{\eta+2} - \frac{B^2}{(\eta+1)(\eta+2)} + \frac{h}{\beta}\frac{BN_s}{(\eta+1)(\eta+2)}. \tag{A19}$$

The expressions for ν and ξ are cumbersome, and are therefore not given here. However, expressions for up to the fourth moment, which involve ν and ξ, have been given in the text.

References

Feltham P 1968 *Phys. Stat. Solidi* **30** 135

—— 1973 *J. Phys. D: Appl. Phys.* **6** 2048

Gilman J J 1968a *Appl. Mech. Rev.* **21** 767

—— 1968b *Dislocation Dynamics* eds A R Rosenfeld, G T Hahn, A L Bement and R I Jaffee (New York: McGraw-Hill) p 3

—— 1969 *Micromechanics of Flow in Solids* (New York: McGraw-Hill)

Gilman J J and Johnston W G 1960 *J. Appl. Phys.* **31** 687

—— 1962 *Solid State Physics* Vol. 13 ed F Seitz and D Turnbull (New York: Academic) p 148

Gupta I and Li J C M 1970 *Mater. Sci. Engng* **6** 20

Johnston W G 1962 *J. Appl. Phys.* **33** 2716

Kendall M G and Stuart A 1969 *The Advanced Theory of Statistics* Vol. 1 (London: Griffin) p 86

Kocks U F, Argon A S and Ashby M F 1975 *Progress in Materials Science* Vol. 19 eds B Chalmers, J W Christian and T B Massalski (Oxford: Pergamon)

Lagneborg R and Forsen R H 1973 *Acta Metall.* **21** 781

Li J C M 1963 *Acta Metall.* **11** 1269

Mott N F and Nabarro F R N 1948 *Report of a Conference on Strength of Solids* (London: The Physical Society) p 1

Ostrom D O and Lagneborg R 1976 *Trans. ASME* **H98** 114

Stratonovich R L 1963 *Topics in the Theory of Random Noise* (New York: Gordon and Breach)

Wang M C and Uhlenbeck G E 1945 *Rev. Mod. Phys.* **17** 323

Webster G A 1966 *Phil. Mag.* **14** 775

Welch D O and Smoluchowski R 1972 *J. Phys. Chem. Solids* **33** 1115

J. Phys. D: Appl. Phys., 14 (1981) 2091–100. Printed in Great Britain

A statistical theory of dislocation dynamics: II. Mathematical properties

G Ananthakrishna
Materials Science Laboratory, Reactor Research Centre, Kalpakkam 603 102, Tamil Nadu, India

Received 30 April 1981

Abstract. We investigate the mathematical properties of the statistical model for dislocation dynamics introduced in the context of creep. The situation corresponds to a nonstationary process in which all the cumulants depend on the density. Based on expressions derived for the first four cumulants via a series expansion derived in our earlier work, we derive an approximate form for the characteristic function. The solution is shown to be a good approximation. The distribution function is platykurtic in nature. The velocity autocorrelation function is also calculated.

1. Introduction

Recently (Ananthakrishna and Sahoo 1981, hereafter referred to as I) we proposed a statistical theory of dislocation dynamics in the context of creep and applied it to creep in LiF. (Creep is time-dependent yielding of material under constant applied stress.) Basically, the phenomenon is one where dislocations multiply, forming dipoles and forest dislocations (Gilman 1969). These in turn act as obstacles for mobile dislocations leading to a reduction in their average velocity V. Generally, for most materials, $V \sim (\sigma^*)^n$ where n is some suitable exponent and $\sigma^* = \sigma_a - A\sqrt{N}$ is the effective stress; σ_a is the applied stress, A a constant and N the total density of dislocations. However, there are simple materials like LiF for which a simpler relation $V = V_0 - AN$ is expected to hold reasonably well, at least for low levels of strain. Here V_0 is a constant for a given temperature and at a given σ_a (Webster 1966, Gilman 1969). Our objective was to construct a statistical theory for such simple materials as a first step in understanding plastic flow. Based on well known mechanisms operating in LiF (and materials like LiF) we wrote an extended Fokker–Planck equation (EFPE) for the conditional density with nonlinear and nonlocal sink terms. We obtained explicit expressions for the first four cumulants via a series expansion in terms of two small parameters. The EFPE has the general feature that all the moments (and the cumulants) depend on time through the total density, i.e. the zeroth moment, which is not conserved. Such a general feature of moments (or the distribution function) depending on time is known to arise in other situations (Clement 1978).

The purpose of this paper is to investigate some mathematical properties of the model introduced in I and to investigate the extent to which the approximation used earlier is valid. In §2 we present the EFPE and explain briefly the physical meanings of the various

0022-3727/81/112091+10 $01.50

terms in the differential equation in the context of creep. We modify some conventional relations in probability theory to accommodate the probability nonconservation. We also identify the initial state of the system. This is essential since the process considered is nonstationary. In §3 we summarise the results obtained in I, i.e. expressions for the first four conditional cumulants k_{nc}, ($n=1$ to 4). For $n=3$ and 4, we find that $k_{nc}=$const. $m_{(n-1)c}$ where m_{nc} is the nth conditional moment. This result suggests that the above relation may be valid for all $n\geqslant 3$. Assuming this relation to hold, we calculate the characteristic function in a closed form. The solution thus obtained satisfies the original differential equation for the characteristic function reasonably well. Some other properties are also investigated. The velocity autocorrelation function is also calculated.

2. The extended Fokker–Planck equation

The central role is played by the conditional probability density (CPD) $\rho(vt|v_0t_0)$ of finding dislocations having velocity v at time t given that they had a velocity v_0 at time t_0. The range of v is taken to be from $-\infty$ to ∞. (For more details see I.) The extended Fokker-Planck equation is

$$\frac{\partial \rho}{\partial t}(vt|v_0t_0)+\frac{\partial J}{\partial v}=S \tag{1a}$$

where

$$J=-(\beta v-f)\rho(vt|v_0t_0)-q\frac{\partial \rho}{\partial v}(vt|v_0t_0) \tag{1b}$$

and

$$S=-(\alpha-\theta v)\rho(vt|v_0t_0)-\mu\int_{-\infty}^{\infty}\mathrm{d}v'\,\rho(v-v',t|v_0t_0)\rho(v't|v_0t_0)$$

$$+h\int_{-\infty}^{\infty}\mathrm{d}v'\,\rho(v-v',t|v_0t_0)\frac{\partial \rho}{\partial v'}(v't|v_0t_0). \tag{1c}$$

The above equation reduces to the usual Fokker–Planck equation if $S=0$. The first term in J, in the context of dislocation dynamics and plastic flow, is related to the dislocation drag, the second to the applied stress and the third to velocity 'diffusion'. The first term in S (the term $-\alpha\rho$) corresponds to the rate at which dislocations of velocity v are stopped at fixed obstacles (e.g. precipitates, grain boundaries, etc). The second term ($\theta v\rho$) corresponds to the production of dislocations by multiple cross-glide (Gilman 1969). The third term represents the depletion of dislocations (monopoles) by pairwise interactions forming 'dipoles' (i.e., a pair of monopoles bound to each other). The last term corresponds to the changes in the distribution of velocities of dislocations due to their mutual interaction. (This term leads to the linear decrease of the average velocity.) This term also leads to change in the density as a function of time. (For detailed explanation of these terms, see I.)

All measurable quantities occur as ratios with respect to β ($\gg 1$), the largest being f/β. This quantity is very much larger than h/β, q/β, α/β and μ/β. However, the quantity $(h/\beta)N$, where N is the total density of dislocations can be comparable to f/β. Wherever there is a need to compare the orders of magnitude of various quantities appearing in our

calculations, we choose the values of these quantities from the physical case applied, namely creep in LiF (Johnston and Gilman 1959, and I). See table 1 where we have listed the values used in calculating the creep curve in I.

The reasons for considering the time evolution of the CPD is that for timescales of the order of β^{-1} the CPD is essentially Markovian and for timescales over which the non-

Table 1. Values of parameters used in calculation of the creep curve for LiF for $\sigma_a = 380$ g mm^{-2}.

Parameter	Value
$B \simeq f/\beta$	3.03×10^{-3} cm s^{-1}
θ	30 cm^{-1}
β	10^9 s^{-1}–10^{13} s^{-1}
α	1.82×10^{-3} s^{-1}
μ	2.271×10^{-10} cm^2 s^{-1}
h/β	3.535×10^{-10} cm^3 s^{-1}
Ns	8.4×10^6 cm^{-2}
N_0	7.5×10^4 cm^{-2}
$2C = q/\beta$	B^2

conservative effects become operative the process essentially becomes a purely random process, i.e. all joint distributions factor into products of the single-variable but non-stationary distributions. Thus in both cases it is sufficient to consider the CPD to describe the process.

Since the process is nonstationary, we have to identify the initial state of the system in order to be able to calculate the final state and the joint probability density (JPD) $\rho(vt; v_0t_0)$. Further, some well known relations of probability theory have to be modified in order to deal with the present problem where the probability is not conserved. The initial state of the system is characterised by the absence of source and sink terms in the equation for the CPD (i.e. $S=0$ in equation (1)). In this case the $t \to \infty$ solution determines the initial distribution of the actual problem, i.e. when S is present. We define

$$\int \rho(v_0)\, dv_0 \equiv N_0 \tag{2}$$

the total (dislocation) density at time t_0:

$$\begin{aligned} \bar{N}_0 \rho(v, t, t_0) &\equiv \int \rho(vt \mid v_0 t_0)\, \rho(v_0, t_0)\, dv_0 \\ &\equiv \int \rho(vt; v_0 t_0)\, dv_0 \end{aligned} \tag{3}$$

and

$$\int \rho(v, t, t_0)\, dv \equiv N(t, t_0) \tag{4}$$

the total density at time t. $\bar{N}_0$ is in principle different from N_0. The deviation of $\bar{N}_0$ from N_0 may be considered as a measure of correlation between the states at v, t and v' t' (see discussion). The initial probability density $\rho(v_0)$ occupies a very special status in our problem since it is at $t = t_0$ that the stress is applied. It is due to this fact that the state at any later time t is fixed by both $\rho(v_0)$ and $\rho(vt; v_0t_0)$. (Note that there is no loss of generality in defining $\rho(v, t, t_0)$ in the above fashion.) However, for calculating a general JPD

for any two arbitrary times $\rho(v', t'; vt)$ $(t_0 < t < t')$, one has to first obtain $\rho(v, t, t_0)$ from equation (3) and use

$$\rho(v't'; vt) \equiv \rho(v't'|vt)\rho(v, t, t_0). \tag{5}$$

We also define the conditional density by

$$\int \rho(vt|v_0t_0)\,dv \equiv N_c(t, t_0). \tag{6}$$

Note that the quantity $N_c(t, t_0)$ is a function of v_0 which has been suppressed.

It is worth emphasising that we are departing from the conventional probability density (Stratonovich 1963) in the following respects:

(i) The probability is not conserved, i.e.

$$\frac{d}{dt}\int \rho(v, t|v_0t_0)\,dv = \frac{dN_c}{dt}(t, t_0) \neq 0.$$

(ii) The JPD does not obey the symmetry relation, i.e.

$$\rho(v't'; vt) \neq \rho(vt; v't').$$

(iii) Although

$$\int dv_0\,\rho(vt; v_0t_0) = \bar{N}_0\rho(v, t, t_0)$$

$$\int dv\,\rho(vt; v_0t_0) \neq N(t, t_0)\rho(v_0t_0) \qquad (t_0 < t)$$

(iv) For $t_0 < t < t'$

$$\int dv\rho(v't'; vt) \neq N(t, t_0)\rho(v', t', t).$$

However, these relations simplify under a decoupling approximation (see discussion). In order to solve equation (1), we use physically reasonable boundary conditions for large v, namely

$$\lim_{v \to \pm\infty} \quad \rho(vt|v_0t_0) \to 0$$

$$\lim_{v \to \pm\infty} \quad \frac{\partial\rho}{\partial v}(vt|v_0t_0) \to 0 \tag{7}$$

and

$$\lim_{v \to \pm\infty} \quad v\rho(vt|v_0t_0) \to 0.$$

We also make use of the initial condition

$$\lim_{t \to t_0} \quad \rho(vt|v_0t_0) = N_0\delta(v - v_0). \tag{8}$$

2.1. Initial probability density

As stated earlier the initial density $\rho(v_0)$ would first be required. The identification of the initial state of the system can only be done by physical considerations. The distribu-

tion $p(v_0)$ is the one induced under the action of applied stress during a time which is short compared to the time for the source and sink terms to become operative. Under these conditions, the probability is conserved. To avoid confusion we shall use a different symbol $p(vt|v_1t_1)$ for the CPD when $S=0$. The solution can be easily obtained (Wang and Uhlenbeck 1945) and is

$$p(vt|v_1t_1)=(4\pi c_1)^{-1/2}\exp\left[-(v-B_1)^2/4c_1\right] \tag{9}$$

where

$$B_1(t)=v_1\psi+(f/\beta)(1-\psi) \tag{10}$$

is the conditional average velocity

$$c_1=(q/2\beta)(1-\psi^2) \tag{11}$$

and

$$\psi=\exp\left[-\beta(t-t_1)\right]. \tag{12}$$

The initial state of the system is then represented by taking the limit $t-t_1\to\infty$, except for a normalisation factor which corresponds to the initial density N_0 of the dislocations. Thus

$$p(v_0)=N_0\left(\frac{2\pi q}{\beta}\right)^{-1/2}\exp\left[-\frac{\beta}{2q}\left(v_0-\frac{f}{\beta}\right)^2\right]. \tag{13}$$

3. An approximate solution of the EFPE

In this section, we summarise the results obtained in I via a power-series solution in terms of two small parameters β^{-1} and ψ (see table 1). We then examine the extent to which the approximation is valid. The characteristic function is defined by

$$\chi(\omega, t, v_0t_0)=\int_{-\infty}^{\infty}dv\,p(vt|v_0t_0)\exp(i\omega v). \tag{14}$$

For simplicity of notation, we shall suppress v_0 and t_0 in χ. Using equation (14) in equation (1), we get

$$\frac{\partial\chi}{\partial t}=-(\alpha+i\omega f+q\omega^2)\chi-(\mu-ih\omega)\chi^2-(\beta\omega-i\theta)\frac{\partial\chi}{\partial\omega}. \tag{15}$$

We have obtained closed-form expressions for the first four cumulants via a power-series expansion in ω using

$$N_c\langle v^n\rangle_c=i^n\left(\frac{\partial^n\chi}{\partial\omega^n}\right)_{\omega=0}. \tag{16}$$

We summarise the results here:

$$N_c(t, t_0)=N_S\{1+\psi^n k_0[(N_S/N_0)\exp(-\theta v_0/\beta)-1]\}^{-1} \tag{17}$$

with $k_0\simeq 1$

$$k_{1c}=\langle v\rangle_c=B-(h/\beta)N_c \tag{18}$$

$$k_{2c}=2C-(h/\beta)N_c\langle v\rangle_c \tag{19}$$

where

$$N_s = \eta\beta^2/(\mu\beta + h\theta) \tag{20}$$

$$\eta\beta = B\theta - \alpha \tag{21}$$

$$B = (f/\beta) + (q\theta/\beta^2) \tag{22}$$

and

$$C = (q/2\beta). \tag{23}$$

The subscript c in the above quantities refer to averaging with respect to the conditional density. The third and the fourth cumulants are given by

$$k_{3c} = -(h/\beta) N_c \langle v^2 \rangle_c \tag{24}$$

and

$$k_{4c} = -(h/\beta) N_c \langle v^3 \rangle_c. \tag{25}$$

Calculation of higher cumulants is rather cumbersome and has not been carried out. The above equations (24) and (25) strongly suggest that within the approximation with which these expressions have been calculated, the following relation may hold even for $n > 4$.

$$k_{nc} = -(h/\beta) N_c m_{(n-1)c} \tag{26}$$

where m_{nc} is the nth conditional moment. If we assume that equation (26) is valid along with equations (17–19), (24) and (25) then we can obtain the characteristic function χ_A which should be expected to hold at least approximately. This χ_A would satisfy a differential equation. This can be compared with the original differential equation (15) for the true χ to determine the extent to which the approximation is valid.

By definition

$$\frac{\chi}{N_c} = 1 + \sum_1^\infty \frac{(i\omega)^n}{n!} m_{nc} = \exp\left(\sum_1^\infty \frac{(i\omega)^n}{n!} k_{nc}\right). \tag{27}$$

The factor N_c would be necessary in order to satisfy $\chi(0, t) = N_c(t)$. Using equations (17–19) and (24–26) in equation (27), we get a differential equation for χ_A

$$\frac{\partial \chi_A}{\partial \omega} = -(iB + 2C\omega)\chi_A + i(h/\beta)\chi_A^2. \tag{28}$$

The solution of this equation with the initial condition that at $\omega = 0$, $\chi(0, t) = N_c(t)$, is

$$\chi_A(\omega, t) = N_c F(\omega)/(1 - i(h/\beta) N_c \varphi(\omega) \tag{29}$$

where

$$F(\omega) = \exp(-iB\omega - C\omega^2) \tag{30}$$

and

$$\varphi(\omega) = \int_0^\omega F(\omega')\, d\omega'. \tag{31}$$

Using equations (20–23) and equation (28), we get

$$-(\beta\omega - i\theta)\frac{\partial \chi_A}{\partial \omega} - (if\omega + q\omega^2 + \alpha)\chi_A + ih\omega\chi_A^2 - \eta\beta\chi_A + (h\theta/\beta)\chi_A^2. \tag{32}$$

Comparing equation (32) with equation (15), we find that if a χ satisfies equation (28),

then it should also satisfy

$$\frac{\partial \chi}{\partial t}=\eta\beta\chi-\left(\frac{h\theta}{\beta}+\mu\right)\chi^2 \tag{33}$$

if it has to be a solution of equation (15). However, from equation (29), we find that χ_A instead satisfies

$$\frac{\partial \chi_A}{\partial t}=\frac{\eta\beta\chi_A}{1-i\,(h/\beta)\,N_c\varphi}-\left(\frac{h\theta}{\beta}+\mu\right)\frac{{\chi_A}^2}{F(\omega)} \tag{34}$$

Equation (34) is similar to equation (33). To see how good an approximation equation (34) is, consider the values of the parameters. We recall that $f/\beta \gg h/\beta \gg \mu/\beta$. Further since $\langle v\rangle_c>0$, $B>(h/\beta)N_c$. (Note that $q\theta/\beta^2 \ll 1$ since $q/\beta=2c$ is the initial dispersion.) So if $(h/\beta)N_c \ll 1$ then the first term in equation (34) can be approximated by $\eta\beta\chi_A$ for all ω. It may be noted that the expressions for the various cumulants does not have this constraint $(h/\beta)N_c \ll 1$. Consider the second term. The fact that the time dependence is correctly satisfied can be seen by setting $\omega=0$. The dependence on ω comes from $F(\omega)$ and $\varphi(\omega)$. For $(h/\beta)N_c \ll 1$, the contribution from $\varphi(\omega)$ in ${\chi_A}^2$ can be approximated reasonably well for all ω. The contribution from $F(\omega)$, however, is reasonable only for small ω. For large ω, it should again be a reasonable approximation since ${\chi_A}^2$ and ${\chi_A}^2/F(\omega)$ have both asymptotic exponential dependence. Thus, $\chi_A(\omega, t)$ given by equation (29) may be considered as a reasonably good approximate solution. We have not been able to invert $\chi_A(\omega, t)$ to obtain the CPD. However, $\rho(v, t, t_0)$ can be obtained numerically for values of parameters in the creep experiment. Earlier (1) we had noted that since both k_3 and k_4 are negative, the distribution should be platykurtic (Kendall and Stuart 1969).

Several observations can be made at this point. The characteristic function χ depends on v_0 through $\exp(-\theta v_0/\beta)$ (see equations (17–25)). All conditional moments also depend on v_0 through N_c, since for the initial state $\langle v\rangle = B \ll \beta/\theta$, and since in our calculation we have taken $\psi \to 0$ for $t-t_0 \gg \tau_1 \sim \beta^{-1}$, for the sake of consistency we should set $\exp(-\theta v_0/\beta) \sim 1$. This is in fact a very good approximation since $\tau_1 \sim \beta^{-1}$ is very small compared to the duration of deformation. In this approximation, the CPD loses memory of its initial velocity but retains its dependence on t_0. This is due to the fact that it identifies the initial density N_0. Then, the CPD goes over to the unconditional density

$$\rho(vt|v_0t_0)\to\rho(v, t-t_0). \tag{35}$$

The dependence on time appears in the form $t-t_0$. A general JPD $\rho(v't';vt)$ with an arbitrary $(v't';vt)$ not representing the initial state v_0t_0, then decouples to

$$\rho(v't';vt)\to\rho(v', t'-t)\,\rho(v, t-t_0). \tag{36}$$

The time dependence is factored in the form $t'-t$ and $t-t_0$, and is due to the nature of the dependence of N_c on time. In particular

$$\rho(vt;v_0t_0)\to\rho(v_0)\,\rho(v, t-t_0). \tag{37}$$

Thus, for $t-t_0 \gg \tau_1$, the process becomes *completely random*. Since the distribution function $\rho(v, t, t_0)$ depends on time, the process is *nonstationary*.

Few more observations can be made. The densities corresponding to $\rho(v', t'-t)$ and $\rho(v, t-t_0)$ are $N(t'-t)$ and $N(t-t_0)$. From equation (17), it is clear that the initial density at a time t is required to define $N(t'-t)$. The only way to fix this unambiguously is to start from the same initial value, N_0 at t_0, when defining both $N(t'-t)$ and $N(t-t_0)$.

Then

$$N(t'-t)=N_S\Big/\left[1+\left(\frac{N_S}{N(t-t_0)}-1\right)\exp\left[-\eta\beta\,(t'-t)\right]\right] \tag{38}$$

Using the expression for $N(t-t_0)$, we get

$$N(t'-t)=N(t'-t_0). \tag{39}$$

Consider a bad sample whose initial density is large, say N_0'; then it would be unrealistic to assume that the initial strain at t_0 is zero. In such a case, the above relation gives a method of estimating the initial strain. This is done by starting from a reasonably pure sample and applying the same stress as that applied to study the creep curve for the bad sample, so as to induce a density N_0'. In addition to this N–t plot of the good sample, we also need the ε–t plot. From these two, the strain corresponding to N_0' can

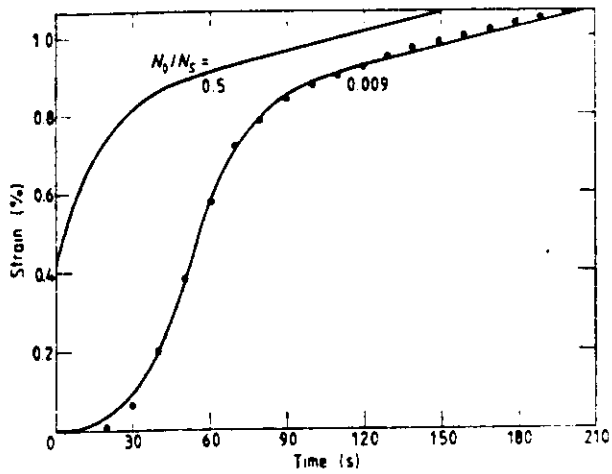

Figure 1. Creep curve for two different values of the initial densities and the choice of initial value of strain for a large initial density. $N_S=8.4\times10^6\ \mathrm{cm}^{-2}$; $\mu\neq0$, $\alpha=0$; $h/\beta=3.535\times10^{-10}\ \mathrm{cm}^3\ \mathrm{s}^{-1}$. Full curves, theory; ●, experimental values.

be assigned as the initial strain for the bad sample. At this point we wish to point out that in I we have taken $\varepsilon_0=0$ for a sample whose initial density is not small (curve D of figure 1 in I). It is because of this unrealistic choice that the curve for large initial N_0 lies below the curve with small N_0. If we used the above procedure, all curves would be asymptotically parallel. In other words if we shift the origin of the creep curve for the bad sample, on to the creep curve of the good sample, they will coincide. Figure 1 shows the creep curve of a bad sample with reference to a good sample.

4. Discussion

We now comment on the broad features of the present theory which perhaps can be used in other areas. The present problem can be looked upon as a problem in transport theory. The analogy between Ohm's law and Orowan's equation has been noted earlier (Gilman 1969). In a conventional transport problem, the response of the system is linearly related to the applied 'force'. This is due to the fact that the 'subsystem' under

consideration is weakly coupled to the 'reservoir' and the application of external force affects the subsystem only. The change in the subsystem does not affect the nature of the reservoir. Under such linear conditions, the CPD (which contains information about the correlation function) can be easily calculated. However, in the present problem the fact that the average velocity and other cumulants are functions of the density suggests that any change in the nature of the 'subsystem' (the ensemble of dislocations) affects the 'reservoir' (the lattice) strongly. This is clear due to the fact that the internal stress field (a property of the lattice) changes as creep proceeds. Under these conditions, the response of the subsystem to the applied force s in general nonlinear. Instead of attempting to handle a nonlinear response, we have included the nonlinearity in the equation for the evolution of the CPD. This procedure allows us to calculate the correlation function as long as we can obtain a solution of the differential equation for the CPD.

It may be recalled that the dependence on the initial velocity comes only through the factor $\exp(-\theta v_0/\beta)$ in N_e. To carry out the calculations, keeping even the linear terms in v_0, is rather cumbersome. However, using the crude decoupling approximation gives some indication of how nonstationarity complicates the situation. In this approximation

$$\langle v\, v'\rangle = [B-(h/\beta)N(t'-t)][B-(h/\beta)N(t-t_0)]. \tag{40}$$

The strain rate autocorrelation function in the same approximation works out to

$$\begin{aligned}\langle \dot\varepsilon(t'-t)\,\dot\varepsilon(t-t_0)\rangle &\overset{\text{det}}{\equiv} b^2\int \mathrm{d}v'\,\mathrm{d}v - v - v'\rho(v't';vt)\\ &\simeq b^2 N(t'-t)N(t-t_0)\langle v v'\rangle\\ &\simeq b^2 N(t'-t_0)N(t-t_0)[B-(h/\beta)N(t'-t_0)][B-(h/\beta)N(t-t_0)]\end{aligned} \tag{41}$$

where we have used equation (39). As a function of t (or t'), this function has the same form as the mobile dislocation density we have obtained elsewhere (Sahoo and Ananthakrishna 1982, Ananthakrishna and Sahoo 1978; see also Gilman 1969). We believe that this autocorrelation function can be related to many measurable quantities (perhaps an example would be the acoustic emission phenomena).

The last observation pertains to the time development of the distribution function. Generally, under conservative effects, an initial delta function for the CPD broadens as time proceeds (as in the case of Brownian motion). In the present problem also, the CPD does broaden initially for a short time corresponding to the evolution under the absence of the source and the sink terms. However, for the rest of the time when the nonconservative effects come into play, both the first and the second cumulant reduce, leading to the sharpening of the distribution. (For a certain choice of the value of the parameters, the dispersion can go to zero.) This general feature of sharpening of the distribution, starting from a broad distribution, arises due to nonlinear nonlocal terms. Such situations do arise in many other problems, for example in the formation of a void lattice under irradiation (Stoneham 1975). In this case what has been understood is that the void lattice is the minimum energy configuration (see for example Stoneham 1975). How exactly a broad distribution in sizes of voids having a certain average size $\langle r\rangle$ goes over to a sharply peaked distribution with average size $r_0 < \langle r\rangle$ is not clearly understood. We believe the present method does throw some light on this problem as well and we are presently looking into this problem.

Acknowledgment

I am very thankful to Dr D Sahoo for many useful discussions.

References

Ananthakrishna G and Sahoo D 1978 *Nucl. Phys. Solid State Phys. (India)* **21C** 771
—— 1981 *J. Phys. D: Appl. Phys.* **14** 699
Clement C F 1978 *Proc. R. Soc.* **A364** 107
Gilman J J 1969 *Micromechanics of Flow in Solids* (New York: McGraw-Hill)
Kendall M G and Stuart A 1969 *The Advanced Theory of Statistics* vol. 1 (London: Charles Griffen) p 86
Johnston W G and Gilman J J 1959 *J. Appl. Phys.* **30** 129
Sahoo D and Ananthakrishna G 1982 *J. Phys. D: Appl. Phys.* **15** at press
Stoneham A M 1975 in *Consultant Symposium, The Physics of Irradiation Produced Voids* ed. R S Nelson AERE-R-7934
Stratonovich R L 1963 *Topics in the Theory of Random Noise* (New York: Gordon and Breach)
Wang M C and Uhlenbeck G E 1945 *Rev. Mod. Phys.* **17** 323
Webster G A 1966 *Phil. Mag.* **14** 775

J. Phys. D: Appl. Phys., 15 (1982) 1439–1449. Printed in Great Britain

A phenomenological dislocation transformation model for the mobile fraction in simple systems

Debendranath Sahoo and G Ananthakrishna
Materials Science Laboratory, Reactor Research Centre, Kalpakkam 603 102, Tamil Nadu, India.

Received 20 March 1981, in final form 3 March 1982

Abstract. We propose, on the basis of well known mechanisms, a dislocation transformation model between mobile and immobile components. An explicit functional form for the mobile fraction of dislocations is derived. The theory is restricted to materials in which the internal stress varies linearly with the total dislocation density. A new creep law is derived and is applied to several materials. Excellent agreement is found between theoretical predictions and experimental results.

1. Introduction

One of the most important variables in dislocation dynamic models of plastic flow is the density N_g of mobile dislocations. There is at present no satisfactory theory relating N_g to the total density N of all dislocations. Gilman (1965, 1969) proposed a relation

$$N_g(\varepsilon) = N(\varepsilon) \exp(-H\varepsilon/\sigma_a)$$

where H is a constant called the hardening coefficient, σ_a is the applied stress and ε denotes strain. Here $N(\varepsilon)$ is assumed to be linear in ε: $N(\varepsilon) = N_0 + M\varepsilon$, where N_0 and M are constants. In deriving this expression, Gilman (1965) has assumed that the average velocity of mobile dislocations remains constant during creep. Gilman (1969) has summarised his view of the statistical description of the situation in the following way. The effect of interactions on the mobile population can be described in either of two ways from a statistical viewpoint. One is to consider that the average dislocation velocity decreases as a result of plastic strain, because collisions tend to reduce the drift velocity. The other is to consider that the moving dislocations continue to move at the same speed, but the fraction of the total density that moves decreases continually as the plastic strain increases. The two viewpoints are statistically equivalent. (See Gilman 1969, p 185.)

One of the purposes of this paper is to investigate the equivalence of the two views within the framework of a simple model in which the dependence of the average velocity V on ε (or equivalently, N) is known. Alternately, assuming the equivalence of the two views, we attempt to relate N_g to N. Generally, for most materials, $V \sim (\sigma^*)^n$ where n is some suitable exponent. Here $\sigma^* = \sigma_a - A\sqrt{N}$ is the effective stress and A is a constant (Alexander and Haasen 1968).

0022-3727/82/081439 + 11 $02.00

Other forms of $V(\sigma^*)$ have also been proposed in the literature, see for example, Gilman (1969). However, in simple materials like LiF, V decreases linearly with increase in N (Webster 1966 and references therein, Gillis and Gilman 1965):

$$V = V_0 - HN. \tag{1}$$

Here H and V_0 are constants for a given temperature at a given σ_a.

Relation (1) has been confirmed experimentally by Gilman and Johnston (1962) for LiF. Often equation (1) is looked upon as an approximation (Webster 1966) to a more general relation given by Gilman (1969). For low levels of strain, Webster (1966) has also applied this equation to other materials. For simplicity, we confine our attention to systems where equation (1) holds, and consider deformation under creep. Based on well known mechanisms, we propose a dislocation transformation model which gives coupled time-evolution equations for N and N_g. This equation for N is identical to the one derived in our earlier work (Ananthakrishna and Sahoo 1981a, to be referred to hereafter as I); V has to be interpreted as the velocity averaged with respect to the distribution function $\rho(v)$ of I. Solving the equation for N and N_g together with relation (1), we obtain an explicit functional form for the mobile fraction $\varphi(t)(\equiv N_g(t)/N(t))$. In order to check whether the time dependence of $N_g(t)$ has been properly incorporated into it, we calculate the average velocity V_g associated with N_g under the assumption of equivalence of the two viewpoints. We find that although V_g is not strictly constant, it is almost so. In order to assess how good is the form of N_g so constructed we derive a creep law assuming that V_g is constant and apply it to creep in LiF (Johnston 1962). We find excellent agreement for three different stresses considered. We also apply it to Al_2O_3 (Webster 1966) and a nickel based alloy (Watchman 1957). An indication that these materials satisfy equation (1) comes from the fact that Webster (1966) has applied a creep law derived on the basis of equation (1). The agreement of our theory with experiments is again very good.

2. The model

We assume that the entire population of dislocations (the individual units denoted by p) consists of single dislocations (monopoles, denoted by g) and pairs of bound monopoles (dipoles, denoted by d). Let $\rho(v, t)$, $\rho_g(v, t)$ and $\rho_d(v, t)$ be their respective velocity distribution functions, and these are related by

$$\rho(v, t) = \rho_g(v, t) + \rho_d(v, t).$$

Let $N(t)$, $N_g(t)$ and $N_d(t)$ denote their respective densities, i.e.

$$N(t) = \int_{-\infty}^{\infty} \rho(v, t)\, dv$$

etc. Clearly we have

$$N = N_g + N_d. \tag{2}$$

We assume the following set of reactions (with the rate constants denoted on the top of the respective arrows),

$$p \xrightarrow{\theta V} p + p \tag{3a}$$

$$p + p \xrightarrow{k\mu 2} d \tag{3b}$$

$$p + p \xrightarrow{(1-k)\mu 2} 0 \tag{3c}$$

$$p + d \xrightarrow{\mu'} p. \tag{3d}$$

The first reaction (3*a*) corresponds to the breeding of new dislocations by the well known cross glide mechanism (Gilman and Johnston 1962); the breeding rate is known to be proportional to the average velocity V of all dislocations, where $V(t) = (1/N)\int_{-\infty}^{\infty} dv\, \rho(v, t)v$ and θ is the breeding constant. The second reaction (3*b*) corresponds to the formation of dipoles and the third (3*c*), to mutual annihilation of two monopoles. The last reaction (3*d*) corresponds to transformation of dipoles into monopoles. A dominant mechanism by which dipoles are formed is by trapping parts of two dislocations as they pass each other on closely spaced parallel glide planes. Annihilation of two dislocations clearly occurs, when their glide planes are the same. Formation of monopoles from dipoles occurs when the glide plane of a passing dislocation is the same as that of one of the dislocations constituting the dipole. In LiF it is well known that the formation of dipoles is the cause of hardening (Gilman 1969, p 147, Alexander and Haasen 1968, pp 97, 105. See also Ananthakrishna 1981, 1982). The last two processes are the recovery processes. We believe that these are the dominant processes operating for the cases we consider here. The constant k is very close to and slightly less than 1 which means the reaction (3*c*) is assumed to be much slower compared to (3*b*). μ and μ' are constants. All these reactions are well known and are listed by Gilman (1969, pp 193–4).

Here it should be pointed out that we have not included a number of other processes. These are: p + p → s + s (e.g. formation of Lommer–Cottrell locks) and s → p (mobilisation of an immobile dislocation due to athermal activation). These have been considered in another paper (Ananthakrishna and Sahoo 1981b). In such a case, the structure of mobile dislocation density and that of creep are similar to that we obtain in the present analysis.

We now reformulate the viewpoints of Gilman: the total flux of dislocations can be written

$$\begin{aligned} NV &= \int_{-\infty}^{\infty} dv\, \rho(v, t)\, v \\ &= \int_{-\infty}^{\infty} dv\, \rho_g(v, t)v + \int_{-\infty}^{\infty} dv\, \rho_d(v, t)v \\ &= N_g V_g + N_d V_d. \end{aligned}$$

It is expected that $V_d \ll V$ and since $N_d < N$, the second term in the right-hand side can be ignored and we then approximate

$$NV \approx N_g V_g. \tag{4}$$

In the first point of view, V decreases with time (the averaging is done with respect to $\rho(v, t)$). This is not inconsistent with the alternate viewpoint in which V_g remains constant and the entire time variation of the flux is due to $N_g(t)$ (the averaging is done with respect to $\rho_g(v, t)$). We have introduced the three distribution functions only to explain the averages involved. However, our entire calculation is done at a phenomenological level. Assuming the statistical equivalence represented by equation (4), we would like to

examine whether it is possible to construct a model based on the second point of view. Thus in our model we assume that equation (1) is valid and the transformations (3) give a prescription to obtain N and N_g. (The first point of view has been investigated in I where equation (1) along with an expression for N has been derived, starting from an equation for $\rho(v, t)$. Equation (3) gives the same expression for N as in I.) Then equation (4) is used as a defining relation for V_g.

The reactions (3*a–d*) lead to the following kinetic equations:

$$\dot{N} = \theta V N - \mu N^2 \cdot \tag{5a}$$

$$\dot{N}_d = k\mu N^2 - \mu' N N_d. \tag{5b}$$

Equation (5*a*) is identical to the one assumed by Webster (1966) except for a constant term in the right-hand side. This equation is also used by Gilman (1965) and Li (1963). According to Webster (1966) and Li (1963) the quantities θ and μ depend on σ_a and temperature. Hence these are constants for deformation under creep. We retain this assumption and also make a similar assumption that μ' is a constant.

Substituting equation (1) in equation (5*a*) we obtain

$$\dot{N} = \theta V_0 N - N^2 \mu'' \tag{6a}$$

where

$$\mu'' = \mu + H\theta. \tag{6b}$$

The parameter H is to be identified with the quantity h/β of I, where its physical meaning has been discussed in detail. The solution of equation (6*a*) with the initial conditions $N = N_0$ at $t = 0$ is the logistic curve

$$N(t) = N_s(1 + a)^{-1} \tag{7a}$$

where

$$a(t) = a_0 \exp(-\theta V_0 t) \tag{7b}$$

$$a_0 = (N_s/N_0) - 1 \tag{7c}$$

$$N_s = \theta V_0/(\mu + H\theta). \tag{7d}$$

The reaction cross-section of one mobile dislocation with another should not be too different from that of a mobile dislocation with a dislocation dipole. This means that μ' and μ'' are of the same order of magnitude and we may assume $\mu' = \mu''$. This assumption is quite good in these crystals where work-hardening occurs due to formation of dipoles. In crystals with a diamond structure where work-hardening is known to occur due to long range stress fields of single dislocations (Alexander and Haasen 1968), it is not expected to hold good. Thus the present theory is not meant to be applicable to such materials. Elsewhere (Ananthakrishna 1982) one of us has considered creep in such materials. Although this choice restricts the direct applicability of our results, the essential feature of our theory is still retained with arbitrary μ' and μ''. Subtracting equation (5*b*) from equation (5*a*) and using equations (1) and (2) with the above assumption, we get

$$\dot{N}_g = \theta V_0 N - k\mu N^2 - \mu' N N_g. \tag{8}$$

Let k' be the fraction of N that is mobile at the start of creep, i.e.

$$N_g = k'N_0 \qquad \text{at } t = 0.$$

Using N as given by equation (7*a*) in equation (8) and with the above initial condition, we obtain

$$N_g(t) = N\left[(1-\bar{k})\left(1-\frac{a}{a_0}\right) + k'\left(\frac{a}{a_0}\right) + a\bar{k}\ln\left(\frac{a_0(1+a)}{a(1+a_0)}\right)\right]$$

$$= N\varphi(t) \tag{9a}$$

where

$$\bar{k} = k(\mu/\mu'). \tag{9b}$$

Physically, the parameter $\bar{k}$ determines the amount of work hardening. It is the ratio of the rates of formation and decomposition of dipoles. The Orowan equation is

$$\dot{\varepsilon} = bV_gN_g. \tag{10}$$

Here we assume that V_g is constant. (This is only approximately valid as we shall show in § 3.) Integrating equation (10) with the initial condition $\varepsilon = \varepsilon_0$ at $t = 0$, we obtain a new creep law:

$$\varepsilon(t) - \varepsilon_0 = bV_gN_sf(t) \tag{11a}$$

where

$$f(t) = \Big([(1-\bar{k}) - \bar{k}\ln(1+a)]\,t + (\bar{k}/\theta V_g)$$
$$\times \ln(1+a_0)\ln(1+a) + (\theta V_g)^{-1}\ln[(1+a)/(1+a_0)]$$
$$\times [(1-\bar{k})(1+a_0)/a_0 - k'/a_0]$$
$$- (\bar{k}/2\theta V_g)[\ln(1+a)]^2 - (\bar{k}/2\theta V_g)[\ln(1+a_0)]^2$$
$$+ \bar{k}\int_0^t \ln(1+a)\,dt\Big). \tag{11b}$$

We note the following features associated with the creep law. The asymptotic value of N_g, from equation (9) is $(1-\bar{k})N_s$ which leads to the creep rate in the secondary creep region

$$\dot{\varepsilon}_{sec} = (1-\bar{k})bV_gN_s. \tag{12}$$

Thus unless $\bar{k}$ is chosen as strictly equal to 1, the creep curve never flattens in the secondary region. For a value of $\bar{k}$ very close to (but less than) unity, one has the strain linearly increasing in time, and the slope of this linear rise is controlled by the parameter $\bar{k}$. (Note that $\bar{k}<1$ since $\mu' = \mu + H\theta > \mu$.) The time at which creep changes over from the transient to the primary region is the time of inflection t_i. At $t = t_i$, $\ddot{\varepsilon} = 0$ which implies $\dot{N}_g = 0$. Using this condition in equation (9), one obtains

$$t_i = \ln(la_0 + l - a_0)/\theta V_0 \tag{13a}$$

where

$$l = \exp[(a_0 - l - \bar{k} - k')/\bar{k}a_0]. \tag{13b}$$

Clearly the point of inflection exists if and only if $t_i > 0$, i.e. if and only if $l > 1$ which implies the condition

$$N_0 < N_s/(\bar{k} + k'). \tag{14}$$

This means there is a point of inflection in creep as long as

$$0 \leq k' \leq 1 - \bar{k} \qquad N_0 < N_s. \tag{15}$$

For $1 - \bar{k} \leq k' \leq 1$ and for any choice of N_0 violating equation (14), there is no point of inflection. Thus there are two classes of qualitatively different creep curves. Note that if k' is chosen as zero, i.e. if there are no mobile dislocations initially, then the initial creep rate is zero. This would always give rise to a point of inflection.

We first apply the creep law to LiF. Except for the value of $\bar{k}$ (which is an adjustable parameter), all other parameters are assumed to have values consistent with those reported in the literature. (We have taken $\theta = 3 \times 10^3\ \mathrm{m}^{-1}$ for LiF.) We describe, in detail, how the theoretical creep curve is calculated for one value of $\sigma_a = 3.73$ MPa. Creep curves calculated for other stresses and for other materials are dealt with later. The approximate value of N_s ($N_s \sim 5.62 \times 10^{10}\ \mathrm{m}^{-2}$) is fixed by the near asymptotic value of ε. (The value of N_s is not given in Johnston (1962).) For the samples used, N_0 is reported to be $3 \times 10^8\ \mathrm{m}^{-2}$ in better samples to about $10^9\ \mathrm{m}^{-2}$ in poorer ones. Our choice is $N_0 = 8 \times 10^8\ \mathrm{m}^{-2}$. From Johnston's (1962) power law $V_g = V_0 = (\sigma_a/5.29)^{16.5}$ (where σ_a is the applied stress in MPa) we obtain $V_g = 3.033 \times 10^{-5}\ \mathrm{m\,s}^{-1}$, for $\sigma_a = 3.73$ MPa, the stress corresponding to the creep experiment (Johnston 1962). We obtain a good fit to Johnston's (1962) recorder tracings for $\bar{k} = 0.9778$ (see figure 1). In figure 1 we have also presented the calculated creep curves corresponding to a slight decrease of $\bar{k}$ ($\bar{k} = 0.965$) from the fitted value and the case corresponding to $\bar{k} = 1$ for which creep saturates. This shows that $\bar{k}$ is a very sensitive parameter in the secondary creep region.

In figure 2 we have drawn a plot of N and N_g normalised to N_s for various values of N_0. (The value of $\bar{k}$ is the one which fits the experimental curve.) For very small values of N_0, the time taken for N to show any appreciable value (compared to its final density) is very long. The mobile density is almost symmetric about its peak except for the flat

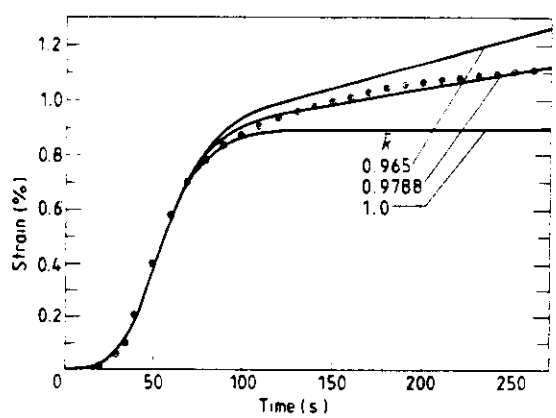

Figure 1. Creep curve for LiF for $\sigma_a = 3.73$ MPa. $N_s = 5.65 \times 10^{10}\ \mathrm{m}^{-2}$; $N_0 = 8 \times 10^8\ \mathrm{m}^{-2}$. The points correspond to experiment and full curves to our theory. Variation of creep with respect to different $\bar{k}$ values is shown.

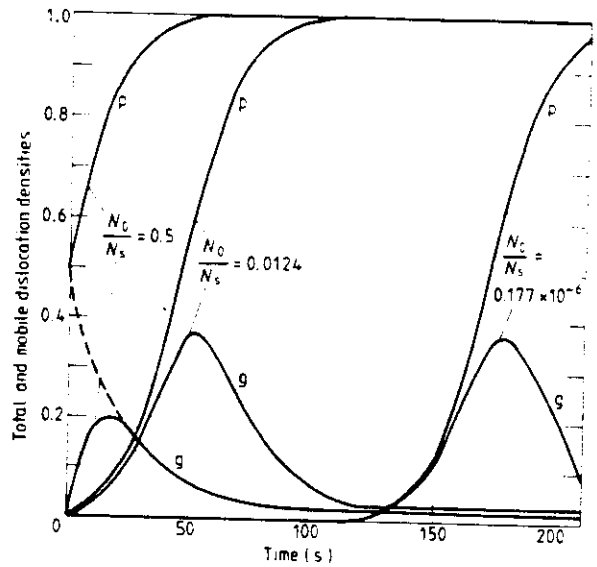

Figure 2. Time variation of the total dislocation density N (denoted by p) and the mobile dislocation density N_g (denoted by g) for different values of initial density N_0. $N_s = 5.65 \times 10^{10}$ m^{-2}; $k = 0.9788$.

(non-zero) asymptotic part which is due to $k \neq 1$. For a large value of N_0 there is a pronounced asymmetry in N_g for $k' = 0$ as can be seen from the curve corresponding to $N_0/N_s = 0.5$. For this value of N_0/N_s, the broken curve corresponds to the choice $k' = 1$.

In figure 3 we have shown that the initial density N_0 controls the transient part of the creep curve. The smaller the value of N_0 the longer it takes to generate a sufficient number of dislocations to contribute to any observable creep. For very large N_0, the initial transient persists slightly for $k' = 0$ in contrast to the initial transient being completely absent when $k' = 1$ is used (broken curve). This can be seen in figure 3 for the value $N_0/N_s = 0.5$. We also note in figure 3 that by increasing N_0 from a reference

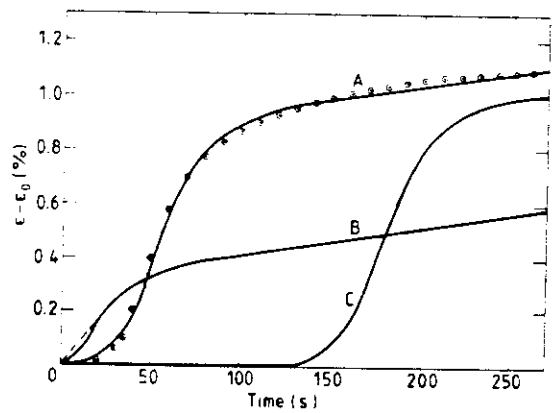

Figure 3. Creep curves calculated for different values of initial dislocation density. Also shown are experimental points. $N_s = 5.65 \times 10^{10}$ m^{-2}; $k = 0.9788$. (A) $N_0/N_s = 0.0124$; (B) $N_0/N_s = 0.5$; (C) $N_0/N_s = 0.177 \times 10^{-6}$.

value of $0.0124 \times N_s$ (curve A) to a value of $0.5 \times N_s$ (curve B), the amount of creep in the secondary creep region is considerably reduced. This is due to the fact that we have subtracted the arbitrary initial strain ε_0 because we lack information about the initial state. Taking the initial strain to be zero is rather artificial when N_0 is large. Ideally one can choose ε_0 to be zero only when N_0 is small compared to N_s. When all other parameters are the same except the initial densities, the respective initial strains would not be the same. One way of knowing the value of ε_0 for large N_0 (say, in a bad sample) is to start from a reasonably pure sample ($N_0 \ll N_s$) and apply an appropriate stress to induce an asymptotic strain ε' which would produce the required value of N_0 in the bad sample. The ε_0 for this case is then ε'. As N_0 is increased, the point of inflection is reached earlier, the peak of the N_g–t curve (see figure 2) is reduced by almost half the corresponding area under the reference curve. By reducing N_0 from the reference value to $(0.177 \times 10^{-6})\, N_s$ (curve C), the above reasoning (also reflected in figure 2) leads to the conclusion that the magnitude of strain should be higher than that of curve A in the secondary stage. This is not shown in figure 3 as the creep curve for the reduced density is still in its primary stage. Eventually it is expected to overtake curve A. We note here that Webster (1966) has reported behaviour similar to that shown in figure 3.

In figure 4, we have plotted N_g/N_s for three different values of $\bar{k}$. For larger deviations of $\bar{k}$ from unity, the position of the peak shifts towards the right, indicating that the point of inflection of the creep curve (which occurs at $t \sim 55$ s for $\bar{k} = 0.9788$) also shifts towards the right.

In order to check the validity of the creep law at other stress levels, we have computed creep curves for LiF at two more stresses $\sigma_a = 3.78$ MPa and 3.63 MPa (figure 5). The same value of θ and N_0 have been used. This is consistent with the fact that Johnston's (1962) samples used in his experiment had almost the same initial density N_0. The parameter $\bar{k}$, being a measure of work hardening, is expected to depend on σ_a, although not too drastically. This is confirmed by our calculation.

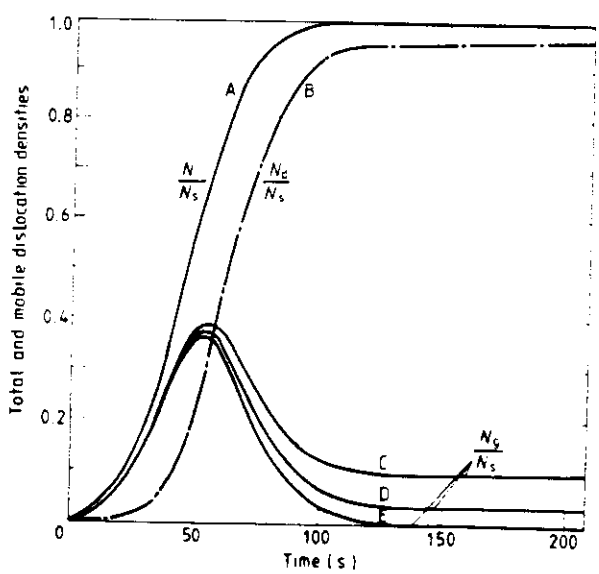

Figure 4. Time variation of the total dislocation density N, the mobile dislocation density N_g and the dipole dislocation density N_d (dashed curve) for different values of the parameter $\bar{k}$: (A), (B), (D), 0.9778; (C) 0.965, (E) 1.0. $N_0 = 8 \times 10^{8}$ m^{-2}; $N_s = 5.65 \times 10^{10}$ m^{-2}.

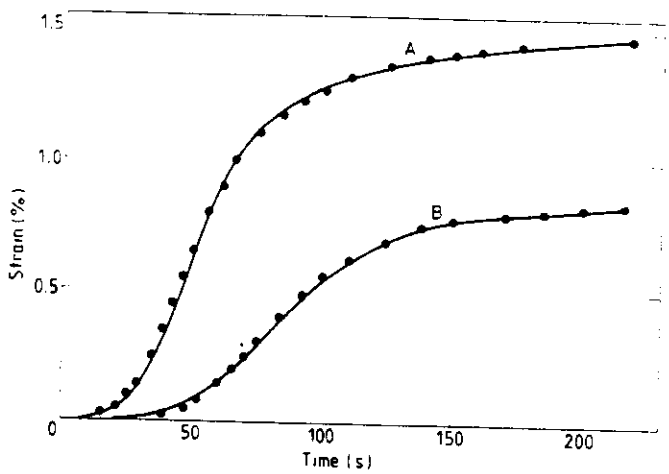

Figure 5. Creep in LiF. (A) $\sigma_a = 3.78$ MPa, $\eta\beta = 0.107\ s^{-1}$, $k = 0.975$, $N_0 = 8 \times 10^6\ m^{-2}$, $N_s = 7.5 \times 10^6\ m^{-2}$; (B) $\sigma_a = 3.63$ MPa, $\eta\beta = 5.66 \times 10^{-2}\ s^{-1}$, $k = 0.977$, $N_0 = 8 \times 10^6\ m^{-2}$, $N_s = 4.9 \times 10^6\ m^{-2}$.

3. Discussion

We now examine the validity of the constancy of V_g assuming the equivalence of the two viewpoints as expressed by equation (4). Substituting equations (1), (7) and (9) in equation (4), we obtain

$$\frac{V_g}{V_0} = \frac{1}{\varphi(t)}\left(1 - \frac{HN}{V_0}\right) = \frac{1}{\varphi(t)}\left(1 - \frac{\lambda}{1 + a(t)}\right) \equiv \psi(t) \tag{16a}$$

where

$$\lambda = HN_s/V_0. \tag{16b}$$

The parameter λ does not occur in our creep law. It can be obtained in two different ways. Since we have investigated creep in LiF using the first point of view in I where the parameter λ appears, we can use the value of λ from I. For LiF $\lambda = 0.979$ for $\sigma_a = 3.73$ MPa. The second way to obtain λ is to demand that the asymptotic creep rates in both the viewpoints (see relation (4)) are equal. Using equations (1), (7*a*) and (9*a*) in equation (4) and assuming $V_g \to V_0$ asymptotically gives $\lambda = k$ (= 0.9788 for this case). In figure 6 we have plotted $\psi(t)$ using $\lambda = 0.979$, together with two values of λ. It can be seen that the maximum variation of ψ occurs around $t = 80$ s, where $\psi \approx 0.4$. In contrast, the ratio V/V_0 reduces to as much as 0.02. Thus our assumption of constancy of V_g is only approximately valid. In spite of this fact, our creep law seems to agree very well with experimental data. This can only imply that the essential time variation is already incorporated in N_g.

We next apply the creep law to two other materials—Al_2O_3 at 1100°C (Watchman 1957) and $\sigma_a = 25.52$ MPa and a nickel based alloy MARM–200 at 760 °C and $\sigma_a = 5.92$ MPa (Webster 1966). This we do in order to stress the wide range of applicability of our model. The results of our calculation together with experimental curves are presented in figures 7 and 8. The agreement is seen to be very good. The values of the parameters we have used to obtain best fit are consistent with those of Webster (1966)

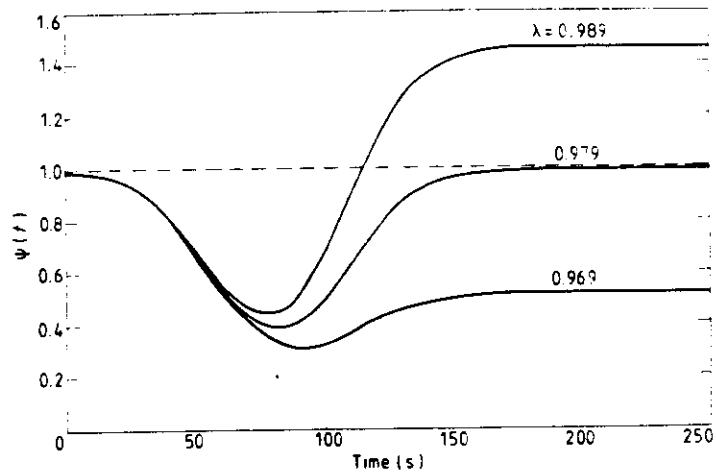

Figure 6. Time variation of the function $\psi(t)$.

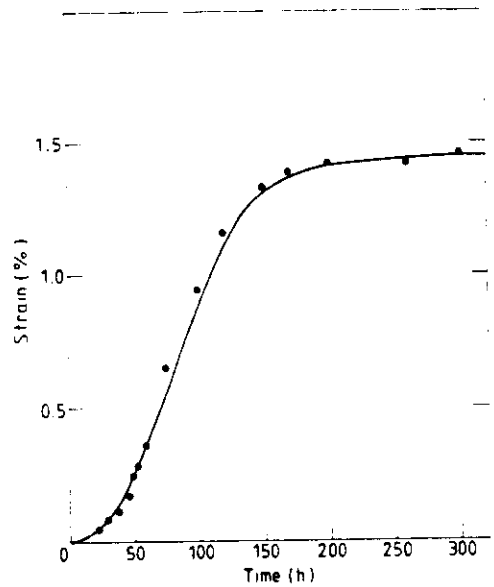

Figure 7. Creep in Al_2O_3 for $\sigma_a = 25.52$ MPa, $\eta\beta = 0.038\ h^{-1}$, $\theta = 2.4 \times 10^{4}$ m, $k = 0.99$, $N_0 = 8.95 \times 10^{8}\ m^{-2}$, $N_s = 9.0 \times 10^{9}\ m^{-2}$.

who has fitted the same data. The consistency is seen by noting that Webster's parameters are related to the creep law derived in I. These parameters themselves have been related to the parameters occurring in our new creep law given in equation (11). (See equation (16*b*) and the discussion that follows.)

The present calculation can be easily extended to crystals with diamond structure. In such cases $V \sim (\sigma^*)^n$ with $n \approx 1$ and $\sigma^* = \sigma_a - AN^{1/2}$. (See Alexander and Haasen 1968.) We have indeed constructed a model (Ananthakrishna 1982) with the same transformations as in equation (3) with the difference that the rate constants depend on N. Again, V_g can be shown to be roughly constant. Elsewhere the present model has

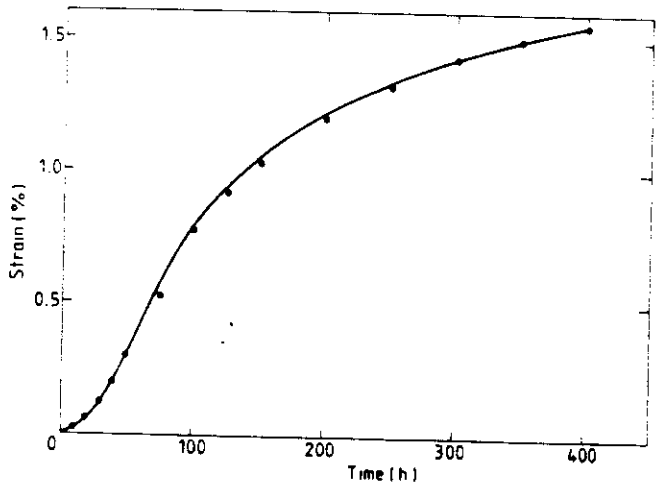

Figure 8. Creep in nickel based alloy MARM-200 for $\sigma_a = 5.92$ MPa, $\eta\beta = 0.029\ h^{-1}$, $\theta = 2 \times 10^4\ m^{-1}$, $k = 0.97$, $N_0 = 5 \times 10^9\ m^{-2}$, $N_s = 1.25 \times 10^{10}\ m^{-2}$.

been used as the starting point in evolving a nonlinear oscillatory model for explaining jumps on creep curve (Ananthakrishna and Sahoo 1981b).

References

Alexander H and Haasen P 1968 *Solid State Physics* vol 22 ed F Seitz and D Turnbull (New York: Academic) p98
Ananthakrishna G 1981 *J. Phys. D: Appl. Phys.* **14** 2091–100
—— 1982 *J. Phys. D: Appl. Phys.* **15** 77
Ananthakrishna G and Sahoo D 1981a *J. Phys. D: Appl. Phys.* **14** 699
—— 1981b *J. Phys. D: Appl. Phys.* **14** 2081
Gillis P P and Gilman J J 1965 *J. Appl. Phys.* **36** 3370
Gilman J J 1965 *J. Appl. Phys.* **36** 2772
—— 1969 *Micromechanics of Flow in Solids* (New York: McGraw-Hill)
Gilman J J and Johnston W G 1962 *Solid State Physics* vol 13 ed F Seitz and D Turnbull (New York: Academic)
Johnston W G 1962 *J. Appl. Phys.* **33** 2716
Li J C M 1963 *Acta Metall.* **11** 1269
Watchman J B 1957 in *ASM Seminar, Creep and Recovery, Cleveland, Ohio* (Ohio: ASM) p 344
Webster G A 1966 *Phil. Mag.* **14** 775

J. Phys. D: Appl. Phys., 15 (1982) 77–87. Printed in Great Britain

Creep in crystals with diamond structure

G Ananthakrishna

Materials Science Laboratory, Reactor Research Centre, Kalpakkam 603 102, Tamil Nadu, India

Received 4 June 1981

Abstract. A slight modification in the starting equation of our earlier model (Ananthakrishna and Sahoo 1981) and the use of method of averages lead to expressions for the average dislocation density and the average velocity. The average velocity varies as the square root of the dislocation density. A new creep law is derived which is expected to hold for crystals with diamond structure. It is applied to creep in Si, giving good agreement with experiments. The creep law is cast into a new form in terms of new scaled variables—time and strain scaled with respect to their values at the point of inflection. The scaled creep law is shown to be independent of both temperature and stress for reasonably small initial densities.

1. Introduction

Recently (Ananthakrishna and Sahoo 1981, hereafter referred to as I) we gave a statistical basis for creep in simple materials like LiF, where the average velocity V decreases linearly with the total density N of dislocations (Gilman 1969). The situation is expected to be applicable to low levels of strain in other materials also (Webster 1966). However, for most other situations $V \sim (\sigma_a - A\sqrt{N})^m$, where σ_a is the applied stress, A is a constant and m is an exponent. For materials with diamond structure like Si, Ge etc, m is known to be close to unity (Alexander and Haasen 1968). The purpose of this note is to extend our earlier theory to materials like Si. The procedure followed is an averaging method applied to a slightly altered equation (from that used in I) describing the velocity distribution function of the dislocations. Under certain approximations, we derive an equation for $\dot{N}$ and an equation for $\dot{V}$. A new creep law is derived and applied to Si with good agreement with experiments. In terms of scaled time and scaled strain (scaled with respect to their values at the point of inflection) the scaled creep function is shown to be independent of temperature and stress.

2. The model

We shall idealise the system to be one-dimensional as in I. Let $\rho(v, t)$ be the velocity distribution function for the dislocations. We shall retain all the assumptions made in I about $\rho(v, t)$. Then the starting equation for us is an extended Fokker–Planck equation for $\rho(v, t)$. It reads

$$\frac{\partial \rho(v, t)}{\partial t} + \frac{\partial J}{\partial v} = S \tag{1a}$$

0022-3727/82/010077 + 11 $02.00

where the current

$$J = -\beta v\rho + f\rho - q\frac{\partial \rho}{\partial v}$$

$$= -\left(\frac{B_0}{M}v - \frac{b\sigma_a}{M}\right)\rho - \frac{Q}{M}\frac{\partial \rho}{\partial v} \tag{1b}$$

and the source

$$S = -(\alpha - \theta v)\rho(v, t) - \frac{\mu}{\sqrt{N}}\int_{-\infty}^{\infty} \rho(v - v', t)\rho(v', t)\, dv'$$

$$+ \frac{h}{\sqrt{N}}\int_{-\infty}^{\infty} \rho(v - v', t)\frac{\partial \rho(v', t)}{\partial v'}\, dv'. \tag{1c}$$

In the above equation, B_0 is the drag coefficient, $b\sigma_a$ is the force acting on a unit length of a dislocation and Q is the velocity diffusion coefficient. M is the effective mass of a dislocation of unit length. The first term in equation (1c) corresponds to stopping of dislocations at precipitates etc with a rate constant α. The second term corresponds to breeding of new dislocations via multiple slip with a rate equal to $\theta v\rho$ (Alexander and Haasen 1968, p 93). We have assumed the breeding coefficient θ to be independent of σ_a as Dew-Hughes has done (1961). The third and the fourth terms correspond to the pairwise interaction of dislocations. These include two dislocations interacting to form a third one which is relatively immobile, the formation of dislocation locks, two dislocations interacting to form two other dislocations, two dislocations of opposite sign forming dipoles and the annihilation of two dislocations of opposite sign. The origin of these terms has been explained at length in I. (These processes are known to lead to the hardening of crystals. See Gilman (1968) p 147). The additional factor $N^{-1/2}$ has been introduced in order to represent the fact that the mechanism of hardening in crystals with diamond structure is different from that of LiF. In LiF, it is known that the internal stress arises due to the formation of dipoles, whereas in the present case it is the long range interaction between dislocations (Alexander and Haasen (1968) pp 97, 105). This includes the interaction of perpendicular dislocations. Thus it is the first three processes represented by the μ and h terms that should be modelled appropriately. To do this, consider two dislocations moving with velocity v and v'. The collision rate of these dislocations should be proportional to an 'impact parameter' which is the closest possible distance at which the interaction becomes significant. (Here it is helpful to see the analogy of our equation with the Boltzmann transport equation which has been stressed in I. In the case of molecules of spherical geometry, the impact parameter has the dimensions of area.) The average value of this distance necessarily decreases with the increase in density and it is to account for this variation of the impact parameter as a function of N that we have introduced the factor $N^{-1/2}$. From the above argument, it is clear that this factor would not arise in the case of LiF since the formation of dipoles is the dominant contribution to the internal stress. (The impact parameter in the case of formation of dipoles is of the order of a few lattice spacings and does not depend on N.)

From the analysis carried out to I, it is clear that it is the last term that gives rise to the change in the average velocity and hence to the change in the internal stress. The introduction of the factor $N^{-1/2}$ in the last two terms will account for the correct variation of the internal stress σ_i, i.e., $\sigma_i \sim N^{1/2}$ in contrast to $\sigma_i \sim N$ in LiF.

We shall assume the coefficients μ and h to be at most weak functions of stress. We shall also assume them to be independent of temperature. In I, we have further assumed

the deformation to be homogeneous. Although we shall retain this assumption some justification is necessary since in the present case, the deformation is inhomogeneous particularly when the initial density N_0 is small ($\sim 200\,\mathrm{cm}^{-2}$). Alexander and Haasen (1968, pp 93, 98, 99, 125) note that the deformation could be made nearly homogeneous by choosing large N_0 ($\sim 10^4\,\mathrm{cm}^{-2}$). Patel (1964) obtains reasonably homogeneous deformation due to oxygen precipitates. Yet another reason for retaining this assumption is that it allows for mathematical simplicity. The fact that this would not be a serious assumption is supported by the fact that the existing theories compare well with some aspects of experiments except when the sample size and N_0 are small (Reppich *et al* 1964, Peissker *et al* 1961, also see Alexander and Haasen 1968). Further, for the case of creep experiments considered here $N_0 \sim 10^4\,\mathrm{cm}^{-2}$. This falls in the region where the deformation is reasonably homogeneous.

It should be pointed out that we have taken simplified forms for f and θ terms in equation (1). Although, we have taken the correct form for the terms representing the interaction of positive and negative dislocations, the f and θ terms should be multiplied by appropriate step functions. We have shown in I that the results do not alter much except that the actual distribution should be bimodal (see § 6 of I).

At this point we would like to point out the differences between the mechanisms included in our starting equation and that of Peissker *et al* (1961). We have taken the breeding coefficient to be constant (as Dew-Hughes 1961 has done) whereas they take it to be proportional to the effective stress. In our theory, we have explicitly taken into account the pairwise interaction of dislocations, which they ignore. (Of course, if their equation for $\dot{N}$ is mathematically interpreted, they would have a loss term proportional to $N^{3/2}$ as in our case.) In spite of these differences, many of their results can be derived, in addition to deriving the expression for average velocity. As we will show most of our expressions are simple and yet they fit the data quite well. We will point out the specific differences as and when it is required.

In principle equation (1) can be solved in terms of a power series expansion developed in I. We will not attempt it here since we are not interested in the full distribution function $\rho(v, t)$. However, the reason for starting with an equation for $\rho(v, t)$ is to show that as the average density increases, an internal stress developes in the sample leading to a decrease in the average velocity. (This point, as well as the fact that all the moments depend on density, was the content of I.)

We shall use natural boundary conditions on $\rho(v, t)$, namely $\rho(v, t)$, $v\rho(v, t)$ and $\partial\rho(v, t)/\partial v$ as $v \to \pm\infty$. Using these and integrating equation (1) over v, we get

$$\frac{\mathrm{d}N}{\mathrm{d}t} = (-\alpha + \theta V)N - \mu N^{3/2} \tag{2}$$

where

$$\int_{-\infty}^{\infty} \rho(v, t)\,\mathrm{d}v = N(t) \tag{3}$$

and

$$\langle v\rangle N = VN = \int_{-\infty}^{\infty} v\rho(v, t)\,\mathrm{d}v. \tag{4}$$

Multiplying equation (1) by v and integrating, we get

$$\frac{\mathrm{d}V}{\mathrm{d}t} + (\beta + \mu N^{1/2})V = f - hN^{1/2} + \theta(\langle v^2\rangle - V^2) \tag{5}$$

where

$$\langle v^2 \rangle N = \int_{-\infty}^{\infty} v^2 \rho(v, t)\, dv. \tag{6}$$

In deriving equation (5) we have made use of equation (2). In a similar way, one can obtain equations for all higher moments. All these equations will be coupled. However, since we need only N and V, we decouple these equations using suitable approximations.

Consider the steady-state value of N

$$N^{1/2}(\infty) = N_S^{1/2} = [\theta V(\infty) - \alpha]/\mu. \tag{7}$$

Since $N_S > N(t)$ for all t (i.e. N is a monotonically increasing function of t), we have

$$\mu N^{1/2}/\beta < [\theta V(\infty) - \alpha]/\beta \ll 1$$

since $\beta \gg 1$ ($\beta \sim 10^9 \sim 10^{12}\ s^{-1}$. See Gilman (1969) p 173 and I. See also table 1.) Thus we can drop the μ term in equation (5). The term $[\langle v^2 \rangle - V^2]$ should be expected to be small since it corresponds to dispersion in velocities. In addition $\theta \ll \beta$. We shall later show that this term can also be ignored. Then we have

$$M \frac{dV}{dt} + B_0 V = b\sigma_a - hN^{1/2}M = b(\sigma_a - \sigma_i) = b\sigma_{eff}. \tag{8}$$

The quantity

$$\sigma_i = hN^{1/2}M/b = f_i M/b \tag{9}$$

corresponds to the internal stress and σ_{eff} is the effective driving stress. (b is the magnitude of the Burgers vector.) Since β^{-1} is very small, the average velocity attains its steady-state value very fast after the stress is applied. Then

$$V(t \gg \beta^{-1}) = \frac{b\sigma_{eff}}{B_0} = \frac{b(\sigma_a - \sigma_i)}{B_0} = \frac{f - hN^{1/2}}{\beta}. \tag{10}$$

We shall call $f/\beta = B$, the initial velocity which is the velocity attained by dislocations under the absence of any internal stress.

There is another time scale which is large compared β^{-1} which corresponds to the duration of plastic flow. This appears explicitly in the equation for $\dot{N}$. If we accept the point that the time scale for the growth of N is much larger than β^{-1}, then we can use equation (10) in equation (2) to obtain

$$\frac{dN}{dt} = (B\theta - \alpha)N - \left(\mu + \frac{h\theta}{\beta}\right) N^{3/2} \tag{11}$$

where $B = f/\beta = b\sigma_a/B_0$. The solution of this equation can be readily obtained and is

$$N(t - t_0) = \frac{N_S}{\{1 + [(N_S/N)^{1/2} - 1] \exp[-\eta\beta(t - t_0)]\}^2} \tag{12a}$$

with

$$N_S = (B\theta - \alpha)^2 \Big/ \left(\mu + \frac{h\theta}{\beta}\right)^2 \tag{12b}$$

$$\eta\beta = (B\theta - \alpha)/2 \qquad N(t = t_0) = N_0. \tag{12c}$$

The equation for N that has been used by Alexander and Haasen (1968) and Piessker *et*

al (1961) has an extra term of N^2. Whereas the solution given by equations (12) is simple, their solution has a complicated form. Indeed, solution of their equation for $N^{1/2}$ is a transcendental equation. Yet many of our results are identical to their results. First, the saturation value of N given by (12*b*) for values of parameters for which creep data fit well, namely, $\alpha = 0$ and $\mu \ll h\theta/\beta$ exactly matches their result

$$N_S = \left(\frac{B}{h/\beta}\right)^2 = (f/h)^2 = \left(\frac{b\sigma_a}{Mh}\right)^2.$$

To see this, consider equation (10) and compare it with their relation

$$V = \bar{B}(T)\,\sigma_{\text{eff}} = \bar{B}(T)(\sigma_a - A\sqrt{N}) = \frac{b}{B_0}\left(\sigma_a - \frac{hM}{b}\sqrt{N}\right) \tag{13}$$

we get

$$A = \frac{hM}{b} \qquad \bar{B}(T) = \frac{b}{B_0(T)} = \frac{b\beta}{M}.$$

Thus

$$N_S = \sigma_a^2/A^2 = f^2/h^2. \tag{14}$$

The second result which agrees with the earlier work is the density at the point of inflection which can be obtained from equation (12)

$$N_{IN}^{1/2} = \tfrac{2}{3}N_S^{1/2} \tag{15}$$

where the subscript corresponds to the point of inflection of N. This is exactly the same as their result. The third result (which we will show later) which agrees with theirs is $\dot{\varepsilon}(t_i) \sim \sigma_a^3$. Perhaps, this is not surprising since the dominant terms in the equation for $\dot{N}$ are of the same nature. However, the point we want to stress is that it is the term corresponding to dislocation interaction in equation (1) that automatically leads to an increase in the interval stress.

In deriving the expression for σ_{eff}, we have assumed that $\theta(\langle v^2\rangle - V^2)$ can be ignored in comparison with the $h\sqrt{N}$ term. We shall show that this assumption is valid. It is reasonable to assume that the dispersion

$$\langle v^2\rangle - V^2 \sim B^2.$$

Although V reduces monotonically, as for the order of terms

$$B \sim (h/\beta)\sqrt{N} \sim (\langle v^2\rangle - V^2)^{1/2}$$

$$\frac{h}{\beta}N^{1/2} \cdot B\theta \sim \theta(\langle v^2\rangle - V^2)^{1/2}B \sim (\langle v^2\rangle - V^2).$$

But $\theta B/\beta \ll 1$ (the ratio of the two time scales in the problem). Thus

$$h\sqrt{N} \gg \theta(\langle v^2\rangle - V^2).$$

3. The creep law

Due to the simplicity of the expressions for both N and V, the Orowan equation

$$\dot{\varepsilon} = bNV$$

can be integrated. The resulting creep law is

$$\varepsilon - \varepsilon_0 = -\frac{bN_S}{\eta\beta}\left(B - \frac{h}{\beta}N_S^{1/2}\right)\left[\ln\frac{N_S^{1/2} - N^{1/2}}{N_S^{1/2} - N_0^{1/2}} + \left(\frac{N}{N_S}\right)^{1/2} - \left(\frac{N_0}{N_S}\right)^{1/2}\right] + \frac{bh}{2\eta\beta^2}N_S^{1/2}(N - N_0). \tag{16}$$

where $\varepsilon_0 = \varepsilon(t = t_0)$ corresponds to ε at an initial density N_0 at t_0. It is possible to estimate the value of N_0 using equations (12) and (16). We shall discuss this a little later.

Table 1. Values of the parameters used in equation (16).

Parameter	Value	Remarks
$B = f\beta$	1.79×10^{-4} cm s †	at $T = 803$°C, $\sigma_a = 0.5$ kg mm^{-2}
β	10^{6} s$^{-1} \sim 10^{13}$ s^{-1} ‡	
θ	10 cm^{-1} §	
μ	$\leqslant 10^{-7}$ cm s^{-1}	
h/β	1.61×10^{-7} cm^2 s^{-1}	at $T = 803$°C
N_S	4.9×10^{6} cm^{-2}	
N_0	2×10^{4} cm^{-2} §	

† Value consistent with near linear power law of Alexander and Haasen (1968).
‡ Ananthakrishna and Sahoo (1981).
§ Alexander and Haasen (1968).

In the following, we shall show that the point of inflection on the creep curve is different from that on the ε curve. Differentiating equation (16), we get

$$N_{i\varepsilon}^{1/2} = \tfrac{2}{3}B/(h/\beta) \tag{17}$$

where the subscript corresponds to the point of inflection on the ε curve. Further, using equation (12), we get

$$t_{i\varepsilon} - t_0 = -\frac{1}{\eta\beta}\ln\frac{(N_S^{1/2} - N_{i\varepsilon}^{1/2})\,N_0^{1/2}}{(N_S^{1/2} - N_0^{1/2})\,N_{i\varepsilon}^{1/2}}. \tag{18}$$

Clearly, $N_{i\varepsilon}^{1/2}$ is different from $N_{iN}^{1/2}$. Since μ and α are positive and nonzero, $N_{i\varepsilon}^{1/2} \geqslant N_{iN}^{1/2}$, the equality holding only when $\mu = \alpha = 0$. Similarly, it can be verified $t_{i\varepsilon} \geqslant t_{iN}$. From equation (18), it can be shown that there will be no point of inflection if $N_{i\varepsilon}^{1/2} \leqslant N_0^{1/2}$.

We shall now show that $\dot{\varepsilon}(t_i) \sim \sigma_a^3$. Using equation (14) in the Orowan equation, we get

$$\dot{\varepsilon}(t_i) = \left(\frac{4}{27}\frac{b\bar{B}(T)}{A^2}\right)\sigma_a^3. \tag{19}$$

This is exactly the same result as derived by Alexander and Haasen (1968). This, of course, is a direct consequence of equation (17). We shall apply equation (16) to creep in Si. The data are that of Reppich *et al* (1964). The parameters which enter into the calculation are N_0, N_S, θ, B, h/β and μ. (We shall use $\alpha = 0$ to minimise the number of adjustable parameters.) The only adjustable parameter is $h\beta$. The values of N_0, θ and

B can be obtained from the experiments. The values of N_0 and θ we use are those given by Reppich *et al* (1964). The average velocity $\langle v \rangle = B$ is obtained by the near linear power law given by Alexander and Haasen (1968). (In principle it can be obtained from experiments on velocity measurement. The data $V \sim \sigma^n$ at the temperature at which creep work is performed are not available.) A rough value of N_S can be obtained by either $N - \varepsilon$ curve for the particular σ and T or it can be estimated from equation (16) and knowing the value of the strain. (For this particular case $N_S \sim 10^7$ cm^{-2}.) An estimate of the value of h/β can be found from the constraint $B \leqslant (h/\beta)N_S^{1/2}$ (see equation (10)). Then a best fit is attempted with the values of parameters in the ranges estimated or those given by experiments. The best fit we obtain for creep at $\sigma_a = 0.5$ kg mm^{-2} at $T = 803$°C is for parameter values $\eta\beta = B\theta/2 = 1.79 \times 10^{-3}$ s^{-1}, $N_S = 4.9 \times 10^6$ cm^{-2} and $h/\beta = 1.61 \times 10^{-7}$ cm^2 s^{-1}. The value of μ is fixed by equation (12b) and $\mu = 9.2 \times 10^{-7}$ cm s^{-1}. Thus *h/β is the only adjustable parameter as in* I. It can be seen from figure 1 that the data fit very well. In order to fit the data at $T = 853$°C, we can assume that the velocity has a Boltzmann temperature dependence with an activation energy 2 eV (Alexander and Haasen 1968) and scale both B and h/β by the factor

$$\exp \frac{E(T_2 - T_1)}{kT_1T_2}$$

where $T_2 > T_1$. Instead we have chosen the best values for B and h/β (keeping both N_S and N_0 fixed) that fit the creep data at $T = 835$°C and used their respective values at $T = 803$°C to obtain E. We get $E = 1.75$ eV which compares well with the experimental value. This is the average of the values obtained for $\eta\beta$ and h/β. (It may be noted that $\beta = M\bar{B}(T)/b$). The calculated creep curve agrees well with the experimental one at $T = 856$°C also (figure 1.)

Creep is a sensitive function of the parameter h/β. Figure 1 contains a plot for a slightly different value of h/β from the one that fits the data.

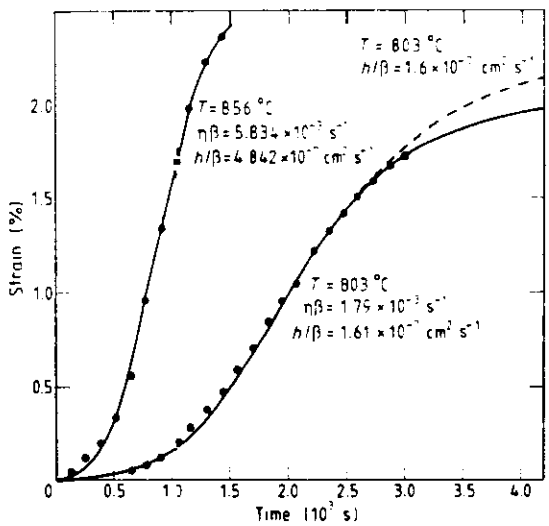

Figure 1. Calculated and experimental creep curves for $\sigma_a = 0.5$ kg mm^{-2} at $T = 803$°C and $T = 856$°C. Variation with respect h/β is also shown (broken curve). $N_S = 4.9 \times 10^6$ cm^{-2}; $N_0 = 2 \times 10^4$ cm^{-2}.

To study the variation with respect to the initial density it is necessary to estimate the value of ε_0 for a bad sample with a large initial density say N_0'. This would be necessary since otherwise, the asymptotic part of the creep curve for large N_0 would lie below that for a creep curve with a small N_0 as in the case of curve D in figure 1 of I. This unphysical feature arises due to the fact that ε_0 is not insignificant for large N_0. This problem has been examined in detail in a paper which mainly discusses the mathematical properties of the statistical model for dislocation dynamics introduced in I (Ananthakrishna 1981, hereafter referred to as II). Here, we shall summarise the results with appropriate modifications. Following II, one can show that

$$N(t' - t) = N(t' - t_0) \tag{20}$$

where $t' > t > t_0$ and t_0 referring to a reasonably pure sample. $N(t' - t)$ is given by

$$N(t' - t) = N_S \Big/ \left\{1 + \left[\left(\frac{N_S}{N'(t - t_0)}\right)^{1/2} - 1\right] \exp - \eta\beta(t' - t)\right\}^2 \tag{21}$$

with the identification that $N'(t - t_0)$ is the density at time t starting with N_0 at t_0. (This can be proved by taking equation (1) as the equation for the conditional density $\rho(vt|v_0t_0)$

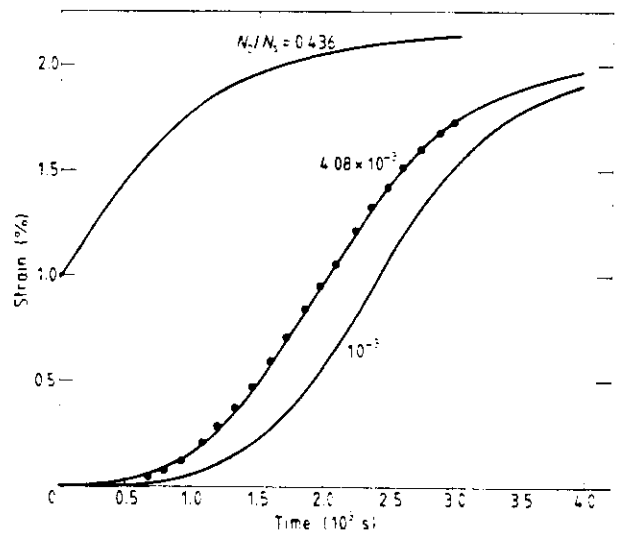

Figure 2. Calculated creep curves for various values of N_0. $N_S = 4.9 \times 10^6\ \text{cm}^{-2}$; $h\beta = 1.61 \times 10^{-7}\ \text{cm}^{-2}\,\text{s}^{-1}$; $\eta\beta = 1.79 \times 10^{-3}\ \text{s}^{-1}$.

and using the fact that decoupling of the initial and the final states occurs for $t \gg \beta^{-1}$. See II.) Similarly, one can obtain an $\varepsilon - t$ plot for a pure sample for which $\varepsilon_0 \simeq 0$ holds. From these two one can assign ε_0' for a bad sample with a large N_0'. This means that one has a unique N–ε curve and different samples correspond to starting from different points on the N–ε curve. Figure 2 shows the ε–t plots for three different values of N_0. (In principle $N_0 = 2 \times 10^4\ \text{cm}^{-2}$ should have a small initial strain, which is quite small and therefore ignored on the plot.) For the creep curve with a large N_0 there is no point of inflection, since it violates the condition (18). The other graphs are self-explanatory.

4. A scaled creep law

We shall first scale N with respect to t_i. We shall also assume that $\alpha = 0$ and $\mu \ll h\theta/\beta$ as has been the case for the creep data. Under these assumptions $N_S^{1/2} \simeq f/h = \sigma_a/A$. Further, $N_{iN} \simeq N_{i\varepsilon} = N_i$, and, $t_{i\varepsilon} \simeq t_{iN} = t_i$ given by equation (18). The dependence of t_i on temperature T comes from $\eta\beta = B\theta/2 = \sigma_a\bar{B}(T)$. Defining $\tau = t/t_i$, and using equation (18) in equation (12), we get

$$N^{1/2}(\tau - \tau_0) = N_S^{1/2}\Big/\left\{1 + \left[\left(\frac{N_S}{N_0}\right)^{1/2} - 1\right]^{1-\tau+\tau_0}\left[\left(\frac{N_S}{N_i}\right)^{1/2} - 1\right]^{\tau-\tau_0} \times \exp[-\eta\beta t_0(\tau - \tau_0)]\right\}. \tag{22}$$

This quantity depends on temperature due to the fact that t_0 is nonzero. However, since t_0 is an arbitrary reference time it can be taken to be zero as long as we require $N_0/N_S \ll 1$. (See § 3.) Using this and equation (15) we get

$$N^{1/2}(\tau) = N_S^{1/2}\Big/\left\{1 + 2^{-\tau}\left[\left(\frac{N_S}{N_0}\right)^{1/2} - 1\right]^{1-\tau}\right\} \simeq N_S^{1/2}\Big/\left[1 + 2^{-\tau}\left(\frac{N_S}{N_0}\right)^{(1-\tau)/2}\right]. \tag{23}$$

Clearly, this quantity is independent of T. (Note that it is not necessary to assume a Boltzmann type of dependence for $\beta^{-1} = \bar{B}(T)(M/b)$). $N(\tau)$ depends only on $\sqrt{N_S}/\sqrt{N_0}$ and τ. From equation (23), $N^{1/2}(1) = \frac{2}{3}N_S^{1/2}$.

Now consider equation (16). It may be readily verified that a variable transformation $t = \tau t_i$ leads to an expression for ε where $N(t)$ is replaced by $N(\tau)$. Then

$$\varepsilon(1) - \varepsilon(0) = -\frac{bN_S}{\eta\beta}\left(B - \frac{h}{\beta}N_S^{1/2}\right)\left[\ln\frac{N_S^{1/2} - N_i^{1/2}}{N_S^{1/2} - N_0^{1/2}} + \left(\frac{N_i}{N_S}\right)^{1/2} - \left(\frac{N_0}{N_S}\right)^{1/2}\right] + \frac{bh}{2\eta\beta^2}N_S^{1/2}(N_i - N_0). \tag{24}$$

Then the scaled creep law takes the form

$$\frac{\varepsilon(\tau) - \varepsilon(0)}{\varepsilon(1) - \varepsilon(0)} = \left\{-N_S^{1/2}(f - hN_S^{1/2}) \times \left[\ln\frac{N_S^{1/2} - N^{1/2}(\tau)}{N_S^{1/2} - N_0^{1/2}} + \left(\frac{N(\tau)}{N_S}\right)^{1/2} - \left(\frac{N_0}{N_S}\right)^{1/2}\right] + \frac{h}{2}(N(\tau) - N_0)\right\}\left\{-N_S^{1/2}(f - hN_S^{1/2})\left[\ln\frac{N_S^{1/2} - N_i^{1/2}}{N_S^{1/2} - N_0^{1/2}} + \left(\frac{N_i}{N_S}\right)^{1/2} - \left(\frac{N_0}{N_S}\right)^{1/2}\right] - \frac{h}{2}(N_i - N_0)\right\}^{-1} \tag{25}$$

where we have used $B = f/\beta$. Since $N(\tau)$ is independent of temperature, the scaled creep law is also independent of temperature. To see that it is independent of stress also, consider the first term in the numerator and the denominator. Since we have assumed $\mu \ll h\theta/\beta$, it follows that $N_S \sim f^2 \sim \sigma_a^2$. The second term in the numerator and the

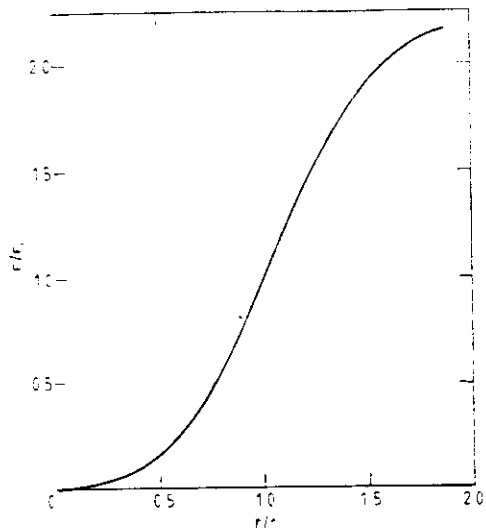

Figure 3. The scaled creep law as a function of the dimensionless parameter $\tau = t/t_c$.

denominator also have a factor N_S, if we drop N_0 (see equation (12)). Thus the dependence on σ_a also disappears. The other terms are in the nature of ratios in which N_S cancels out if we use $N_0/N_S \ll 1$. Thus, the scaled creep law is independent of stress and temperature for small N_0. The applicability is restricted to such values of N_0 for which homogeneous deformation occurs. Experimentally it is found that below a certain threshold value of N_0 the deformation proceeds inhomogeneously (Alexander and Haasen 1968, p 39). (Of course, we have used the assumption that μ and h are weak functions of stress.) It depends weakly on the ratio N_S/N_0, even for small N_0. For a fixed value of N_S/N_0, the scaled creep law is identical for various $\eta\beta$ and h/β values as long as $\mu \ll h\theta/\beta$. Figure 3 shows the scaled creep law as a function of τ. Experiments on Si support the above prediction that results for different σ_a and T but with the same N_0 fall on one single creep curve (Peissker *et al* 1961).

It is also clear that the creep law derived in I for LiF can be easily cast into the scaled form.

5. Discussion

Following the method developed in I and starting from a slightly different form for the term representing the pairwise interaction of dislocations, we have shown that the average velocity decreases as the square root of the average density, i.e., $\sigma_i \sim N^{1/2}$. A new creep law is derived and applied to Si. The form of the creep law is simple and can be cast into a scaled form. The scaled creep law is shown to be independent of stress and temperature for small N_0, μ and $\alpha = 0$. The value of the saturation density we estimate is perhaps lower than the experimental value by a factor of four. This might suggest that the time development of N should be slower than that given by equation (12). In spite of this several of our results agree with Peissker *et al* (1961) and with experimental findings.

The above crep law is perhaps applicable to other materials where $\sigma_i \sim N^{1/2}$. In

particular, if $V \sim (\sigma_a - A\sqrt{N})^m$ and if m can be approximated to be an integer, then for such stresses where $nAN^{1/2} < \sigma_a$ holds, it is fair to approximate $V \sim \sigma_a^n[1 - (nA/\sigma_a)N^{1/2}]$. Attempts are under way to test the applicability of the creep law to other materials and to tensile test situations.

References

Alexander H and Haasen P 1968 *Solid State Physics* **13** 27 (New York: Academic)
Ananthakrishna G 1981 *J. Phys. D: Appl. Phys.* **14** 2091
Ananthakrishna G and Sahoo D 1981 *J. Phys. D: Appl. Phys.* **14** 699
Dew-Hughes D 1961 *IBM J. Res. Dev.* **5** 279
Gilman J J 1969 *Micromechanics of Flow in Solids* (New York: McGraw Hill)
Patel J R 1964 *Disc. Faraday Soc.* **38** 201
Peissker E, Haasen P and Alexander H 1961 *Phil. Mag.* **7** 1279
Reppich B, Haasen P and Ilschner B 1964 *Acta Metall.* **12** 1283
Webster G A 1966 *Phil. Mag.* **14** 775

J. Phys. D: Appl. Phys., 14 (1981) 2081–90. Printed in Great Britain

A model based on nonlinear oscillations to explain jumps on creep curves

G Ananthakrishna and Debendranath Sahoo
Materials Science Laboratory, Reactor Research Centre, Kalpakkam 603 102, Tamil Nadu, India

Received 25 February 1981

Abstract. A dislocation transformation model with three types of dislocations—namely the mobile, the immobile and those with clouds of solute atoms—is considered. Some physically reasonably reactions are postulated, leading to a coupled set of nonlinear differential equations for the rate of change of their densities. The basic idea of Cottrell's mechanism has been incorporated. It is shown that these equations admit a class of periodic solutions called limit cycles which are typical of nonlinear systems, suggesting that nonlinearity plays a fundamental role in our model. The rate equations are solved on a computer to obtain the oscillatory behaviour of the densities and hence leading to steps on the creep curve. The theory predicts that there is a range of temperature over which the phenomenon can occur, in agreement with the experiment of Zagorukuyko *et al*. The theory also reproduces other normal forms of creep curves.

1. Introduction

The phenomenon of repeated discontinuous yielding of materials is of considerable interest in materials science since it touches upon the basic question of the stability of materials. This phenomenon manifests itself either as serrations (also known as jerky flow and as the Portevin–Le Chatelier effect) or as steps on the stress–strain curve depending on whether the material is subjected to a constant strain rate or to a constant stress rate, respectively. Bell (1973) has discussed these effects, especially the case of stepped response. In a creep test, a material is subjected to a constant stress, i.e. to zero stress rate and hence stepped response is also to be expected in a creep test. This has been observed in β-brass by Ardley and Cottrell (1953), in zinc by Zagorukuyko *et al* (1977), and in steel by Da Silveira and Monteiro (1979). According to Lubahn and Felgar (1961), steps on creep curves were first observed in copper by Andrade (1910) who called it 'copper quakes'. Lubahn and Felgar (1961) cite some further references. In contrast to the case of constant strain rate and that of constant (non-zero) stress rate, the data available on stepped response on creep curves (to be referred to as staircase creep, or SCC) are rather limited. There seems to be no detailed theory for SCC in the literature. Explanations for discontinuous yielding that have been proposed include the solute atom hypothesis of Cottrell (1953), an improved version of this theory by McCormic (1972) and Van den Beukel (1975, 1980), the Coulomb friction analogue of Bodner and Rosen (1967) and the particle-wave hypothesis of Fitzgerald (1966).

In this paper we propose a dislocation transformation model for SCC. It is an extension of our earlier work (Ananthakrishna and Sahoo 1978, Sahoo and Ananthakrishna

0022-3727/81/112081+10 $01.50

1982) in which we developed a theory of creep with the assumption that mobile (denoted as 'g') and immobile (denoted as 's') dislocations interact and transform into each other. In the present paper, which can be read independently of this earlier work, we introduce a third species of dislocations (denoted as 'i') which are surrounded by clouds of solute atoms. These are dislocations moving much slower compared to the mobile species and ultimately becoming immobile. Introduction of the species i is reminiscent of the basic feature of Cottrell's (1953) theory of dynamic strain-aging, i.e., as the dislocations move with a velocity below a certain threshold, the solute atoms diffuse and catch up with them, thereby arresting their motion. Thus we have tried to incorporate the essence of Cottrell's (1953) theory. The repetition of this mechanism is brought about via interactions among the three species of dislocations. The rate equations for the densities of the three species form a coupled system of nonlinear differential equations. *Nonlinearity plays a crucial role* in our theory. For a certain range of values of the rate constants, this system of equations exhibits time-periodic solutions called limit cycles which are characteristic of nonlinear systems (Minorsky 1962). The existence of a limit cycle is proved. A computer analysis of these rate equations is carried out to obtain the periodic solutions. Numerical integration of the Orowan equation gives rise to SCC. We obtain only the secondary creep region. It is shown that there is a fixed range of strain-rate values and of temperature over which SCC can be observed, consistent with the experimental results of Zagorukuyko *et al* (1977). For values of rate constants outside the domain of instability, normal creep curves are obtained. Finally we wish to emphasise that we have made no attempt to explain any particular data and that *our interest is only to suggest a possible mechanism which can give rise to* SCC.

2. The model

We propose the following reactions or transformations between the species g, s and i.

$$g \xrightarrow{\theta V_g} g+g \tag{1a}$$

$$g+g \xrightarrow{k\mu'/2} s+s \tag{1b}$$

$$g+g \xrightarrow{(1-k)\mu'/2} 0 \tag{1c}$$

$$g+s \xrightarrow{\mu} 0 \tag{1d}$$

$$s \xrightarrow{\lambda} g \tag{1e}$$

$$g \xrightarrow{\alpha} i \tag{1f}$$

$$i \xrightarrow{\alpha'} s. \tag{1g}$$

The first reaction describes generation of dislocations by the multiple cross-glide mechanism (Gilman and Johnston 1962 and references therein); θ is the breeding constant and V_g, the average velocity of the species g. The second reaction (1*b*) describes the conversion of two g's into two s's. The reactions (1*c*, *d*) describe the annihilation of g with g and g with s. Here k is a number very close to but less than unity, i.e. the reaction (1*c*) is very slow. The reaction (1*e*) describes mobilisation of s due to the applied stress or due to thermal activation. The reaction (1*f*) corresponds to a dislocation acquiring a cloud of

solute atoms and moving along with the cloud. As the solute atoms progressively gather around dislocations, these slow down and finally stop. When this process is complete, i is regarded as having transformed into s with a rate α'. This is expressed by the reaction (1*g*). We disregard the continuous decrease in the velocity of i and assume that i moves with a constant velocity (much less than V_g) till it stops suddenly, changing thereafter to s. Admittedly, this is a gross idealisation, but we feel that it still retains the essential features of dynamic strain-aging.

Let N_g, N_s and N_i denote the densities of g, s and i species respectively. The rate equations are:

$$\dot{N}_g = \theta V_g N_g - \mu' N_g^2 - \mu N_g N_s + \lambda N_s - \alpha N_g \tag{2}$$

$$\dot{N}_s = k\mu' N_g^2 - \mu N_g N_s - \lambda N_s + \alpha' N_i \tag{3}$$

$$\dot{N}_i = \alpha N_g - \alpha' N_i. \tag{4}$$

Here we assume that θ, μ, μ', α, α' and λ are constants for a given stress at a given temperature, i.e. these are constants in a creep test. (In reality, these could be weakly dependent on stress.) The assumption that θ and μ are constants has been made earlier by Webster (1966), Li (1963) and Gilman (1965). The parameter α is expected to depend on the diffusion constant of the solutes, their concentration and the velocity of i. The parameter α' is the drag coefficient of i. It may be noted that the reactions (1(*a*)–(*f*)) are assumed to be occurring homogeneously over the entire sample.

For convenience, we make equations (2)–(4) dimensionless by substituting

$$\left.\begin{aligned} x &= (\mu/\lambda) N_g \\ y &= (\mu/\theta V_g) N_s \\ \text{and} \\ z &= (\mu\alpha'/\lambda\alpha) N_i. \end{aligned}\right\} \tag{5}$$

Then we obtain

$$\frac{dx}{d\tau} = (1-a)x - bx^2 - xy + y \tag{6}$$

$$\frac{dx}{d\tau} = b(kbx^2 - xy - y + az) \tag{7}$$

$$\frac{dz}{d\tau} = c(x-z) \tag{8}$$

where

$$\left.\begin{aligned} \tau &= \theta V_g t \\ a &= \alpha/\theta V_g \\ b &= \lambda/\theta V_g \end{aligned}\right\} \tag{9}$$

and

$$c = \alpha'/V_g\theta.$$

Here we have taken $\mu = \mu'$ in order to minimise the number of parameters.

3. Stability analysis and existence of limit cycles

The above set of equations form a nonlinear system. Under well known conditions (Minorsky 1962), these admit periodic solutions called limit cycles for a certain range of values of parameters a, b, c and k. Although the method of investigation pursued is well known, for the sake of completeness we briefly outline the procedure used. Limit cycles are special classes of solutions which are isolated closed trajectories in the phase plane (x, y, z) such that any trajectory which is sufficiently close to it either approaches or recedes from it. Such closed trajectories can only arise in nonlinear systems. The existence of limit cycles is generally preceded and aided by an investigation of the global properties of these equations by linearising around the steady-state values x_s, y_s and z_s. The stability of the system is decided by the nature of singular points, namely node, focus, saddle point and centre. These correspond to the four possible combinations of the eigenvalues ω_1, ω_2 and ω_3 of the linearised forms of equations (6)–(8) namely

$$\frac{d\psi}{d\tau} = \mathbf{W}\psi \tag{10}$$

where ψ is a column vector $(x-x_s, y-y_s, z-z_s)$ and $\mathbf{W}$ is a 3×3 linearised matrix (around x_s, y_s and z_s). A node arises when all ω are of the same sign, and a saddle point when one of these is of opposite sign; a focus occurs when two complex conjugate roots exist and a centre when one root is identically zero and the other two are purely imaginary. (In the last case the nature of the singular point may have to be analysed more carefully. See Minorsky 1962.)

An attractive limit cycle exists if there is a surface surrounding an unstable focus into which all trajectories enter. For this we first look for a domain in the parameter space (a, b, c, k) when two of the roots are complex with at least one of them having a positive real part and then show that such a surface exists. Using this procedure we have shown in the Appendix that a limit cycle exists. The only constraints that we have on the values of the parameters are that $a \leqslant 1$ (which is a consequence of the fact that the total rate of production of dislocations is positive), $k \lesssim 1$ and a, b and $c > 0$. Also we have N_g, N_s and $N_i > 0$.

4. Staircase creep

Analytical solution of the rate equations (6)–(8) for arbitrary values of the parameters is difficult to obtain. (The stability analysis and the existence of a limit cycle are given in the Appendix.) However, these equations can be solved on a computer. To do this, the form of V_g as a function of the effective stress σ^* should be known. σ^* is itself a function of the total density of dislocations $N\ (=N_g+N_i+N_s)$. For simplicity of calculation we assume V_g to be constant. We shall show shortly that this assumption, although unphysical, retains the qualitative aspects of SCC. With this assumption we have solved equations (6)–(8) for some values of parameters in the instability range using the Harwell subroutine package DCO1AD. (Although for all $0.5 \leqslant k \leqslant 1$, the instability and the limit cycle exist, all the results reported are for $k = 1$.) Figure 1 shows the oscillatory patterns of N_g, N_s and N_i. The density N_i has the same pattern as N_g (not shown in the figure). As can be seen from figure 1, N_g varies over two orders with fast rise and fall times. In contrast, both N_s and N vary slowly except for the initial fast rise. (See figure 1.) The total density has an initial fast rise time reaching a near steady-state value about which it

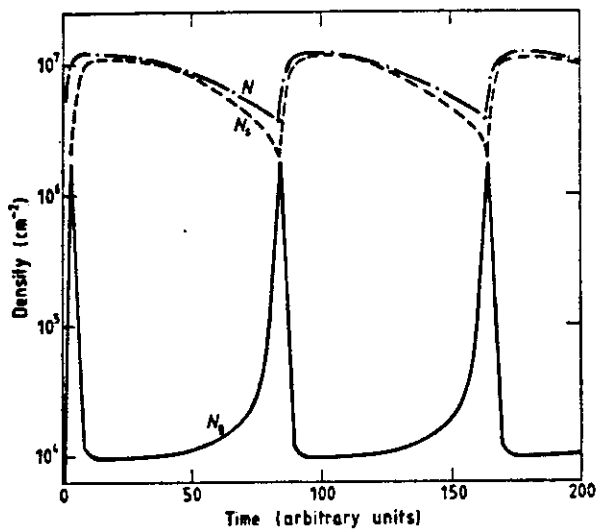

Figure 1. A plot of N_g, N_s and N as a function of time for $a=0.43$, $b=0.0007$, $c=0.04$. $V=0.3$ cm s^{-1}; $\mu=10^{-6}$ cm^2 s^{-1}; $N_{g0}=N_{s0}=N_{i0}=10^5$ cm^{-2}.

changes with a subsequent *slow* periodic variation. For this reason, V_g which depends on time only through $N(t)$ (since σ^* is a function of $N(t)$), changes from its initial value to a near steady-state value very quickly, determined by the near steady value of $N(t)$. Hence any different choice of V_g as a function $\sigma^*(N)$, should not result in any qualitative change in the densities or in the nature of the creep curve. The period of oscillation of x, y and z depends on the imaginary part of the eigenvalue of $\mathbf{W}$. From our numerical calculation, we find that $10^{-4} < \mathrm{Im}\,\omega_l \lesssim 10^{-1}$ and in most cases $\mathrm{Im}\,\omega_l < 10^{-2}$. In order that the oscillatory patterns of N_g, N_s and N_i are observable, an appropriate value of θV_g should be chosen. The value we have chosen is $V_g \sim 0.1$ s^{-1} and $\theta = 30$ cm^{-1}. We have chosen reasonable values of N_s, N_g and N_i compatible with strains of the order of 1 or 2%. This is done by fixing $\mu \sim 10^{-6}$ cm^2 s^{-1}. Then SCC is obtained by numerically integrating the Orowan equation $\dot{\epsilon} = b(V_g N_g + V_i N_i)$ with V_i chosen to be a fraction of V_g (b is the magnitude of the Burgers vector). The staircase creep obtained for the special case $V_i = 0$ is presented in figure 2. It may be noted that we obtain only the secondary creep due to the fact that all the densities attain their oscillatory states very fast. Very often this phenomenon sets in after the primary stage only (see for example, Zagorukuyko *et al* 1977 and Da Silveira and Monteiro 1979). Therefore, this feature is not unphysical. However, if we desire to have a primary creep region, it would be necessary to introduce another time scale slower than $(\theta V_g)^{-1}$.

Our model also predicts a crucial result which is in agreement with experiment—namely, that there is an upper and a lower bound for the asymptotic creep rates for which the SCC occurs. This can be seen from the fact that the period of oscillation $T \sim 2\pi/\theta V_g \mathrm{Im}\,\omega_l$, with $10^{-4} \leqslant \mathrm{Im}\,\omega_l \lesssim 10^{-1}$. The exact range of $\mathrm{Im}\,\omega_l$ is unimportant as we have not modelled any particular system. (The range of $\mathrm{Im}\,\omega_l$ will depend on the nature of the system and hence the basic mechanisms prevailing in the system.) So, corresponding to the bounds of $\mathrm{Im}\,\omega_l$, V_g has to have appropriate bounds (over three orders in this case) if we wish to have observable steps. This implies that the phenomenon can only be observed over a fixed range (at most three orders) of $\dot{\epsilon}$. For the present case, if the variation in densities as functions of parameter θV_g is considered, the range of $\dot{\epsilon}$ will be

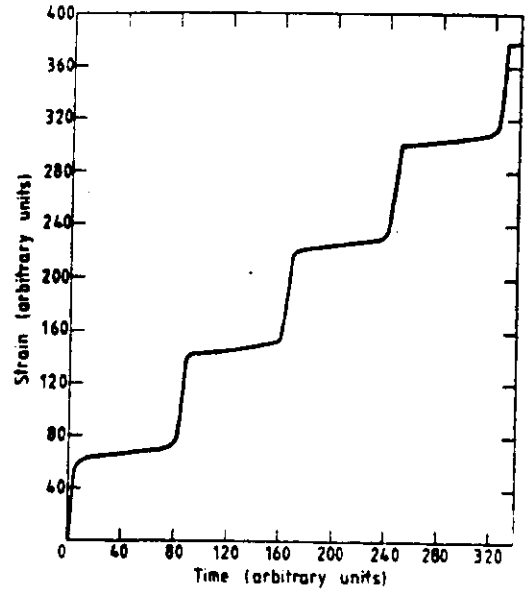

Figure 2. scc for the same values of parameters a, b and c as figure 1.

slightly less than three orders. Since V_g is temperature dependent (for a fixed stress), this phenomenon can only occur over a fixed range of temperature as corroborated by the experimental result of Zagorukuyko *et al* (1977). Another result that can be seen is that the phenomenon should start smoothly as temperature is raised, which is also confirmed by Zagorukuyko *et al* (1977).

The model generates a scc with slowly damping steps for values of parameters just outside the instability domain in the parameter space (a, b, c) as shown in figure 3. In this case, we do not have a limit cycle. The oscillatory part arises due to $\mathrm{Im}\,\omega_i$; but $\mathrm{Re}\,\omega_i$ for all i is negative, which damps the oscillations in N_g, N_i and N_s.

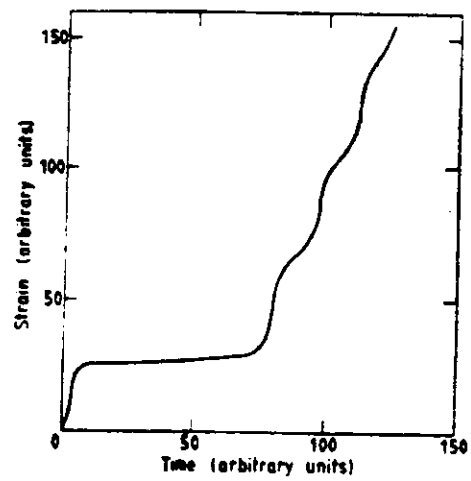

Figure 3. Damped scc for values of parameters just outside the instability domain $a=0.41$, $b=0.0003$, $c=0.16$.

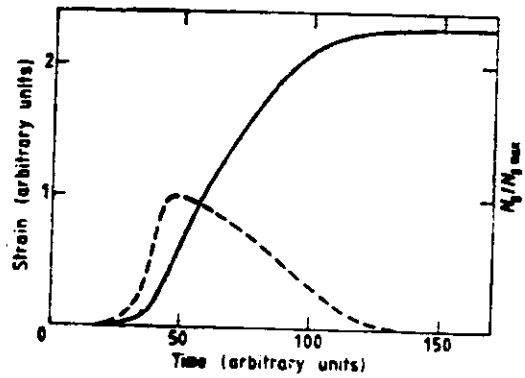

Figure 4. A normal type of creep curve for a value of c much outside the instability domain (full curve). $a=0.41$, $b=0.0001$, $c=0.0200$. The broken curve shows the behaviour of the mobile dislocation density.

Finally, it produces the usual type of creep curve for values of parameters falling outside the instability domain. To see the correspondence, consider the value of c to be small compared to a and lying outside the instability domain. This means that gradually dislocations are retarded and surrounded by solute atoms but cannot get rid of these. This leads to the same kind of variation of the mobile dislocations as we have obtained earlier by a dislocation transformation model containing only two types of dislocations (Sahoo and Ananthakrishna 1981, Ananthakrishna and Sahoo 1978). The creep curve for a typical case is shown in figure 4, together with the variation of N_g.

Figure 5 shows the projection of the limit cycle on the N_g–N_i plane. As can be seen from the figure, no matter what the initial values of the densities, the trajectories quickly reach the limit cycle. The full curve corresponds to the limit cycle and the broken curves to arbitrary initial states. The choice of the initial densities matching the asymptotic

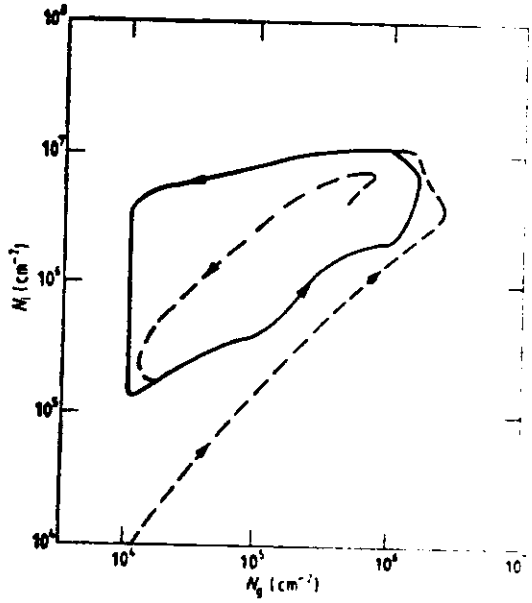

Figure 5. A projection of the limit cycle on N_g–N_i plane. Parameters a, b and c have the same values as in figure 1.

densities, i.e., $N_g(t=0)=N_{g_0}$ and $N_i(t=0)=N_{i_0}$ is not of much physical interest in the creep problem but has been considered only to show that the limit cycle is approached even when the initial state is inside the limit cycle. The bounds on the limit cycle are calculated in the Appendix. The projection of the limit cycle on the other two planes are similar to figure 5.

5. Summary and discussion

The basic idea we have used is to model systems exhibiting SCC as nonlinear systems. The underlying physical mechanisms operating decide the nature of the equations. However, since plasticity is basically a nonlinear phenomenon (in densities), we have tried to incorporate some well established mechanisms to show that some basic features of SCC emerge. We have not tried to fit any data. Although we have incorporated the essential features of Cottrell's theory, we stress that *it is the nonlinear interaction that leads to* SCC. We have checked this point by incorporating another mechanism in place of Cottrell's mechanism, namely, stopping of dislocation at athermal 'locks' and release of these and production of new ones via the Frack–Read mechanism.

The essential feature that emerges from our theory, apart from explaining SCC, is that there are bounds on $\dot{\epsilon}$ and the temperature over which the phenomenon occurs. Our theory also gives rise to the usual type of creep curves outside the instability range.

We believe that both steps in the stress–strain curve in the constant stress-rate test and the Portevin–Le Chatelier effect can be explained along these lines. Further work is in progress.

Appendix

Consider equations (6)–(8). The procedure we adopt is the same as that for the Oregonator model (Nicolis and Prigogine 1977) representing Zhabotinski's oscillating chemical reaction. The model is similar to Oregonator. These equations can be written as

$$\frac{dr}{d\tau}=F(r, a, b, c, k)$$

with

$$r=(x, y, z). \tag{A1}$$

The first point that should be noted is that V_g is some known function of N which itself varies with time according to the set of equations (6)–(8). Therefore the function F does not explicitly depend on time. So the system is an autonomous one. Thus, the stability analysis can be used to get some useful information. The singular points denoted by (x_a, y_a, z_a) are obtained by equating the left-hand side of equations (6)–(8) to zero. There are only two singular points (0, 0, 0) and (x_a, y_a, z_a).

$$x_a=\frac{-B\pm(B^2+4A)^{1/2}}{2A} \tag{A2}$$

$$y_a=-(b/2)(1-k)x_a+\tfrac{1}{2} \tag{A3}$$

$$z_a=x_a \tag{A4}$$

with

$$B=2a-1+b(1-k) \tag{A5}$$

and

$$A = b(1+k). \tag{A6}$$

The stability of the singular points depends on the eigenvalues of the matrix obtained by linearising F around the singular points, namely the roots of the cubic equation

$$\omega^3 - \omega^2(A_1 + A_4 - c) + \omega[-c(A_1 + A_4) + A_1A_4 - A_2A_3] - c[A_2A_5 + A_2A_3 - A_1A_4] = 0$$

or

$$\omega^3 - T\omega^2 + \delta\omega - \Delta = 0 \tag{A7}$$

where

$$A_1 = 1 - a - 2bx_0 - y_0 \tag{A8}$$

$$A_2 = 1 - x_0 \tag{A9}$$

$$A_3 = 2kb^2x_0 - by_0 \tag{A10}$$

$$A_4 = -bx_0 - b \tag{A11}$$

$$A_5 = ab. \tag{A12}$$

The origin is an unstable point since there is at least one root with a positive real part. The nontrivial singular point r_a can become an unstable focus when one of the following conditions is violated (see Nicolis and Prigogine 1977).

$$T < 0 \qquad \Delta < 0 \qquad \Delta - T\delta > 0. \tag{A13}$$

Rough bounds on (a, b, c) can be obtained for the unstable domain by demanding that one of the above relations be violated (and using the assumption that b is small compared to a). Below, we give the bounds, obtained on a computer for $k = 1$:

$$\begin{aligned} &0.33 < a_1(b, c) \leqslant a \leqslant a_2(b, c) < 0.69 \\ &0.0001 < c_1(a, b) \leqslant c \leqslant c_2(a, b) < 0.201 \\ &0 < b_1(a, c) \leqslant b \leqslant b_2(a, c) < 0.011 \end{aligned} \tag{A14}$$

where a_2 etc. are the actual cut-off values.

For all $0.5 \leqslant k \leqslant 1$, we find that there is an instability domain. We have not investigated for smaller values of k.

In order to prove the existence of the oscillatory solution of finite amplitude, we look for a surface S on which every solution trajectory of equations (6)–(8) or (A1) enters, i.e., $\mathrm{d}r/\mathrm{d}\tau$ always points inwards for any point r on S, i.e.

$$n \frac{\mathrm{d}r}{\mathrm{d}\tau} < 0 \text{ for } r \text{ on } S \tag{A15}$$

where n is the outward normal to S. Following Murray (1974), it is easy to show that S is the rectangular box given by

$$1 \leqslant x \leqslant 1/b \qquad y_1 \leqslant y \leqslant y_2 \qquad 1 \leqslant z \leqslant 1/b$$

where

$$y_1 = ab/(1+b) \qquad y_2 = (a + kb^2)/2b. \tag{A16}$$

In the above we have used the fact that $b \ll a$ which follows from equation (A3). Since r_a given by equations (A2)–(A4) is an unstable focus and S surrounds r_a, it contains an attractive limit cycle. We have plotted the limit cycle obtained by numerically solving equations (6)–(8) and this is shown in figure 5.

References

Ananthakrishna G and Sahoo D 1978 *Nucl. Phys. Solid State Phys. (India)* **21C** 771
Andrade E N da C 1910 *Proc. R. Soc.* **84** 1
Ardley G W and Cottrell A H 1953 *Proc. R. Soc.* **A219** 328
Bell J F 1973 *Handbuch der Physik Band VIa/1* (Berlin: Springer-Verlag)
Bodner S R and Rosen A 1967 *J. Mech. Phys. Solids* **15** 63
Cottrell A H 1953 *Phil. Mag.* **44** 829
Da Silveira T L and Monteiro S N 1979 *Met. Trans.* **A10** 1795
Fitzgerald E R 1966 *Particle Waves and Deformation in Crystalline Solids* (New York: Interscience)
Gilman J J 1965 *J. Appl. Phys.* **36** 2772
Gilman J J and Johnston W G 1962 *Solid State Phys.* **13** 148 (New York: Academic Press)
Li J C M 1963 *Acta Metall.* **11** 1269
Lubahn J D and Felgar R P 1961 *Plasticity and Creep of Metals* (New York: John Wiley)
McCormic P G 1972 *Acta Metall.* **20** 351
Minorsky N 1962 *Nonlinear Oscillations* (New Jersey: Van Nostrand)
Murray J D 1974 *J. Chem. Phys.* **61** 3160
Nicolis G and Prigogine I 1977 *Self Organization in Non-equilibrium Systems* (New York: Wiley)
Sahoo D and Ananthakrishna G 1982 *J. Phys. D: Appl. Phys.* **15** at press
Van den Beukel A 1975 *Phys. Stat. Solidi* a **30** 197
—— 1980 *Acta Metall.* **28** 965
Webster G A 1966 *Phil. Mag.* **14** 775
Zagorukuyko L N, Osetskiy A I and Soldatov V P 1977 *Phys. Met. Metallogr.* **43** 156

J. Phys. D: Appl. Phys., 16 (1983) 1055–1068. Printed in Great Britain

A model based on nonlinear oscillations to explain jumps on creep curves: II. Approximate solutions

M C Valsakumar and G Ananthakrishna
Materials Science Laboratory, Reactor Research Centre, Kalpakkam 603 102, India

Received 6 August 1982

Abstract. Using the method of relaxation oscillations, we derive approximate expressions for the amplitude, period and the waveform of the limit cycle solutions. Using these, an expression for the step size per cycle on the creep curve is derived. It is shown that these approximate solutions agree well with the numerical solutions. The theory predicts bounds on temperature and stress over which the steps are seen. The dependence of the step size and the period of the oscillation on stress and temperature permits mapping of the theoretical parameters on to the experimental ones. It is shown that this dependence is in agreement with the experimental results of Zagorukuyko *et al*.

1. Introduction

Instabilities in plastic deformation which manifest as steps on creep curves (creep is time dependent deformation at constant stress), or as jumps on stress–strain curves in a constant stress rate test, or as repeated yield drops in a tensile test (deformation at constant strain rate) have been of immense interest in metallurgical literature (see for example Bell 1973). Though there exist many phenomenological treatments of the phenomenon (Cottrell 1953, Bodner and Rosen 1967, Penning 1972, Van den Beukel 1975, 1980, Bell 1973) there has been no attempt to understand how this periodic temporal state develops. Recently, Ananthakrishna and Sahoo (1981, hereafter referred to as I) proposed a model which exploited the intrinsic nonlinear character of dislocation interactions (or equivalently that of plastic flow) to explain the periodic temporal state, thereby explaining jumps on creep curves. The model consists of three types of dislocations (mobile, immobile and those with clouds of solute atoms to mimic Cottrell's (1953) idea) and some transformations between them, leading to a coupled set of nonlinear differential equations for the dislocation densities. It was shown that for a range of values of the rate constants, these equations admit oscillatory solutions, called limit cycles. The model has been subsequently extended to the constant strain rate case with good success (Ananthakrishna and Valsakumar 1982).

In I as well as in its extension to constant strain rate (Ananthakrishna and Valsakumar 1982), only qualitative comparisons with experiments were attempted. However, it is desirable to make better contact with experiments (in terms of quantitative comparison). This would require a knowledge of the dependence of the rate constant (at the level at which they are introduced in the theory) on such parameters as stress (σ), temperature (T), concentration of solute atoms (C), etc. This however is lacking, although there is

a limited knowledge of some of the rate constants. Even if these are known, it would be difficult to achieve the above objective without obtaining closed-form expressions for such physically measurable quantities as the period of the steps (or of serrations), amplitude of steps (or of serrations), etc. Generally, the dependence of these experimental quantities can be measured as functions of σ, T and C and are expressed through some phenomenological relations. Once closed-form expressions are derived, comparison with experiments is possible. This can also be used to give some insight into the dependence of the theoretical rate constants on σ, T and C, where such knowledge is lacking.

The purpose of this paper is to derive approximate closed-form expressions for the above mentioned quantities. The analysis proceeds along the lines of Tyson (1977) for the Belousov–Zhabotinski oscillating chemical reaction. Using standard methods (Minorsky 1962), in § 2, we perform the stability analysis of the equations used in I. We present the domain of the parameters for which the steady state becomes an unstable focus. On scaling these equations appropriately, we identify the fast variable and adiabatically eliminate it to obtain a reduced set of two coupled equations. Using the method of relaxation oscillations (Minorsky 1962, Tyson 1977), in § 3, we show the existence of limit cycle solutions. We also obtain approximate expressions for the amplitude, the period and the waveform of these solutions. We show that the results agree quite well with the numerical solutions of the original set and the reduced set of differential equations. In § 4, we derive an expression for the steady-state creep curve and compare it with the numerical solutions obtained for the original set and the reduced set of equations. Many qualitative features of the phenomenon are shown to follow from these results. Expressions for the step height and the period of the jumps on the creep curves as a function of σ and T are shown to be consistent with the results of zinc (Zagorukuyko *et al* 1977). In analogy with equilibrium phase transition, the transition is shown to be a first-order transition or a hard transition.

2. Stability analysis

The rate equations for the densities of the three types of dislocations introduced in I are

$$\frac{dN_g}{dt} = \theta V_g N_g - \mu' N_g^2 - \mu N_g N_s + \lambda N_s - \alpha N_g \tag{1a}$$

$$\frac{dN_s}{dt} = k\mu' N_g^2 - \mu N_g N_s - \lambda N_s + \alpha' N_i \tag{1b}$$

and

$$\frac{dN_i}{dt} = \alpha N_g - \alpha' N_i \tag{1c}$$

where N_g, N_s and N_i correspond to the densities of the mobile species, the relatively immobile species, and those with clouds of solute atoms, respectively. We have shown in I that these equations describe the dynamics of dislocations under constant stress. (For details of the reactions and the rate constants, see I.) The plastic strain rate $\dot{\epsilon}_p$ and the plastic strain ϵ_p are given by

$$\dot{\epsilon}_p = b_0 N_g V_g \tag{2a}$$

and

$$\varepsilon_p = \int_0^t \dot{\varepsilon}_p(t')\,dt' \tag{2b}$$

where b_0 and V_g are the Burgers vector and the velocity of mobile dislocations respectively. (The qualitative nature of the oscillatory solutions supported by these equations will not change if V_g is allowed to depend on the effective stress σ^*. See I and Ananthakrishna and Valsakumar (1982).)

For convenience we define a new set of dimensionless variables

$$x = (\mu/\lambda)N_g \qquad y = (\mu/\theta V_g)N_g \qquad z = (\mu\alpha'/\lambda\alpha)N_i. \tag{3}$$

Then we obtain

$$\frac{dx}{d\tau} = (1-a)x - bx^2 - xy + y \tag{4a}$$

$$\frac{dy}{d\tau} = b(bx^2 - xy - y + az) \tag{4a}$$

and

$$\frac{dz}{d\tau} = c(x - z) \tag{4c}$$

where

$$\tau = \theta V_g t \qquad a = \alpha/\theta V_g \qquad b = \lambda/\theta V_g \qquad c = \alpha'/\theta V_g \tag{5}$$

(We have taken $\mu' = \mu$ and $k = 1$ to minimise the number of parameters.) Since the parameter b is related to stress or thermal activation, b is expected to be small compared to a. We will restrict our attention to the situation when $b \ll a$, $c \leqslant b$, and $b \ll 1$ (although there is a range of values of $c > b$).

Equations (4a)–(4c) admit a trivial steady state $x_a = y_a = z_a = 0$ which can be shown to be unstable. The only positive nontrivial solution for the steady state is

$$\left.\begin{aligned} x_a = z_a &= \frac{1 - 2a + [(1-2a)^2 + 8b]^{1/2}}{4b} \\ y_a &= \tfrac{1}{2}. \end{aligned}\right\} \tag{6}$$

For subsequent analysis it is convenient to express equations (4a)–(4c) in terms of the deviations from the steady state

$$X = x - x_a \qquad Y = y - y_a \qquad Z = z - z_a. \tag{7}$$

The time evolution is given by

$$\dot{X} = -(\alpha X + \beta Y + bX^2 + XY) \tag{8a}$$

$$\dot{Y} = -b(\gamma X + \delta Y + XY - bX^2 - aZ) \tag{8b}$$

and

$$\dot{Z} = c(X - Z) \tag{8c}$$

where the dot denotes differentiation with respect to the scaled time τ and

$$\alpha = a + 2bx_a + y_a - 1$$
$$\beta = x_a - 1$$
$$\gamma = y_a - 2bx_a$$
$$\delta = x_a + 1. \tag{9}$$

When $|X| \ll 1$, $|Y| \ll 1$ and $|Z| \ll 1$ we may neglect the quadratic terms in equations (8*a*)–(8*c*). The resulting equations read

$$\frac{d\psi}{d\tau} = W\psi \tag{10}$$

where ψ is the column vector $(X, Y, Z)^T$ and W is the matrix associated with the linearised system of equations. The eigenvalues ω_i, $i = 1$ to 3, are given by

$$\omega^3 - T\omega^2 + P\omega - \Delta = 0 \tag{11}$$

where

$$T = -(\alpha + \delta b + c)$$
$$\Delta = -bc[\alpha\delta + \beta(a - \gamma)]$$

and

$$P = \delta bc + \alpha(\delta b + c) - \beta\gamma b. \tag{12}$$

The nontrivial singular point becomes an unstable focus when one of the following conditions are violated (Murray 1974):

$$T < 0 \qquad \Delta < 0 \qquad \text{or} \quad \Delta - PT > 0. \tag{13}$$

It is easy to show that the first two inequalities cannot be violated. Substituting for Δ, P and T we get

$$(\alpha + \delta b)c^2 + [(\alpha + \delta b)^2 - \beta ab]c + b(\alpha + \delta b)(\alpha\delta - \beta\gamma) < 0 \tag{14}$$

for instability. Using the equality sign in equation (14) we get a critical value of $c = c_{crit}$ for fixed a and b. For $c < c_{crit}$ the steady state is unstable. For further analysis it is expedient to use the power series expansion in b of the parameters α, β, γ and δ given in table 1. Using these expressions in equation (14) and demanding $c_{crit} \geqslant 0$ we get the bounds on a for which the system is unstable and is given by

$$\tfrac{1}{3} \leqslant a \leqslant 1/\sqrt{2}. \tag{15a}$$

The expressions for c_{crit} are given by

$$c_{crit} = \begin{cases} \dfrac{5a - 2 + (-23a^2 + 20a - 4)^{1/2}}{4} & \text{for} \quad \tfrac{1}{3} < a < \tfrac{1}{2} \\ \tfrac{1}{8} & \text{for} \quad a = \tfrac{1}{2} \\ \dfrac{2b(1 - 2a^2)}{(2a - 1)^2} & \text{for} \quad \tfrac{1}{2} < a < 1/\sqrt{2}. \end{cases} \tag{15b}$$

In figure 1 we have shown a plot of $1/c_{crit}$ as a function of a for $b = 10^{-4}$. The domain as

Table 1. Leading terms in the expansion of the parameters α, β, γ and δ in terms of b.

	$a < \frac{1}{2}$	$a = \frac{1}{2}$	$a > \frac{1}{2}$
α	$\frac{1-2a}{2} - \frac{2b}{1-2a}$	$\sqrt{2b}$	$\frac{2a-1}{2} - \frac{2b}{2a-1}$
β	$\frac{1-2a}{2b} - \frac{2a}{1-2a}$	$\frac{1}{\sqrt{2b}} - 1$	$\frac{2(1-a)}{2a-1} - \frac{2b}{(2a-1)^2}$
γ	$\frac{4a-1}{2} - \frac{2b}{1-2a}$	$\frac{1}{2} - \sqrt{2b}$	$\frac{1}{2} - \frac{2b}{(2a-1)}$
δ	$\frac{1-2a}{2b} - \frac{2(1-a)}{1-2a}$	$\frac{1}{\sqrt{2b}} + 1$	$\frac{2a}{2a-1} - \frac{2b}{(2a-1)^2}$

given by equation (15b) is open in the c–a plane, i.e., $c \to 0$ as $a \to a_c$. This is due to the fact that we have ignored terms of higher order in b^{-1}. If this is included, c versus a is a closed curve.

3. Limit cycle, amplitude, period and waveform

Now we rescale time as $\tau' = b\tau$. Using a dot to denote differentiation with respect to τ' we get

$$b\dot{X} = -(\alpha X + \beta Y + bX^2 + XY) \tag{16a}$$

$$\dot{Y} = -(\gamma X + \delta Y - bX^2 + XY - aZ) \tag{16b}$$

and

$$\dot{Z} = \frac{c}{b}(X - Z). \tag{16c}$$

It is clear that in the limit $b \to 0, |\dot{X}| \to \infty$ unless the right-hand side vanishes identically. Physically this amounts to saying that X changes with a characteristic time $\sim b$ to maintain

$$\alpha X + \beta Y + bX^2 + XY = 0.$$

Table 2. Leading terms in the expansion of the nonlinear function $X(Y)$ in terms of b.

$a < \frac{1}{2}$	$-\frac{1}{2} < Y < \frac{1}{2} - a$	$X = -\frac{Y}{b} - \frac{1}{1-2a} - \frac{Y+\frac{1}{2}}{Y+a-\frac{1}{2}}$
	$Y > \frac{1}{2} - a$	$X = -\left(\frac{1-2a}{2b} + \frac{1}{1-2a}\right) + \frac{Y+\frac{1}{2}}{Y+a-\frac{1}{2}}$
$a > \frac{1}{2}$	$-\frac{1}{2} < Y < \frac{1}{2} - a$	$X = -\frac{(Y+a-\frac{1}{2})}{b} - \frac{1}{2a-1} - \frac{Y-\frac{1}{2}}{Y-a-\frac{1}{2}}$
	$Y > \frac{1}{2} - a$	$X = -\frac{1}{2a-1} + \frac{Y+\frac{1}{2}}{Y+a-\frac{1}{2}}$

Table 3. Expression for the null cline Z_1 in terms of b.

$a < \frac{1}{2}$	$-\frac{1}{2} < Y < \frac{1}{2} - a$	$Z_1 = -\dfrac{2Y^2 + (3a-1)Y}{ab} - \dfrac{(2Y+a)(Y-\frac{1}{2})}{a(Y+a-\frac{1}{2})} - \dfrac{1}{1-2a}$
	$Y > \frac{1}{2} - a$	$Z_1 = -\left(\dfrac{1-2a}{2b} + \dfrac{1}{1-2a}\right) - \dfrac{(2Y+a)(Y+\frac{1}{2})}{a(Y+a-\frac{1}{2})}$
$a > \frac{1}{2}$	$-\frac{1}{2} < Y < \frac{1}{2} - a$	$Z_1 = -\dfrac{(2Y+a)}{a}\left(\dfrac{Y+a-\frac{1}{2}}{b} + \dfrac{Y+\frac{1}{2}}{Y+a-\frac{1}{2}}\right)$
	$Y > \frac{1}{2} - a$	$Z_1 = -\dfrac{1}{2a-1} + \dfrac{(Y+\frac{1}{2})(a+2Y)}{a(Y+a-\frac{1}{2})}$

This enables us to define X as a function of

$$X = \frac{[(\alpha + Y)^2 - 4b\beta Y]^{1/2} - (\alpha + Y)}{2b}. \tag{17}$$

(Only the positive square root is meaningful because the other root corresponds to negative dislocation density.) Table 2 gives a power series expansion of X.

Since X is a fast variable, we have to solve only equations (16b) and (16c) with equation (17) i.e.

$$\frac{dY}{d\tau} = -b[aX - 2(x_s + X)Y - aZ] \tag{18a}$$

and

$$\frac{dZ}{d\tau} = c(X - Z) \tag{18b}$$

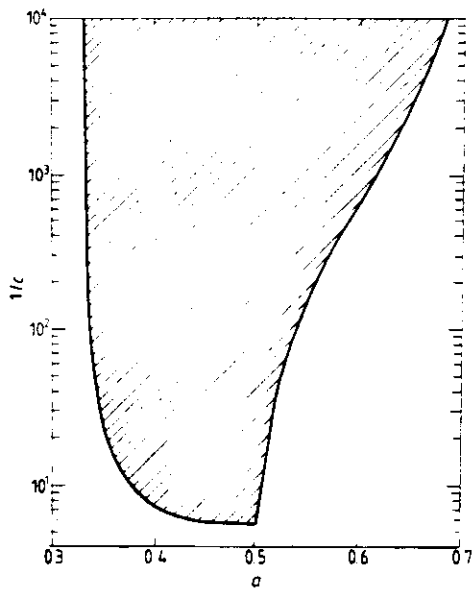

Figure 1. Domain of instability of the steady state for $b = 10^{-4}$. c_{crit}^{-1} is plotted as a function of a. The shaded region is unstable.

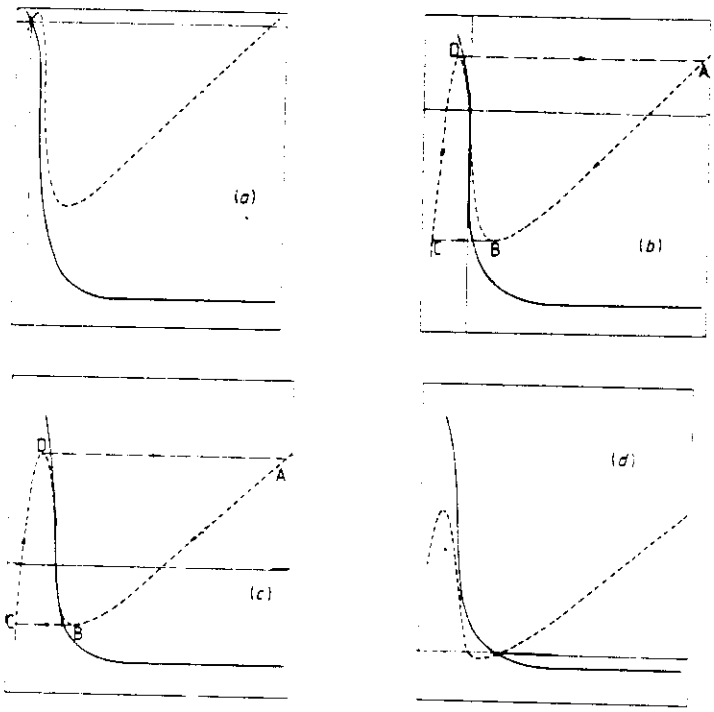

Figure 2. Phase plane portrait. The null clines Z_1 and Z_2 are plotted as a function of Y. The broken curve corresponds to Z_1 and the full curve represents Z_2. (*a*) For $a < \frac{1}{3}$, the steady state is stable; (*b*) anc (*c*), for $\frac{1}{3} < a < \frac{1}{2}$ and $\frac{1}{2} < a < 1/\sqrt{2}$ respectively, the steady state is unstable. The limit cycle $A \to B \to C \to D \to A$ exists. (*d*) The steady state is stable for $1 > a > 1/\sqrt{2}$.

where X is given by equation (17).

3.1. Limit cycle

Consider the phase plane $Y - Z$. Using standard phase plane techniques (Minorsky 1962) we determine the null clines

$$\dot{Y} = 0 \leftrightarrow Z_1 = Z(Y) = X(Y) + \frac{2}{a}[x_a + X(Y)]Y \tag{19}$$

and

$$\dot{X} = 0 \leftrightarrow Z_2 = X(Y).$$

Table 3 gives the power series expansion of $Z(Y)$ in b. To find the existence of a limit cycle, we look for the intersection of the null clines in the region of negative slope.

From the expressions for the null clines Z_1 and Z_2 we can have a reasonable idea of the phase portrait which is schematically summarised in figures 2(*a*)–(*d*). (Z_1 always shows a negative slope region.) Z_1 and Z_2 are plotted as a function of Y. For $0 < a < \frac{1}{3}$ and $1/\sqrt{2} < a < 1$ the null clines intersect in the positive slope region (actual bounds are obtained by demanding the maximum in Z_1 to occur for $Y \leqslant 0$ and minimum in Z_1 to occur for $Y \geqslant 0$). This means that the steady state of the reduced equations

$Y_a = Z_a = 0$ is stable for $0 < a < \frac{1}{3}$ and $\frac{1}{2} < a < 1/\sqrt{2}$. On the other hand for $\frac{1}{3} < a < \frac{1}{2}$ and $\frac{1}{2} < a < 1/\sqrt{2}$ the null clines intersect in the negative slope region which means that a limit cycle exists for $\frac{1}{3} < a < 1/\sqrt{2}$. Starting from an arbitrary point P, the trajectory moves along the null cline $\dot{Y} = 0$ until it reaches the turning point D from where it almost instantaneously jumps to A. Thereafter it moves along this branch of the null cline $\dot{Y} = 0$ (slowly) until it reaches the second turning point B from where it jumps to C and the process continues. Thus the trajectory is a closed one and the limit cycle is A → B → C → D → A.

3.2. *Period, amplitude and waveform*

Before proceeding further we emphasise that the subsequent analysis is applicable only when $c \ll b$. When $\frac{1}{3} < a < \frac{1}{2}$, there is a large region of the unstable domain lying outside this and hence care should be exercised in applying these results. However for $\frac{1}{2} < a < 1/\sqrt{2}$ the above condition ($c \ll b$) is always satisfied.

Table 4. Expressions for X, Y and Z at the characteristic points of the limit cycle. (*i*) $a < \frac{1}{2}$; (*ii*) $a > \frac{1}{2}$.

(*i*)

	A	B	C	D
X	$-\frac{1-2a}{2b} - \frac{2a}{1-2a}$	$-\frac{1-2a}{2b} - \frac{2a}{1-2a} + \sqrt{2}$	$\frac{a}{2b}$	$\frac{3a-1}{4b}$
Y	$\frac{(1-a)^2}{16b}$	$\frac{1-2a+\sqrt{2}(1-a)}{2}$	$-\frac{a}{2}$	$-\frac{3a-1}{4}$
Z	$-\frac{(1-3a)^2}{8ab}$	$-\frac{1-2a}{2b} - \frac{1}{1-2a}$ $-(1+\sqrt{2})^2\frac{(1-a)}{a}$	Z_B	Z_A

(*ii*)

	A	B	C	D
X	$-\frac{2(1-a)}{2a-1}$	$-\frac{2(1-a)}{2a-1} - \sqrt{2}$	$\frac{1-a}{2b}$	$\frac{1-a}{4b}$
Y	$\frac{(1-a)^2}{16b}$	$\frac{1-2a+\sqrt{2}(1-a)}{2}$	$-\frac{a}{2}$	$-\frac{3a-1}{4}$
Z	$\frac{(1-a)^2}{8ab}$	$-\frac{1}{2a-1}$ $+(1+\sqrt{2})^2\frac{(1-a)}{a}$	Z_B	Z_A

Table 4 summarises the values of X, Y and Z at the characteristic values of the values of the limit cycle A, B, C and D. X is approximately a constant ($\cong X_A = -\beta$) in the branch AB of the limit cycle. At B, X makes a jump to its maximum ($= X_C$). Thereafter

it decreases to X_D and jumps down to X_A. The amplitude in X

$$X_{amp} \sim X_C - X_B = \frac{1-a}{2b} \qquad \text{for } \tfrac{1}{3} < a < 1/\sqrt{2}. \tag{20}$$

Now we consider calculating the period and the waveform of the oscillation. This is accomplished by integrating equations (18*a*) and (18*b*), piecewise (by using the power series expressions for X and Z in the appropriate branches of the limit cycle). Substituting for X and Z in terms of Y, and integrating, we get along branch AB

$$\frac{(1-2a^2)}{1-2a}\ln Y + (1-a)\ln(Y+\tfrac{1}{2}) - \frac{1-a}{1-2a}\ln(Y+a-\tfrac{1}{2}) = -c\tau + \text{constant}$$

for

$$\tfrac{1}{3} < a < \tfrac{1}{2} \qquad \tfrac{1}{2} < a < 1/\sqrt{2}.$$

Hence

$$\tau_{AB} = \frac{1}{c}\left(\frac{1-2a^2}{1-2a}\ln\frac{Y_A}{Y_B} + (1-a)\ln\frac{Y_A+\tfrac{1}{2}}{Y_B+\tfrac{1}{2}} - \frac{1-a}{1-2a}\ln\frac{Y_A+a-\tfrac{1}{2}}{Y_B+a-\tfrac{1}{2}}\right).$$

Since X is nearly a constant we can simply integrate equation (18*b*) and get a maximum estimate of τ_{AB}. The result is

$$X = -x_a + 1 \qquad \text{for} \qquad 0 < \tau < \tau_{AB} \tag{21a}$$

and

$$\tau_{AB} \cong \frac{1}{c}\ln\left(\frac{(1-a)^2}{8b(1+\sqrt{2})^2(1-a\sqrt{2})}\right) \tag{21b}$$

for

$$\tfrac{1}{3} < a < \tfrac{1}{2} \qquad \tfrac{1}{2} < a < \frac{1}{\sqrt{2}}.$$

Similarly integrating equations (18*a*) and (18*b*) along the branch CD of the limit cycle, we get for $\frac{1}{3} < a < \frac{1}{2}$ and $\frac{1}{2} < a < 1/\sqrt{2}$

$$(3a-1)\ln(-Y) - (1-a)\ln(-Y+\tfrac{1}{2}-a) = -(2a-1)c\tau + \text{constant}. \tag{22a}$$

Substituting for Y_A and Y_B from table 4 we get

$$\tau_{CD} = \frac{1}{c}\left(2\ln 2 + \frac{3a-1}{2a-1}\ln\frac{a}{3a-1}\right). \tag{22b}$$

The period of oscillation is

$$\tau_P = \tau_{AB} + \tau_{CD}.$$

Substituting for Y in terms of X and applying initial conditions we get from equation (21*a*)

$$\frac{(bX+\tfrac{1}{2}-a)^{1-a}}{(bX)^{3a-1}} = \frac{[(1-a)/2]^{1-a}}{(a/2)^{3a-1}}\exp[-(1-2a)c(\tau-\tau_{AB})] \tag{23a}$$

for

$$\tau_{AB} \leqslant \tau \leqslant \tau_P \qquad \tfrac{1}{3} < a < \tfrac{1}{2}$$

and

$$\frac{(bX + a - \frac{1}{2})^{3a-1}}{(bX)^{1-a}} = \frac{(a/2)^{3a-1}}{[(1-a)/2]^{1-a}} \exp[-(2a-1)c(\tau - \tau_{AB})] \qquad (23b)$$

for

$$\tau_{AB} \leqslant \tau \leqslant \tau_P \qquad \tfrac{1}{2} < a < 1/\sqrt{2}.$$

A plot of $x = x_a + X$ versus τ for one cycle of oscillation is shown in figure 3 for $a = 0.63$ and $b = c = 10^{-4}$ (the full curve). Also shown in the figure are the numerical solutions of the three original equations (the dotted curve) and that of the reduced set of equations (the dashed curve). But for a small change at the jump down part (resulting in a loss for the integral of the density) the numerical solutions are in remarkable agreement. The elimination of the fast mode appears to have practically no effect on the shape and the position of the waveform as can be seen by the two numerical solutions except for the discrepancy at the jump down part. The shape of the wave as calculated by the approximate expression is not significantly different, but a phase lag is induced. The error in this is of the order of 7% for this particular choice of a, b and c. The agreement with the numerical solution improves if c is reduced. For values of c larger than b the approximation becomes worse. The nature of the waveform also changes from the one indicated in figure 3 to the one given in figure 1 of paper 1.

4. The creep curve

The results derived in the previous sections can be used to derive the steady-state creep curve. Using equations (2*a*), (2*b*) and (3), creep

$$\varepsilon_p = \frac{bb_0V_a}{\mu}\int_0^\tau x(\tau')\,d\tau' \qquad (24)$$

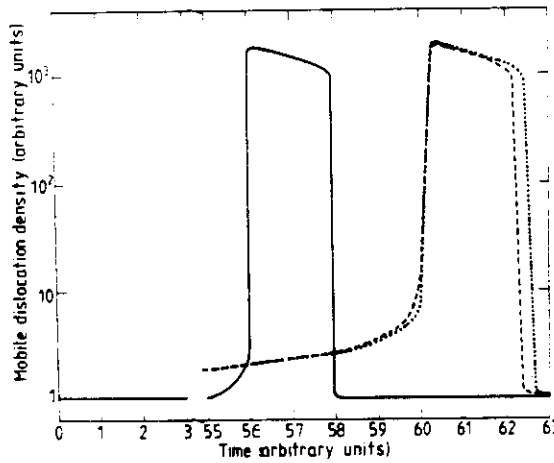

Figure 3. Comparison of the waveforms obtained by various methods for $a = 0.63$, and $b = c = 10^{-4}$. The full curve corresponds to the approximate closed-form solution. The dotted curve represents the numerical solution with all the three equations and the dashed curve corresponds to the solution obtained with the two equations.

$$\tilde{\varepsilon} = \frac{\mu\varepsilon_p}{bb_0V_g} = \int_0^\tau x(\tau')\,d\tau'$$

$$= \tau x_a + \int_{X(0)}^{X(\tau)} X(\tau)\frac{d\tau}{dX(\tau)}\,dX(\tau). \tag{25}$$

Integrating, we get for

$$\tfrac{1}{3} < a < \tfrac{1}{2} \qquad 0 \leqslant \tau \leqslant \tau_{AB}$$

$$\tilde{\varepsilon} = \tau \tag{26}$$

and for

$$\tau_{AB} \leqslant \tau \leqslant \tau_P$$

$$\tilde{\varepsilon} = \tau_{AB} + \frac{1-2a}{2b}(\tau - \tau_{AB}) + \frac{2}{c}[X(\tau_{AB}) - X(\tau)] - \frac{1-a}{2bc}\ln\left(\frac{bX(\tau_{AB}) + \frac{1}{2} - a}{bX(\tau) + \frac{1}{2} - a}\right) \tag{27a}$$

for

$$\tfrac{1}{3} < a < \tfrac{1}{2}$$

and

$$\tilde{\varepsilon} = \tau_{AB} - \frac{\tau - \tau_{AB}}{2a-1} + \frac{2}{c}[X(\tau_{AB}) - X(\tau)] - \frac{3a-1}{2bc}\ln\left\{\frac{bX(\tau_{AB}) + a - \frac{1}{2}}{bX(\tau) - a - \frac{1}{2}}\right\} \tag{27b}$$

for

$$\tfrac{1}{2} < a < 1/\sqrt{2}.$$

The step size on the reduced creep curve is given by

$$\Delta\tilde{\varepsilon}_p = \int_{\tau_{AB}}^{\tau_P} X(\tau)\,d\tau = \begin{cases} \dfrac{1-a}{2bc}[1 - \ln 2] & \text{for } \frac{1}{3} < a < \frac{1}{2} \\ \dfrac{1-a}{2bc} - \dfrac{3a-1}{2bc}\ln\dfrac{2a}{3a-1} & \text{for } \frac{1}{2} < a < 1/\sqrt{2}. \end{cases} \tag{28}$$

Let us examine $\Delta\varepsilon_p$ and $T_P = \tau_P/\theta V_g$ as a function of σ. For this we first get the bounds on σ using the bounds on a. (It is also possible to obtain bounds on σ using bounds on c, but the limited variation in c allowed by our approximation does not permit the full range of σ allowed. Note that $c \leqslant b$ and $b \ll 1$.) Choosing a power law

$$V_g = V_0(\sigma/\sigma_0)^m$$

we get

$$\sigma = \left(\frac{\xi\alpha}{\theta V_0}\right)^{1/m}\sigma_0 \qquad \sqrt{2} < \xi < 3$$

for a fixed α. Then for a fixed α, α' and λ, we get

$$\Delta\varepsilon_p(\sigma, T) = \begin{cases} \dfrac{b_0\alpha^2}{2\mu\alpha'\theta}\xi(\xi-1)(1-\ln 2) & \text{for } \sqrt{2} < \xi < 2 \quad (29a) \\ \dfrac{b_0\alpha^2}{2\mu\alpha'\theta}\xi(\xi-1) - \dfrac{b_0\alpha^2}{2\mu\alpha'\theta}\xi(3-\xi)\ln\dfrac{2}{3-\xi} & \text{for } 2 < \xi < 3. \quad (29b) \end{cases}$$

Similarly

$$T_P(\sigma, T) = \frac{1}{\alpha'}\left(2\ln 2 + \frac{3-\xi}{2-\xi}\ln\frac{1}{3-\xi} + \ln\frac{(1-\xi)^2}{8\lambda(1+\sqrt{2})^2(\xi-\sqrt{2})}\right). \tag{30}$$

Note that α, α', λ and V_0 are functions of T. It is clear that $\Delta\varepsilon_p$ is a rapidly increasing function of ξ and hence of σ. In contrast $T_P(\sigma)$ is a weak decreasing function of σ for most part of the allowed values of σ. It slightly increases for value of $\xi(\sigma^m) \sim 3$. This slight increase is however due to the overestimation of τ_{AB} given by equation (21*b*) which corresponds to the third term in equation (30).

It is obvious that the full steady-state creep curve can be obtained by repeating the single cycle over successive cycles. Figure 4 displays one such cycle on the creep curve

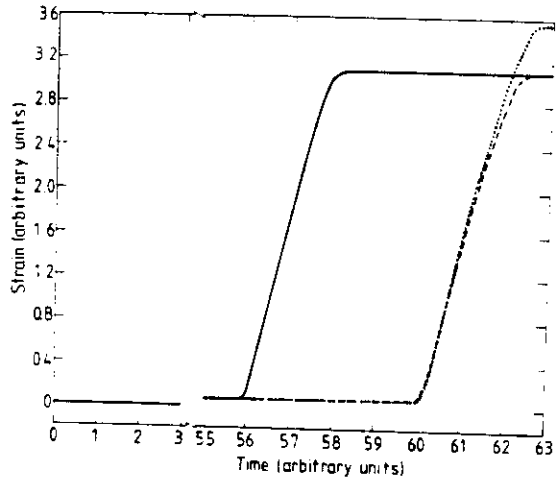

Figure 4. One step in the creep curve generated by various methods. The full curve corresponds to the closed-form solution. The dotted and the dashed curves represent the numerical solutions, corresponding to the original set of three equations and the reduced set of two equations.

$\tilde{\varepsilon} - \tau$ for $a = 0.63$ and $b = c = 10^{-4}$. Also shown are the numerical results of the original set and the reduced set of equations. The agreement is seen to be very good.

5. Results and discussion

Many qualitative features of the theory are in agreement with the experimental results. The fact that there are bounds on a, b and c over which steps occur implies similar bounds on σ, T and C. This is consistent with results available on steps on creeps and other inferred results from experiments on serrated flow. There are very few experiments reported which display steps on creep curves (Ardley and Cottrell 1953. Da Silveira and Monteiro 1979, Zagorukuyko *et al* 1977). Even among these, detailed measurements.

much in the nature of those we mentioned in the introduction, have been carried out only on zinc (Zagorukuyko *et al* 1977). Although the theory in its present form is not directly applicable, it still permits qualitative comparison. These authors (as well as Da Silveira and Monteiro 1979, Lubahn and Felgar 1961) report that steps are seen in the secondary (steady-state) creep only. It is obvious that this result is consistent with our theory since the theory corresponds to bifurcation of the steady-state solution into temporal periodic solutions. Zagorukuyko *et al* (1977) report a rapid monotonic increase of $\Delta\varepsilon_p$ as a function of σ and a weak decreasing dependence of T_p on σ. Clearly both these are consistent with our results of $\Delta\varepsilon_p(\sigma)$ and $T_P(\sigma)$ given by equations (29) and (30) respectively. They also report that the overall slope (given by $\Delta\varepsilon_p/T_P$) increases till the steps become indistinguishable. This result is also compatible with our results.

These authors also report results for $\Delta\varepsilon_p(T)$ and $T_P(T)$. Comparison with our work is slightly more difficult, since the dependence on T comes through all the variables α, α', V and λ. If more experiments show a common trend, it is then possible to use them to guess the dependence of α, α', V and λ on T. If we assume Arrhenius dependence of α and α' with respective activation energies E and E', such that $2E < E'$, then it is clear that $\Delta\varepsilon_p(T, \sigma)$ is an increasing function of T and $T_P(T, \sigma)$ is a decreasing function of T (note that the additional temperature dependence comes from V_0). We want to emphasise that the purpose of this comparison with the results on zinc is not so much to show that results on functional forms on σ and T are consistent with experiments, but to demonstrate how the theoretical parameters can be mapped on the experimental parameters. Since detailed experiments are lacking, we intend performing a similar calculation in the case of the Portevin–Le Chatelier effect, where more detailed results are available.

Often an analogy can be established between systems which exhibit instabilities and systems which undergo equilibrium phase transitions. In the former, new solutions emerge beyond critical values of parameters (called drive parameters). In the present case, the new state of order is one of the oscillatory solutions. It is conventional to associate the radius (or (area)$^{1/2}$) of the limit cycle as the order of parameter. In the present problem a natural choice appears to be step size per cycle per period, namely $\Delta\varepsilon_p/T_P$. It should be noticed that both are proportional to $1/c$. As $a \to a_c^*$, $(a_c^* = \frac{1}{3})$, $c \to 0$ i.e., both $\Delta\varepsilon_p \to \infty$ and $T_P \to \infty$ at the same rate and there is one single creep curve (or jump). (Note that T_P is not defined for $a < 1/\sqrt{2}$ and $a < \frac{1}{3}$.) However, for any finite $\Delta a = a - a_c$, $\Delta\varepsilon_p/T_P$ takes on a finite (but small) value. This implies that the transition is a hard transition or a first-order transition (Nicolis and Prigogine 1977, Nitzan *et al* 1974).

6. Summary

With a view to mapping the theoretical parameters to the experimental ones, we have derived approximate expressions for jump size on the creep curve and the period of cycle. The method used is that of relaxation oscillations. We have demonstrated a way of comparing theoretical results with experimental results. This gives us an insight into the dependence of the theoretical parameters on σ and T. Due to lack of experimental results only functional forms of $\Delta\varepsilon_p$ and T_P (as functions of σ and T) are compared with experimental results on zinc (Zagorukuyko *et al* 1977). Since detailed experiments on serrated yielding are available, a similar calculation will be undertaken.

References

Ananthakrishna G and Sahoo D 1981 *J. Phys. D: Appl. Phys.* **14** 2081
Ananthakrishna G and Valsakumar M C 1982 *J. Phys. D: Appl. Phys.* **15** L171
Ardley G W and Cottrell A H 1953 *Proc. R. Soc.* A **219** 328
Bell J F 1973 *Handbuch der Physik Band VIa/I* (Berlin: Springer-Verlag)
Bodner S R and Rosen A 1967 *J. Mech. Phys. Solids* **15** 63
Cottrell A H 1953 *Phil. Mag.* **44** 829
Da Silveira T L and Monteiro S N 1979 *Met. Trans.* **A10** 1795
Lubahn J D and Felgar R P 1961 *Plasticity and Creep of Metals* (New York: Wiley)
Nicolis G and Prigogine I 1977 *Self Organization in Nonequilibrium Systems* (New York: Wiley)
Nitzan R, Ortolava P, Deutch J and Ross J 1974 *J. Chem. Phys.* **61** 1056
Minorsky N 1962 *Nonlinear Oscillations* (New Jersey: Van Nostrand)
Murray J D 1974 *J. Chem. Phys.* **61** 3160
Penning P 1972 *Acta Metall.* **20** 1169
Tyson J J 1977 *J. Chem. Phys.* **66** 905
Van den Beukel A 1975 *Phys. Status Solidi* a **30** 197
—— 1980 *Acta Metall.* **28** 965
Zagorukuyko L N, Osetskiy A I and Soldatov U P 1977 *Phys. Met. Metallogr.* **43** 156

J. Phys. D: Appl. Phys., 15 (1982) L171–L175. Printed in Great Britain

LETTER TO THE EDITOR

Repeated yield drop phenomenon: a temporal dissipative structure

G Ananthakrishna and M C Valsakumar
Materials Science Laboratory, Reactor Research Centre, Kalpakkam 603 102, Tamil Nadu, India

Received 20 September 1982

Abstract. Based on well known mechanisms, we set up a system of coupled nonlinear rate equations for the densities of three types of dislocations, namely, the mobile, the immobile and those with clouds of solute atoms, and for the load sensed by the load cell. For a range of values of the parameters, these equations admit periodic solutions called limit cycles, leading to repeated yield drops. The model exhibits many experimentally observed features. The new temporal order is an example of a dissipative structure.

There are many phenomenological treatments (Bell 1973, Bodner and Rosen 1967, Cottrell 1953, McCormic 1972, Penning 1972, Van den Beukel 1975, 1980) of repeated yielding (RY) (which is also referred to as serrated yielding (SY)). The best known model is Cottrell's dynamic strain aging model (Cottrell 1953) and its improved versions (McCormic 1972, Van den Beukel 1975, 1980). However, there has been no attempt to use the well established solute dislocation interaction mechanism along with other dislocation interactions to show that the temporal behaviour of SY (and other experimentally observed features) follow naturally. From this point of view Cottrell's model (and its extensions) has remained a static one. Once the dislocations break away from the cloud, unless the solute atoms catch up again (or vice versa) another yield drop cannot follow. In the present analysis, we consider the phenomenon of SY only to the extent of what the load cell senses (space average over the sample) and we will not attempt to explain the inhomogeneous deformation that most often accompanies SY. However, we point out that inhomogeneous deformation should follow from our model once the appropriate space dependence is included. The support for this view comes from two complementary points of view and will be discussed at the end. In spite of this idealisation, we show that the model which is an extension of our earlier work (Ananthakrishna and Sahoo 1981a, hereafter referred to as I) on creep curves exhibits several experimentally observed features of SY. Here, we stress that in the present analysis we will not attempt to fit any data.

The purpose of this study is twofold. First, starting from dislocation interactions, we show that the model exhibits several experimentally observed features, apart from demonstrating that the temporal state naturally emerges. Second, the analysis shows that the phenomenon of SY is an example of a dissipative structure (Nicolis and Prigogine 1977) or a non-equilibrium phase transition.

The model consists of three types of dislocations, namely, 'g' type dislocations which

0022-3727/82/120171 + 05 $02.00

are mobile with density N_g, 's' type dislocations which are relatively immobile with density N_s and 'i' type dislocations with clouds of solute atoms with density N_i. The last one is introduced to mimic Cottrell's idea of dynamic strain aging. On the basis of well established mechanisms (see I), we incorporate some transformations between these dislocations. This gives rise to a set of coupled nonlinear differential equations for the rate of change of densities. These equations are coupled to the machine equation representing the load sensed by the load cell. The rate equations are

$$\dot{N}_g = \theta V_g(\sigma^*) N_g - \mu N_g^2 - \alpha N_g + \lambda N_s - \mu' N_g N_s \tag{1}$$

$$\dot{N}_s = k\mu N_g^2 - \mu' N_g N_s - \lambda N_s + \alpha' N_i \tag{2}$$

$$\dot{N}_i = \alpha N_g - \alpha' N_i \tag{3}$$

$$\dot{\sigma}_a = K[\dot{\varepsilon} - b_0(N_g + \gamma N_i) V_g(\sigma^*)] \tag{4}$$

where the dot refers to the time derivative. Equations (1–3) are identical to the system of equations in I (see I for the details of the mechanisms involved). In equation (4), $\dot{\varepsilon}$ is the imposed strain rate, K is the effective compliance and b_0 is the Burgers vector. The second term in equation (4) is the plastic strain rate $\dot{\varepsilon}_p$. We have used a power law

$$V_g = V_0(\sigma^*/\sigma_0)^m$$

with $\sigma^* = \sigma_a - HN^{1/2}$, where σ^*, σ_a, H, N and m are the effective stress, the applied stress, the stress required to induce a velocity V_0, a constant characteristic of hardening, the total dislocation density ($=N_g + N_s + N_i$) and a velocity exponent respectively.

To keep the analysis simple we have included only simple transformations with further idealisations on the rate constants. For example, in some situations μ should be proportional to $N^{-1/2}$ to account for the variation of the density (Ananthakrishna 1982). It is straightforward to include such changes. Here we assume that θ, $\mu(=\mu')$, λ, α' and α are independent of stress. α is expected to depend on the concentration of solute atoms, their diffusion constant and the velocity of 'i'. α' depends on the drag coefficient of 'i' and on the critical size of the cloud.

All these constants are taken as parameters. Here, we make no attempt to relate them to the existing parameters in the literature. (Such an attempt calls for analytical approach in finding amplitude, period of the yield drop, etc. We have performed such a calculation in the creep case (Valsakumar and Ananthakrishna 1982), where the step size and the period have been obtained as a function of the parameters or equivalently as a function of stress and temperature. Thus the experimental parameters and theoretical ones have been related. These results agree with the experiments of Zagarukuyko *et al* (1977). A similar calculation for the present case is in progress.)

Let us define

$$\left.\begin{array}{llll} \mu N_g = \lambda x & \mu N_s = \theta V_0 y & \mu\alpha' N_i = \lambda\alpha z & \sigma = \varphi\sigma_0 \\ \tau = \theta V_0 t & bx + y + (ab/c)z = \eta. & & \end{array}\right\} \tag{5}$$

Then

$$\dot{x} = (\varphi - h\eta^{1/2})^m x - bx^2 - ax + y - xy \tag{6}$$

$$\dot{y} = b(kbx^2 - xy - y + az) \tag{7}$$

$$\dot{z} = c(x - z) \tag{8}$$

$$\dot{\varphi} = d[e - (\varphi - h\eta^{1/2})^m (x + \gamma' z)] \tag{9}$$

where the dot corresponds to derivative with respect to τ and

$$\left.\begin{aligned} &\alpha = \theta V_0 a \quad \lambda = \theta V_0 b \quad \alpha' = \theta V_0 c \quad c'\gamma' = a\gamma \\ &\theta\mu\sigma_0 d = \lambda b_0 K \quad eb_0 V_0 = \dot{\varepsilon}\mu \quad h\sigma_0 = H(\theta V_0 U/\mu)^{1/2} \end{aligned}\right\} \tag{10}$$

Under well known conditions (Minorsky 1962) these coupled sets of nonlinear equations admit periodic solutions called *limit cycles* which are characteristic of only nonlinear systems; we have carried out the analysis along the lines given in I). Physically, these periodic solutions arise due to the feedback loop g → i → s → g. First, stability of the steady states

$$P_a = (x_a, y_a, z_a, \varphi_a)$$

(for which $\dot{x}$, $\dot{y}$, $\dot{z}$ and $\dot{\varphi}$ are zero) is investigated, i.e., we look for a region in the parameter space $(a, b, c, d, h, k, e, \gamma')$ in which eigenvalues ω_i of the linearised form of equations (6–9) around P_a are complex with Re $\omega_i > 0$. This ensures the spiralling out of the trajectories in the phase space (x, y, z, φ). Then we look for a surface S surrounding P_a into which all trajectories enter. These conditions ensure a bounded variation of trajectories often leading to a limit cycle. We have carried out the above programme and we find that there is unstable domain in $(a, b, c, d, e, h, k, \gamma')$ and an associated limit cycle. Most of this has to be carried out on a computer. The details of the above calculation will be given elsewhere.

Equations (6–9) have been numerically solved on IBM 370 and Honeywell Bull DPS8 computers for some values of the parameters in the domain of instability. These are chosen to be consistent with the expected dislocation densities and the magnitude of the yield drops. (Our earlier calculation (Valsakumar and Ananthakrishna 1982) shows that the value of N_g is determined by the value of μ. The magnitude of the yield drop depends on μ and σ_0. For a given material σ_0 is fixed by the power law and thus it would depend on μ only.) Various characteristic features of the SY exhibited by our model are studied. Almost all of these qualitative features are consistent with the experimental results. (Note that the latter are in the nature of averages over the sample dimensions.)

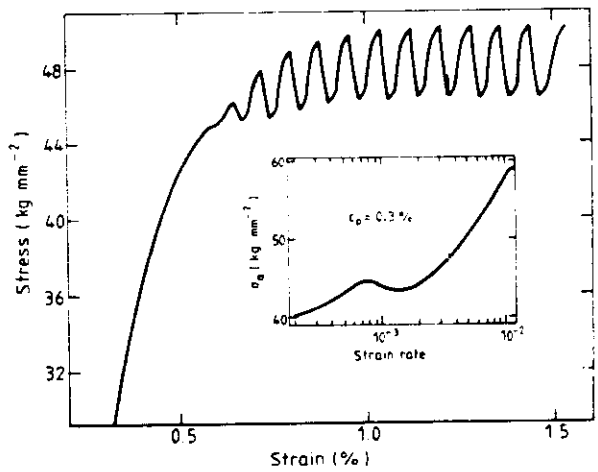

Figure 1. Stress–strain curve showing repeated yielding for $a = 0.2$, $b = 0.002$, $c = 0.008$, $d = 0.001$, $\gamma = 0$, $h = 0.2$, $k = 0.8$ and $m = 2$. Shown in the inset is a graph of σ versus $\dot{\varepsilon}_p$ for the same values of the parameters.

We list here some important ones, with explanations only where it is found necessary. (*a*) There is a range of $\dot{\epsilon}$ over which serrations are seen. (*b*) The model exhibits the negative strain rate behaviour of the flow stress at a fixed plastic strain, ϵ_p. The inset of figure 1 shows a typical plot of $\sigma_a - \dot{\epsilon}_p$ for $k = 0.8$, $h = 0.2$ and $m = 2$. The minimum in σ_a at $\dot{\epsilon}_p = \dot{\epsilon}_m$ is clearly seen. Curves corresponding to larger ϵ_p are displaced successively upwards. This feature has been theoretically established (Penning 1972) and experimentally verified (Bodner and Rosen 1967). We have also investigated the dependence of $\sigma_a(\dot{\epsilon}_p)$ with respect to k and h. We find that the dependence is qualitatively the same as was indicated by our earlier analysis (Sahoo and Ananthakrishna 1982). (*c*) Figure 1 shows a typical plot of SY. The serrations are seen to be periodic (asymptotically). Since it is not possible to identify them as type A or type B (from the nature of the plot), a strain rate change test (Wijler and van Westrum 1971) had to be carried out, from which we find that beyond $\dot{\epsilon}_m$ it is of type B. (*d*) The amplitude of the serration increases up to $\dot{\epsilon}_m$ and thereafter decreases. (*e*) The amplitude increases and saturates as a function of ϵ, consistent with experiments (McCormic 1971). (*f*) Another important feature exhibited by our model consistent with experiments is that there are upper and lower bounds on α within which SY is seen. Since α depends on the concentration of solute atoms, this implies that there are bounds on the concentration of solute atoms in which SY is allowed. We find the usual kind of $\sigma_a(\epsilon)$ beyond these bounds. (*g*) ϵ_c (the critical strain), as a function of $\dot{\epsilon}$, decreases and thereafter increases (McCormic 1971). (*h*) Beyond the range of $\dot{\epsilon}$ where SY occurs, normal behaviour of $\sigma_a(\epsilon)$ is also found.

Here we would like to point out that there has so far been no attempt to derive the negative strain rate behaviour of flow stress (which is most crucial for any meaningful description of the phenomenon) starting from dislocation interactions. In the existing theories this is either assumed (Penning 1972) or derived through phenomenological treatment of waiting time (Van den Beukel 1975). In contrast, in our model this property comes out naturally starting from dislocation interactions.

Below we argue that although we have considered space averaged quantities, inhomogeneous deformation should follow from our model once appropriate space dependent terms are included. The support for this comes from Penning's analysis, which assumes a form of $\sigma(\dot{\epsilon}_p)$ shown in the inset of figure 1. Under the assumption that $\dot{\epsilon}_p$ is localised in space (which is equivalent to N_g localised in space), he shows that inhomogeneous deformation follows. Since, we have shown that our model predicts the form of $\sigma(\dot{\epsilon}_p)$ he assumes, similar results should follow from our model once space dependent density functions are introduced. This can be done by an extension of our earlier work (Ananthakrishna and Sahoo 1981b, Ananthakrishna 1981). Define

$$N_g(t) = \int n_g(x, t)\, dx$$

etc. The equation for $\dot{n}_g(x, t)$ will contain, apart from other terms

$$\tilde{v}_g(x, t) \frac{\partial n_g}{\partial x}(x, t)$$

where $\tilde{v}_g(x, t)$ is the velocity associated with $n_g(x, t)$. Additional support comes from the fact that generally, a system of nonlinear equations which admits limit cycle solutions also supports spatial inhomogeneous solutions when appropriate space dependence is incorporated, the exact nature of which depends on the boundary conditions and geometry. (See for example Brusselator model in Nicolis and Prigogine (1977).) Thus, our model is consistent with inhomogeneous deformation.

We have shown that the new temporal order is a consequence of a bifurcation from

a homogeneous (in time, in the present analysis) steady-state plastic flow beyond some critical values of the parameters. From the analysis it is clear that this order is a result of a balance between the energy input (in the forms of dislocation multiplication) and dissipation (annihilation, immobilisation and other processes). The phenomenon is obviously a far from equilibrium situation and is an example of a dissipative structure (Nicolis and Prigogine 1977).

We thank Dr G Venkataraman for arousing interest in this problem and Dr P Rodriguez for useful discussions.

References

Ananthakrishna G 1981 *J. Phys. D: Appl. Phys.* **14** 2091
—— 1982 *J. Phys. D: Appl. Phys.* **15** 77
Ananthakrishna G and Sahoo D 1981a *J. Phys. D: Appl. Phys.* **14** 2081
—— 1981b *J. Phys. D: Appl. Phys.* **14** 699
Bell J F 1973 *Handbuch der Physik* Band VIa/1 (Berlin: Springer)
Bodner S R and Rosen A 1967 *J. Mech. Phys. Solids* **15** 63
Cottrell A H 1953 *Phil. Mag.* **44** 829
McCormic P G 1971 *Acta Metall.* **19** 463
—— 1972 *Acta Metall.* **20** 351
Minorsky N 1962 *Nonlinear Oscillations* (New York: Van Nostrand)
Nicolis G and Prigogine I 1977 *Self Organisation in Non-Equilibrium Systems* (New York: Wiley)
Penning P 1972 *Acta Metall.* **20** 1169
Sahoo D and Ananthakrishna G 1982 *J. Phys. D: Appl. Phys.* **15** 1439
Valsakumar M C and Ananthakrishna G 1982 *J. Phys. D: Appl. Phys.* at press
Van den Beukel A 1975 *Phys. Status Solidi* a **30** 197
—— 1980 *Acta Metall.* **28** 965
Wijler A and van Westrum S 1971 *Scr. Metall.* **5** 531
Zagarukuyko L N, Osetskiy A I and Soldatov V P 1977 *Phys. Met. Metallogr.* **43** 156.

CHAOTIC FLOW IN A MODEL FOR REPEATED YIELDING

G. ANANTHAKRISHNA and M.C. VALSAKUMAR
Materials Science Laboratory, Reactor Research Centre, Kalpakkam 603 102, Tamil Nadu, India

Received 14 December 1982

Chaos exhibited by a model introduced in the context of repeated yielding is studied. The model shows an infinite sequence of period-doubling bifurcations with an exponent $\delta = 4.67 \pm 0.1$. The associated one-dimensional map and the projection of the strange attractor are also studied.

Recently we [1–3] have been interested in modelling the phenomenon of repeated yielding of materials and its other manifestations [1,2]. Repeated yielding (RY) of materials has been known to be some kind of instability [4] and has been an object of much investigation in metallurgical literature. Our interest in the subject arose out of a need to understand and explain the full temporal behaviour of RY. In a sense, the model we have proposed is a generalization of Cottrell's model [5] by including the time dependence. The basic idea was to make use of the intrinsic nature of plastic flow, namely the nonlinear interaction between dislocations, and to show that limit cycle solutions are supported for certain values of the parameters. We thus identified the emergence of limit cycle solutions as the mathematical mechanism of RY.

The purpose of this note is to report the chaotic flow [6,7] exhibited by our model over a certain range of the drive parameter. (There is some evidence for such a flow in experimental situations also. We shall discuss this briefly later.) This adds to the growing list of models as well as physical situations exhibiting chaos [6–9]. The model shows an infinite sequence of period-doubling bifurcations eventually leading to chaos. The drive parameter is the applied strain rate. The region over which chaos is exhibited is very small compared to the range of strain rate over which RY is seen. (RY is considered to be periodic.) We have calculated the value of the associated exponent and found it to be the same as Feigenbaum's exponent for the quadratic map. We have also obtained the associated one-dimensional map.

Briefly the model consists of three types of dislocations, namely the mobile, the relatively immobile and those with clouds of solute atoms (Cottrell type). There are many well-known mechanisms which transform one type of dislocation to an other, leading to a coupled set of rate equations for their respective densities. The rate constants are functions of stress, temperature and other parameters. In constant-strain-rate experiments, the stress is changing. The rate of change of stress is described by the machine equation which involves all the dislocation densities. (For the interested reader we refer to ref. [1–3].) Here we will not give any description of the equations, except those that will be essential for our discussion. We shall work with dimensionless variables. The rate equations are

$$\dot{x} = (\phi - h\eta^{1.2})^m x - bx^2 - ax + y - xy \,, \tag{1}$$

$$\dot{y} = b(kbx^2 - xy - y + az) \,, \tag{2}$$

$$\dot{z} = c(x - z) \,, \tag{3}$$

$$\dot{\phi} = d[e - (\phi - h\eta^{1/2})^m (x + \gamma' z)] \,. \tag{4}$$

The dot refers to the derivative with respect to a dimensionless variable τ (the dimensionless strain or time). In the above equations x, y, z and ϕ correspond to the mobile density, the immobile density, the density of those with clouds of solute atoms and the stress, respectively. All the parameters (a, b, c, d, e, h, k, γ')

0 031-9163/83/0000–0000/$ 03.00

are parameters that can be varied. In the actual physical situation all the parameters are positive and so are the variables x, y, z and ϕ. Further, the initial values for x, y, z are never strictly zero.

The two steady states are $(0, 0, 0, 0)$ and (x_a, y_a, z_a, ϕ_a). The trivial steady state is always unstable and is not allowed by the physical conditions. Linear-stability analysis around (x_a, y_a, z_a, ϕ_a) shows that there is an unstable domain in the parameter space for which a limit cycle solution is supported. The parameter of interest (even in the physical case) is the applied strain rate. We therefore fix the values of other parameters within the instability region and study the bifurcation sequence with respect to e (the strain rate). The entire numerical work has been carried out on a Honeywell Bull DPS 8. The values of the parameters are fixed at $(0.7, 2 \times 10^{-3}, 8 \times 10^{-3}, 10^{-4}, e, 0.2, 0.9, 0)$.

The region over which the period-doubling bifurcation occurs is small and this region is located near the upper end of the domain of e (the dimensionless strain rate) over which RY is observed. The first bifurcation from the periodic state with period T to a state with period $2T$ occurs at $e_1 = 159.9844$. The successive bifurcations 2^2T, 2^3T, 2^4T and 2^5T occur at $e_2 = 173.7178$, $e_3 = 175.8974$, $e_4 = 176.3462$ and $e_5 = 176.4423$, respectively. The exponents defined by

$$\delta_n = (e_n - e_{n-1})/(e_{n+1} - e_n) ,$$

for $n = 2, 3$ and 4 are respectively 6.30 ± 0.1, 4.86 ± 0.1 and 4.67 ± 0.1. (We have not tried to obtain a better estimate of δ due to limitations on computer time.) It is clear that the value of δ in our case is very close to that obtained by Feigenbaum [10,11] for the quadratic map. Figs. 1, 2 and 3 show graphs of $\phi(\tau)$

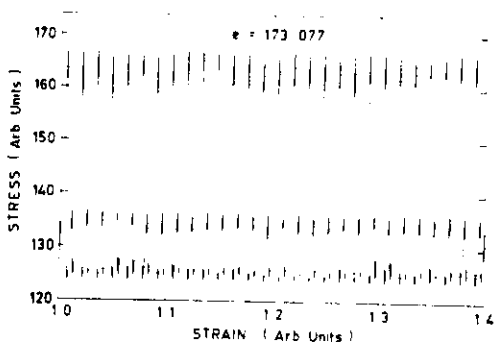

Fig. 1. Stress–strain curve for $e = 173.077$ with period $2T$.

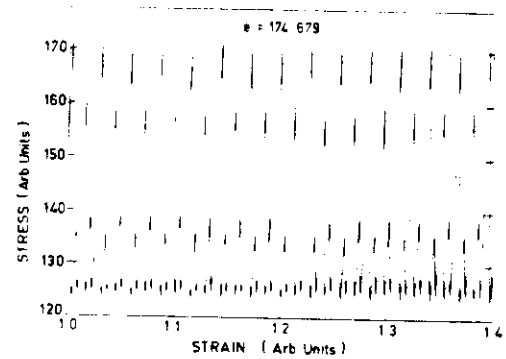

Fig. 2. Stress–strain curve for $e = 174.679$ with period $4T$.

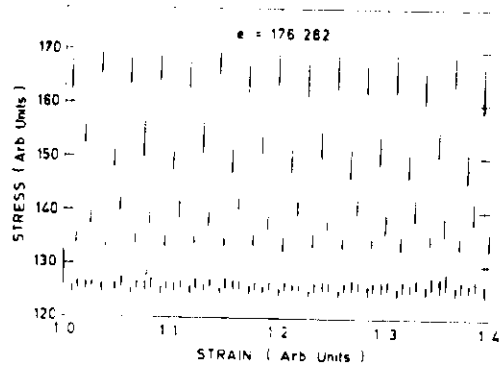

Fig. 3. Stress–strain curve for $e = 176.282$ with period $8T$.

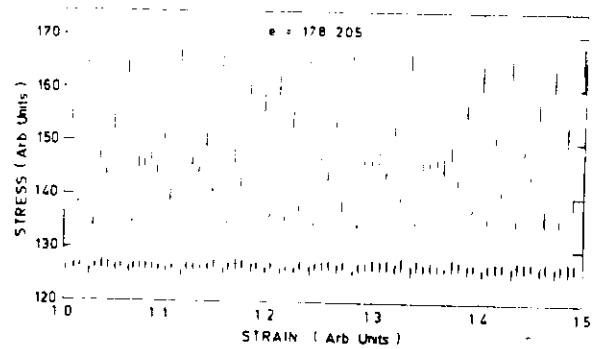

Fig. 4. Stress–strain curve for $e = 178.205$ well within the chaotic regime.

with periods $2T$, 2^2T and 2^3T, respectively. The estimated value of e_∞ is 176.4669. Beyond this value of e_∞ we find chaotic motion. Fig. 4 shows a graph of $\phi(\tau)$ for $e = 178.205$ well in the chaotic domain. We

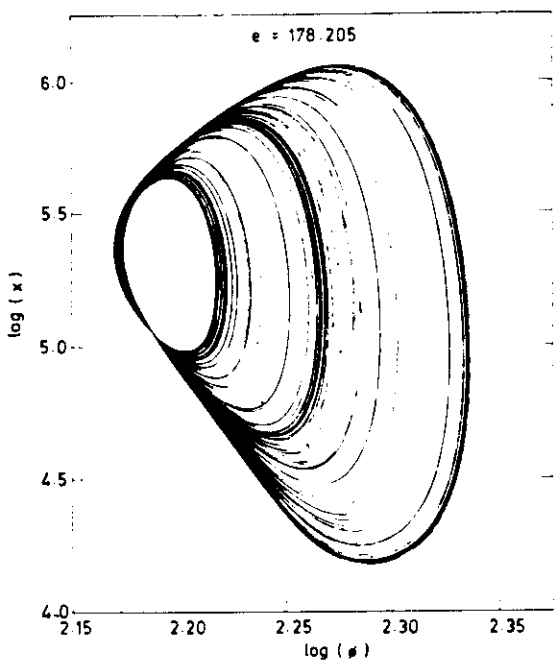

Fig. 5. A log–log plot of the strange attractor for $e = 178.205$ on the $x-\phi$ plane.

have also obtained the projection of the strange attractor in the $x-\phi$ plane. A log–log plot of this projection is shown in fig. 5.

In order to check the precise nature of the one-dimensional map associated with our system of equations, we have plotted M_{n+1} versus M_n, where M_n is the nth maximum of the $\phi(\tau)$ graph. The number of points used is 1000 and we have passed a smooth curve since these points form almost a continuous line. The plot so generated is shown in fig. 6. Unlike the one-dimensional map associated with the Lorenz model [6], our map has a smooth rounded maximum similar to the quadratic map, except that it is very much skewed.

The fact that our model exhibits a chaotic flow has prompted us to look for such experimental plots in repeated yield drops. (Of course, the values of the parameter which controls the magnitude of variation in ϕ, i.e. the magnitude of yield drop has to be chosen appropriately.) Even though we are constrained by the fact that the average level of ϕ (stress) remains flat in our model, we have found evidence in support of such flows [12]. Experimentally such regions also occur at the end of the region of the strain rate for

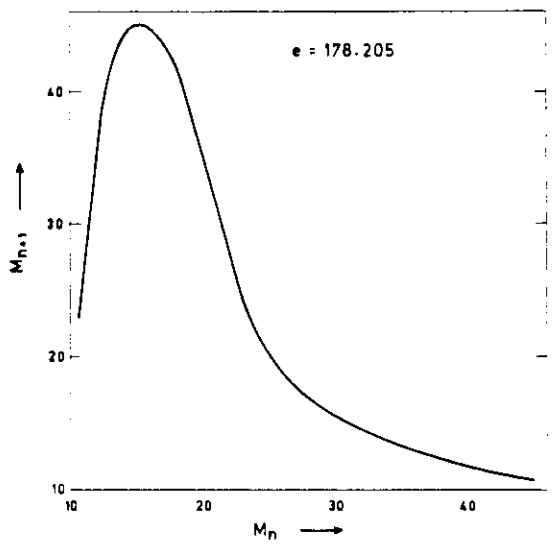

Fig. 6. A one-dimensional map associated with the model.

which RY is seen. If we subtract the slow increase in the base level of stress normally observed, there appear many more situations which are perhaps chaotic [13].

A more detailed analysis of the model including the period-undoubling phenomena seen will be reported elsewhere.

We thank Mr. K. Anantharaman for the help in preparing the computer plots.

References

[1] G. Ananthakrishna and D. Sahoo, J. Phys. D14 (1981) 2081.
[2] G. Ananthakrishna and M.C. Valsakumar, J. Phys. D15 (1982), to be published.
[3] M.C. Valsakumar and G. Ananthakrishna, submitted to J. Phys. D.
[4] J.F. Bell, in: Handbuch der Physik, Vol. VIa/1 (Springer, Berlin, 1973).
[5] A.H. Cottrell, Phil. Mag. 44 (1953) 829.
[6] E. Ott, Rev. Mod. Phys. 53 (1981) 655.
[7] J.P. Eckmann, Rev. Mod. Phys. 53 (1981) 643.
[8] W. Lauterborn and E. Cramer, Phys. Rev. Lett. 47 (1981) 1445.
[9] D.J. Jefferies, Phys. Lett. 90A (1982) 317.
[10] M.J. Feigenbaum, J. Stat. Phys. 19 (1978) 25.
[11] M.J. Feigenbaum, J. Stat. Phys. 21 (1979) 669.
[12] E.O. Hall, Yield point phenomena in metals and alloys (Macmillan, London, 1970).
[13] A. Rosen and S.R. Bodner, Mater. Sci. Eng. 4 (1969) 115.